

HEAT AND MASS TRANSFER IN SPRAY DRYING

A

THESIS

BY

JAN DLOUHY, B.Eng.

Chemical Engineering Laboratory - McGill University

Under Supervision of Dr. W. H. Gauvin

Submitted to the Faculty of Graduate Studies
and Research of McGill University in partial
fulfillment of the requirements for
the degree of Doctor of Philosophy

McGill University

April 15th, 1957

ACKNOWLEDGEMENTS

The author wishes to express his thanks to all those who, in various ways, have contributed to this work:

To the staff and graduate students of the Chemical Engineering Department, for their willing contributions and suggestions.

To the Pulp and Paper Research Institute of Canada, for the loan and construction of certain pieces of equipment.

To his wife, for her assistance with the spray dryer operation and analytical work.

To the National Research Council, for the award of a Bursary and two Studentships which greatly facilitated the carrying out of this research.

TABLE OF CONTENTS

A. HISTORICAL REVIEW

INTRODUCTION	1
I. THE SPRAY DRYING PROCESS	4
1. ATOMIZATION	4
a) Theory of Atomization	4
b) Atomizing Nozzles	6
i) Pressure Nozzles	6
ii) Spinning-disk Atomizers	10
iii) Pneumatic Atomizers	14
iv) Other Atomizers	17
2. DRYING CHAMBER	17
a) Chamber Design	18
b) Drying Gases	21
3. PRODUCT COLLECTION	22
II. EVAPORATION AND DRYING OF SPRAYS	24
1. HEAT AND MASS TRANSFER TO SINGLE DROPS	24
2. HEAT AND MASS TRANSFER TO CLOUDS OF PARTICLES	30
3. EVAPORATION AND DRYING OF DROPS CONTAINING SOLIDS	35
4. EFFECT OF HIGH EVAPORATION RATES ON THE HEAT TRANSFER COEFFICIENTS	37

B. EXPERIMENTAL SECTION

INTRODUCTION	39
I. METHODS OF MEASUREMENT	41

1.	DETERMINATION OF AIR HUMIDITY	41
a)	Volumetric Method	43
i)	Equipment	43
ii)	Procedure and Calibration	45
b)	Sample Collection	48
2.	MEASUREMENT OF AIR TEMPERATURE	49
3.	PARTICLE SIZE DETERMINATION	52
a)	Sample Collection	53
b)	Particle Counting	56
4.	DETERMINATION OF SOLID CONCENTRATION	58
a)	Sample Collection	59
b)	Analysis for Concentration	60
5.	PHYSICAL PROPERTIES OF LIGNOSOL SOLUTIONS	63
a)	Density	63
b)	Heat of Solution	64
c)	Specific Heat	65
d)	Vapour Pressure	66
i)	Equipment and Procedure	66
ii)	Results	68
II.	HEAT AND MASS TRANSFER COEFFICIENTS	72
1.	EQUIPMENT	72
a)	Air Supply	74
b)	Air Heating	78
c)	Drying Chamber	79
d)	Atomization and Feed Supply	80
2.	PROCEDURE	82
3.	CALCULATIONS	85
a)	Determination of the Rate of Evaporation	85
b)	Calculation of the Heat Transfer Coefficient and the Nusselt Number	86
c)	Calculation of the Mass Transfer Coefficient and the Modified Nusselt Number	88

4.	RESULTS	89
5.	DISCUSSION	99
a)	Temperature Distribution	107
b)	Heat and Material Balance	109
c)	Droplet Mean Statistical Diameter	110
d)	Heat Transfer Coefficients	112
III.	EVAPORATION AND DRYING OF LIGNOSOL SPRAYS	117
1.	EQUIPMENT	117
2.	PROCEDURE	118
3.	CALCULATIONS	119
4.	RESULTS	120
a)	Spray Drying of Lignosol BD	120
b)	Spray Drying of Lignosol TS	132
c)	Tray Drying	136
5.	DISCUSSION	136
a)	Spray Drying of Lignosol BD	136
b)	Drying of Lignosol TS	142
c)	Calculation of Drying Time	143
	NOMENCLATURE	153
	CONCLUSIONS	157
	SUMMARY AND CONTRIBUTION TO KNOWLEDGE	166
	BIBLIOGRAPHY	169

LIST OF ILLUSTRATIONS

Figure 1	Apparatus for the Determination of Air Humidities.....	44
Figure 2	Sampling Devices and the Thermometer Shield.....	50
Figure 3	Calibration Curve for the Fisher Neffluoro-Photometer.....	62
Figure 4	Dew Point Apparatus.....	67
Figure 5	Saturation Humidities of Lignosol Solutions.....	71
Figure 6	Spray Drying Apparatus.....	73
Figure 7	Schematic Arrangement of the Spray Drying Apparatus.....	75
Figure 8	Control Panel.....	76
Figure 9	Blower Orifice Calibration Curve.....	77
Figure 10	Temperature Distribution along the Drying Chamber at Different Air Velocities.....	100
Figure 11	Temperature Distribution along the Drying Chamber at High Inlet Air Temperatures.....	101
Figure 12	Temperature Distribution along the Drying Chamber at Various Average Droplet Diameters.....	102
Figure 13	Dependence of the Water Vaporization on the Average Droplet Diameter and Inlet Air Temperature.....	103
Figure 14	Dependence of the Water Vaporization on the Average Droplet Diameter and Inlet Air Temperature.....	104
Figure 15	Dependence of the Water Vaporization on the Average Droplet Diameter and Inlet Air Temperature.....	105
Figure 16	Photomicrograph of Large Water Droplets.....	106
Figure 17	Photomicrograph of Small Water Droplets.....	107
Figure 18	Calculated and Experimentally Determined Particle Size Distribution (Run No. 2, $x = 5.2$ -feet).....	113

Figure 19	Variation of the Heat Transfer Coefficient with the Droplet Diameter.....	114
Figure 20	Correlation of the Heat Transfer Coefficient in Terms of the Nusselt Number.....	115
Figure 21	Photomicrographs of Lignosol Particles, Run No. 23, (220X).....	126
Figure 22	Photomicrograph of Lignosol Particles, Run No. 20, (220X).....	127
Figure 23	Temperature and Humidity Distribution in the Spray Dryer, Run No. 20.....	128
Figure 24	Temperature and Humidity Distribution in the Spray Dryer, Run No. 21.....	129
Figure 25	Temperature and Humidity Distribution in the Spray Dryer, Run No. 22.....	130
Figure 26	Temperature and Humidity Distribution in the Spray Dryer, Run No. 23.....	131
Figure 27	Drying of Lignosol Sprays.....	133
Figure 28	Drying of Lignosol Sprays.....	134
Figure 29	Photomicrograph of Spray Dried Lignosol TS (220X).....	135
Figure 30	Tray Drying.....	137
Figure 31	Particle Size Distribution (Run No. 20).....	140
Figure 32	Particle Size Distribution (Run No. 20).....	145
Figure 33	Calculated and Experimental Rate of Drying of Lignosol Sprays.....	151

LIST OF TABLES

<u>Table No.</u>		<u>page</u>
I	Calibration of Air Humidity Apparatus.....	47
II	Saturation Humidities of Lignosol Solutions.....	70
III	Location of Sampling Points.....	81
IV	Heat and Mass Transfer to Water Droplets at High Air Velocity (Run 1).....	90
V	Heat and Mass Transfer to Water Droplets at High Air Velocity (Run 2).....	91
VI	Heat and Mass Transfer to Water Droplets at Low Air Velocity (Run 3).....	92
VII	Heat and Mass Transfer to Water Droplets at Low Air Temperature (Run 4).....	93
VIII	Heat and Mass Transfer to Water Droplets at High Air Velocity (Run 5).....	94
IX	Heat and Mass Transfer to Water Droplets at High Air Temperature (Run 6).....	95
X	Heat and Mass Transfer to Water Droplets of Large Average Diameter (Run 7).....	96
XI	Heat and Mass Transfer to Water Droplets of Large Average Diameter (Run 8).....	97
XII	Heat and Mass Transfer to Water Droplets of Small Average Diameter (Run 9).....	98
XIII	Heat and Mass Transfer to Water Droplets of Small Average Diameter (Run 10).....	98A

<u>Table No.</u>		<u>page</u>
XIV	Spray Drying of Lignosol (Run 20).....	121
XV	Spray Drying of Lignosol (Run 21).....	122
XVI	Spray Drying of Lignosol (Run 22).....	123
XVII	Spray Drying of Lignosol BD and Lignosol TS (Run 23).....	124
XVIII	Mean Volume Diameters.....	141
XIX	Calculated Drying Time for Lignosol Solutions.....	148
XX	Calculated Drying Time for Lignosol Solutions.....	149
XXI	Calculated Drying Time for Lignosol Solutions.....	150

A. HISTORICAL REVIEW

INTRODUCTION

Of all the operations of chemical engineering, very few have enjoyed a more spectacular development than spray-drying, particularly during the past two decades. This remarkable growth has, in turn, stimulated a considerable amount of research work in an attempt to minimize the empirical nature of spray dryer design. In addition, contributions from studies in the fields of fluid mechanics, boundary layer behaviour and particle dynamics have resulted in a much better understanding of the fundamental principles which underly this operation. The purpose of this Literature Survey is to summarize these recent advances, with particular reference to their heat and mass transfer aspects.

Spray drying may be defined as the drying of an atomized solution or slurry in contact with a stream of hot gases, under conditions which permit the recovery of the dried product. This definition indicates only partly the complexities of the operation, and its wide acceptance today is due to the desirable properties of the product obtained, rather than to the simplicity of the equipment necessary.

The advantages of spray drying have been widely discussed (78)(91), and depend chiefly on the high rate of drying and on the fact that the particles remain at or close to the wet-bulb temperature of the drying air during most of the short time of exposure. This results in little or no decomposition of the material being dried, even if it is highly heat sensitive. Other advantages include the uniformity, good colour and free-flowing characteristics of the dried product, which is thus

ready for immediate packaging without further handling. From the operational point of view, absence of pretreatment steps such as precipitation and filtration, which are often necessary in conventional dryers, should be noted. Disadvantages include relatively high investment costs, inflexibility of operation, and low bulk density of the product.

European engineers were the first to recognize the special advantages of this drying process and it was not until the beginning of World War II that its potentialities were felt in America. During that time the question of transportation was of paramount importance and the dehydration of foodstuffs such as powdered eggs (19)(37)(48), milk (32)(76)(102)(125)(126)(132), ice cream mix, whipped cream (26) and potato purees (16)(101) was carried out by spray drying because these materials are generally heat sensitive and the product is required in a readily soluble form.

Pharmaceutical products such as thermobile (7), blood plasma (138), yeast, penicillin and drugs in general (14)(145) obtained by spray drying are superior to those produced by sublimation, freeze drying or vacuum drying. Soaps and detergents are also commonly spray-dried in America, and in Europe and Asia (8)(15)(111)(112)(113)(114)(134)(139) because of the "anti-sneeze" properties of the product, which are due to the almost complete absence of fines.

A host of other products such as waste liquors from industrial processes (32), pigments, polymers and many inorganic materials have been spray-dried economically, showing the versatility of the process and its importance in the present day industry.

In its broader aspects the spray drying operation can be divided into three major operations:

1. atomization of the solution, slurry or colloidal suspension;
2. evaporation and drying of the liquid droplets so produced;
3. separation of the dried particles from the drying gaseous medium and their collection.

Recent studies have made it abundantly clear that atomization has far reaching consequences not only on the rate of drying but also on the physical properties of the product. The first section of this survey is therefore devoted to a brief description of the more common atomizing nozzles presently available, particularly from the point of view of the particle size and size distribution that can be expected from them.

Following atomization, the liquid droplets are mixed with the hot gases in the drying chamber. The design of this chamber must provide adequate residence time for the droplets to be dried, and the various flow patterns encountered in drying chambers constitute the next section. Finally a section is also devoted to the various methods of separation and collection of the dried product.

The evaporation of the liquid spray involves simultaneous consideration of heat, mass and momentum transfer, and although a considerable amount of work has been done on the evaporation and drying of single droplets, only limited data are available for the evaporation and drying of clouds of particles, particularly in turbulent gas streams. These considerations are discussed separately and in considerable detail in the second chapter of this review.

I. THE SPRAY DRYING PROCESS

1. ATOMIZATION

The most important single step in any spray drying process is, without doubt, atomization. Under given operating conditions, the initial particle size will have a direct bearing on the product's moisture content, recovery, appearance, bulk density and wetting properties, and must therefore be closely controlled.

Atomization is, moreover, of great importance in many other fields outside the process industries. In agriculture the spraying of liquid chemicals such as insecticides, herbicides, fungicides and defoliant is achieved by means of atomization. The use of liquid fuels for combustion in boilers, furnaces, internal combustion piston engines, jet engines and rocket engines has also led to the increased use of atomizers and, consequently, further stimulated research in the field of atomization.

a) Theory of Atomization

In analyzing the performance of any atomizing nozzle, it would be desirable to arrive at an expression which would correlate the drop size, size distribution and spatial distribution of the spray in terms of the variables of the system including pressure, density, surface tension, viscosity, flow rate and the general geometry of the atomizing device.

Atomization depends mostly on the break-up of jets or plane fluid sheets. Considerable study by high speed photography has undoubtedly led to a better understanding of the mechanism of drop formation

(30)(35)(50)(56)(80)(91)(98)(124) but no unified theory has as yet been presented. However, several mechanisms have been proposed, depending on the initial velocity of the jet or plane fluid sheet, and on the turbulence of the fluid.

At very low velocities the liquid is held to the nozzle by surface tension and if the force separating the liquid from the nozzle exceeds the force holding it there, drops will form and separate. This would be the mechanism of drop formation from a hypodermic needle at low pressures; Edeling (31) has shown that the energy necessary to overcome the surface tension is given by:

$$W = (6\sigma)/(D) \dots\dots\dots(1)$$

where W - energy per liter of liquid, (Kg.)(m.)/(l.);

σ - surface tension of the liquid, (Kg.)/(m.);

D - diameter of droplets formed, (m.).

At somewhat higher velocities, Castelman (22) suggested that the mechanism of break-up is due to the formation of filaments by air friction, followed by the disruption of these filaments into drops according to Rayleigh's theory (110). Hinze and Milborn (59) also postulated the above two mechanisms but they also mentioned film formation, as studied by Hagerty (50), as an alternative intermediate. Fogler (34) suggested that the break-down of the filaments or films is due to the combined action of surface tension, internal viscous forces and turbulence. The relative importance of these forces will depend on the type of nozzle used, on the rate of flow of the liquid

and on its physical properties.

Richardson (115) considered the formation of filaments to be essential for the atomization of liquids and proposed three regions for the liquid jet break-up into filaments: a) capillary ripples; b) sinuous oscillation of the cylinder axis of the jet; c) filament formation due to air friction.

For the case of atomization of a liquid breaking up without the influence of the surrounding air, the mechanism of jet break-up can be predicted to be dependent on jet diameter d , jet velocity v , liquid density ρ_L , surface tension σ , and viscosity μ . The break-up mechanism of a jet as predicted by dimensional analysis would appear to be a function of the jet Reynolds number $dv\rho_L/\mu$ and a dimensionless group, $\mu/\sqrt{\sigma\rho_L d}$, sometimes referred to as the Z-number (91).

b) Atomizing Nozzles

Depending on the type of energy used for the atomization, the various atomizing nozzles can be divided into several distinct categories. A very complete survey of these was made by Marshall in 1954 (91) and only a brief summary will therefore be given here.

i. Pressure Nozzles

In this type of nozzle, pressure energy is used to break up the liquid into droplets. Several different types exist, chief among which are the single-hole nozzles, swirl-spray nozzles and impact nozzles. Apart from the physical properties of the liquid atomized, the particle size produced

will be a function of the nozzle orifice diameter and the pressure used. Since the liquid rate will also be a function of these variables, there is no way of controlling independently the particle size distribution. As a result of this, pressure nozzles are rather inflexible, but they are simple to operate and give fairly uniform size distributions.

From dimensional analysis, Dorman (29) has shown that if the particle size can be taken as a function of the surface tension to the one third power, as given by Rayleigh (110), then the diameter of the particles produced in a spray will be given by:

$$D = C(Q/\theta)^{1/3} \gamma^{1/3} \rho_L^{1/6} p^{-1/2} \dots\dots\dots(2)$$

where D - a statistical diameter; *

C - constant;

Q - liquid flow rate;

θ - angle of spray;

γ - surface tension;

ρ_L - density of the liquid;

p - pressure of the liquid.

This correlation neglects the effect of the liquid viscosity, assuming it to be negligibly small. A limited study on the atomization of water and kerosene gave good results. Straus (141) studied the disintegration of flat sheets from a single hole fan spray nozzle and expressed the diameter as:

* The units of the original authors are used in the equations presented in this chapter because most of these equations are semi-empirical, and a general list of symbols would not be practicable.

$$d_s = 160 (\sigma/p)^{0.25} (FN/\theta)^{0.37} \rho_L^{0.065} / K_q^{0.98} \dots\dots\dots(3)$$

where d_s - statistical surface mean diameter, microns;

FN - (flow rate, g.p.h.)/(pressure, p.s.i.)^{1/2};

K_q - discharge coefficient.

The constant was derived empirically, but since all the work was done on water only, the effect of viscosity would not be apparent. The equation is, however, very similar to that of Dorman (29).

Tate and Marshall (143) studied the atomization from centrifugal pressure nozzles. Drop size distributions from grooved-core-type and spin-chamber-type nozzles were determined and the results expressed as:

$$d_{vs} = 286(d + 0.17)\exp(13/V_v - 0.0094V_t) \dots\dots\dots(4)$$

where d_{vs} - mean Sauter diameter, microns;

d - orifice diameter, (in.);

V_v - vertical velocity component of the liquid, (ft.)/(sec.);

V_t - tangential velocity component of the liquid, (ft.)/(sec.).

Again, this correlation was tested for water only and hence no viscosity term is included. Some work was done using liquids of different viscosities, but the range was too small to assess the effect of viscosity. The liquid inlet tangential velocity was a function of the internal design features of the nozzle and was expressed as:

$$V_t = 0.320(\cos a)/N_G A_G \dots\dots\dots(5)$$

where a - angle made by the grooves in the nozzle with the horizontal;

N_G - number of grooves;

A_G - cross-sectional area of a single groove, (sq.in.).

while the vertical velocity component was given by:

$$V_v = 0.407C/d^2 \dots\dots\dots(6)$$

where C - capacity of nozzle, (gal./min.);

d - orifice diameter, (in.).

Nozzles of several different configurations were used and the equation appears to be generally applicable for the atomization of water from nozzles of this type. The particle size distribution was also given.

Turner and Moulton (148) studied hollow cone pressure nozzles of a specific design by spraying organic materials into the air and allowing the particles so produced to freeze before being collected.

For the two nozzles used they correlated the mean diameter as follows:

$$x' = 16.56D^{1.520}w^{-0.444}\sigma^{0.713}\mu^{0.159} \dots\dots\dots(7)$$

and $x' = 41.40D^{1.589}w^{-0.537}\sigma^{0.594}\mu^{0.220} \dots\dots\dots(8)$

where x' - mean diameter, microns;

D - nozzle orifice diameter, (mm.);

w - flow rate, (gm.)/(sec.);

σ - liquid surface tension, (dynes)/(cm.);

μ - liquid viscosity, centipoises.

Equations (7) and (8) are empirical and specific to the nozzles studied, but they do show the effect of some of the physical properties of the liquid on the particle size produced. However, the range of liquid density, viscosity and surface tension studied was rather small making the results of little value for general purposes, and the difference in exponents in the two equations indicates the limited theoretical significance.

Many other experimental results are reported in literature, but most of these - like the above - apply only to specific nozzle designs and are useful only to indicate general trends.

ii. Spinning-Disk Atomizers

Spinning-disk atomizers are comparable to pressure nozzles but they utilize centrifugal energy rather than pressure energy to separate the liquid from the nozzle. They also produce sprays of a fairly narrow size distribution and the particle size can be controlled independently of the liquid rate by changing the r.p.m. of the disk. This is of considerable advantage since it imparts flexibility to a given system, but the spray pattern is very wide, consisting of a flat sheet perpendicular - at least initially - to the axis of rotation. Special consideration must therefore be given to this spray pattern in designing the drying chamber.

Spinning-disks of a great variety of design have been used, depending on the material to be atomized. The principal advantage of these atomizers is that practically any liquid or slurry can be atomized to a desired particle size, without danger of plugging, in contrast with the operation of pressure nozzles.

The question of particle size distribution from spinning-disk atomizers was the subject of several recent studies. Frazer (35) studied the drop size from a square edge glass plate at speeds of up to 2,500 r.p.m. and correlated his results on the basis of the equation given by Harkins and Brown (53) for the determination of the surface tension of liquids when drops are formed under the influence of gravity. The equation given by Frazer is:

$$d_M = 360,000(\sigma/D\rho_L)^{1/2}/(S)\dots\dots\dots(9)$$

where d_M - diameter of the main drop formed, microns;

σ - surface tension, (dynes)/(cm.);

D - diameter of disk, (cm.);

ρ_L - density of the liquid, (gm.)/(cm.³);

S - disk velocity, (r.p.m.).

The "main drop" as defined above was the diameter of the largest majority of the drops formed. Other drops of a diameter of $0.50d_M$ and $0.36d_M$ were also formed, but these accounted for only 17% of the total volume of the liquid atomized.

These results agree very well with those of Walton and Prewett (150) but they are applicable only to low liquid rates; the periphery of the

disk must be completely wetted, but when the liquid rate is increased and flooding of the plate occurs equation (9) no longer holds. This deviation is probably due to a different mechanism of atomization coming into play and a new fundamental equation would have to be used. Frazer (35) also noted that if the edge of the plate is not square the constant in the above correlation changes.

Friedman et al (38) studied a wide range of disk designs and speeds as well as a number of different liquids and correlated their results by means of dimensional analysis to give the equation:

$$d_{vs}/r = 0.4(G/\rho nr^2)^{0.6}(\mu/G)^{0.2}(\sigma\rho L/G^2)^{0.1}\dots\dots\dots(10)$$

where d_{vs} - mean Sauter diameter, (ft.);

r - radius of disk, (ft.);

G - feed rate of liquid atomized, based on wetted periphery,
(lb.)/(min.)(ft.);

ρ - density of feed, (lb.)/(cu.ft.);

n - speed of disk, (r.p.m.);

μ - viscosity of feed, (lb.)/(ft.)(min.);

σ - surface tension of feed, (lb.)/(min.)(min.);

L - wetted periphery of disk stream, (ft.).

The above equation disagrees with equation (9) in the number of variables included as well as in the exponents of some of the variables. This discrepancy is at least partly due to the much wider applicability of equation (10) and due to the fact that a particle size spectrum was obtained rather than particles of a uniform diameter. Friedman et al (38)

expressed this distribution by means of the Hatch dispersion coefficient, which is the ratio of the 84.13% diameter to the 50% diameter.

In an attempt to correlate the liquid feed rate and design characteristics of vaned disk atomizers with the particle size distribution, Herring and Marshall (56) studied twelve experimental disks. Water only was used in this study and the results were correlated by means of equation (11):

$$y = d(ND)^{0.83}(nb)^{0.12}/(w)^{0.24} \dots\dots\dots(11)$$

where y - ordinate value on probability plots;

d - drop diameter, microns;

N - speed of disk, (r.p.m.);

D - disk diameter, (in.);

n - number of vanes for a disk;

b - vane height, (in.);

w - liquid feed rate, (lb.)/(min.).

The parameter y was plotted against d on a probability plot and the line obtained is shown in the original paper. The importance of the peripheral velocity of the disk can be clearly seen from this equation. Equation (11) agreed quite well with the results obtained by Adler and Marshall (3) who also studied water only, but the results of Friedman et al (38) fall below the proposed line.

Apart from the drop size distribution, atomization introduces two other factors which are of considerable importance in spray dryer design.

The first of these is the diameter of the largest drops produced. This can be deduced from the probability plot of Herring and Marshall (56). Friedman et al (38) suggested that the largest drop has a diameter three times as large as the mean Sauter diameter of the spray.

The second consideration is the trajectory of the spray; atomization will obviously be of little use if the particles coalesce again on the walls of the drying chamber. Herring and Marshall (56) presented the following empirical equation:

$$R_{99} = 12D^{0.21}w^{0.25}/N^{0.16} \dots\dots\dots(12)$$

where R_{99} - radial distance at which 99% of the spray has fallen
36 in. below the plane of the disk, (ft.);

D - disk diameter, (in.);

w - liquid feed rate, (lb.)/(min.);

N - speed of disk, (r.p.m.).

Other correlations were also presented (2)(38)(100), but none of these are really applicable to spray dryers since the tests were carried out in still air. It is impossible to ignore the effect of the drying gas on the path of the droplets in these calculations, which are therefore specific to each application.

iii. Pneumatic Atomizers

Pneumatic or two-fluid atomizers utilize the energy of a secondary compressed gas to produce sprays. In general, the liquid jet is broken up by means of a gas introduced in an annulus surrounding the jet; the

mechanism of this break-up was discussed by Lane (80), Castelman (22), Marshall (91) and others (84)(98).

Pneumatic atomizers have the advantage of independent control of the particle size produced, as contrasted with pressure nozzles, because the atomizing gas pressure may be varied independently of the liquid rate. On the other hand, the capacities of such nozzles are low and the size distribution obtained is rather wide, particularly if fine atomization is necessary. Large amounts of energy are also required.

Rasbash (109) reported that a uniform particle size may be obtained by using a battery of hypodermic needles around which low pressure air was passed. The capacity per needle was low but the overall capacity of the 169 needles used ranged from 20 to 160 gallons per minute, and the particle size ranged from 200 to 1000 microns. This is rather high, particularly since pneumatic atomizers are used when a fine spray is desired; pressure nozzles are generally preferable if the required particle size is in the above range.

Nukiyama and Tanasawa (98) made an extensive study of the particle size resulting from small pneumatic atomizers and established the correlation:

$$d_{vs} = 585\sigma^{0.5}/(v\rho_s)^{0.5} + 597[\mu/(\rho_s\sigma)^{0.5}]^{0.45}(1000Q_s/Q_a)^{1.5} \dots (13)$$

where d_{vs} - mean Sauter diameter, microns;

v - relative velocity between the liquid and air stream, (m.)/(sec.);

ρ_s - density of the liquid, (gm.)/(cm³.);

μ - viscosity of the liquid, poises;

σ - surface tension of liquid, (dynes)/(cm.);

Q_s - volumetric flow rate of the liquid, (cm³.)/(sec.);

Q_a - volumetric flow rate of the air, (cm³.)/(sec.).

This equation was established for liquid densities from 0.8 to 1.2 (gm.)/(cm³.), surface tensions from 3 to 73 (dynes)/(cm.) and viscosities from 1 to 30 centipoises. Since air only was used as the atomizing gas, no correction is included for the variations of the physical properties of the gas. Subsequent studies with ethylene and nitrogen have shown that the drop size is nearly proportional to the gas viscosity, while the correction for the density variations is negligibly small (84).

In spite of the fact that the above equation is not dimensionally consistent, it was found to be in substantial agreement with other data published (84) and its applicability was extended by Briton (12) to supersonic atomization. Outside the range of variables studied, however, considerable disagreement was noted (91).

The particle size distribution was correlated by Nukiyama and Tanasawa (98) by means of the following distribution function:

$$N = ad^2e^{-bd^q} \dots\dots\dots(14)$$

where N - number of drops in size group $d \pm \Delta d/2$;

d - diameter of drop, microns;

a, b - constants;

q - dispersion coefficient.

The dispersion coefficient q was found to be a constant for a given

nozzle over a wide range of variables, but changes considerably with different nozzle designs.

From equation (13) it can be seen that if the ratio of the liquid flow rate to the gas flow rate is very small, the viscosity of the liquid is of minor importance in determining the particle size, since the first group on the right hand side of the equation predominates. On the other hand when this ratio becomes large, the surface tension of the liquid becomes of lesser importance.

iv. Other Atomizers

Several other types of energy may be used for the breaking up of liquid into sprays (91). Supersonic vibrations and mechanical vibrations have been tried as well as the use of high voltage electricity. The impingement of jets onto solid surfaces and the impingement of two liquid jets upon each other have also been studied, but none of these methods have as yet been applied to spray drying.

2. DRYING CHAMBER

Following the atomization of the liquid, the spray is mixed with hot gases which permit the evaporation and drying of the droplets. The design of the drying chamber, in which this step takes place, has received little attention from experimenters. Only qualitative measurements have been made so far, but these measurements indicate the importance of the gas flow patterns on the efficiency of the drying operation as well as on the quality of the product produced.

i. Chamber Design

Several important factors must be borne in mind when considering the design of a drying chamber. First of all the hot gases must mix effectively with the atomized spray, and this will depend not only on the flow pattern of the gas but also on the type of atomizing nozzle used. The effect of the spray from the nozzle on the flow patterns of a pilot plant scale spray dryer was recently studied (49), and it was shown that pneumatic and spinning disk atomizers had a predominating influence on the air flow within the dryer because of the large kinetic energy associated with the atomization process. In plant scale dryers this effect will probably be of lesser importance. The location of the nozzle with respect to the gas inlet ports can also have a large effect on the capacity of a unit (78).

The second consideration is product build-up in the drying chamber. Wet particles coming into contact with the walls of the chamber will stick there with the resulting loss of product and maintenance difficulty. Again this will be dependent on the type of nozzle used, but proper gas flow patterns may minimize the problem. In certain cases secondary air may have to be introduced into the chamber to give the desired particle trajectory. The problem of droplet deposition on the chamber wall was studied by Alexander and Coldren (5) for the case of droplets suspended in a turbulent air stream in a duct, but no conclusive results were obtained.

The third and most important consideration is the particle trajectory and residence time in the chamber. Obviously a sufficient quantity of hot gases must be supplied to permit the complete drying of the spray,

and their flow pattern must be such that none of the particles will leave the chamber until they are completely dried.

In general the basic designs of spray drying chambers may be divided into three categories: cocurrent, countercurrent and mixed-flow. The various possible flow patterns in these categories have been discussed in some detail by Marshall (91) and a description of commercial spray dryers was also given by Marshall and Seltzer (93).

In cocurrent flow, as the name implies, the spray and the hot gases are introduced in the same direction. The high temperature gradient around the nozzle causes a high rate of evaporation, resulting in the formation of back eddies, an undesirable feature since the particles swept back will be exposed to the hot gases for a prolonged period. On the other hand the dried product leaves the chamber with gases that are already cooled, and decomposition is thus minimized for the bulk of the material.

Countercurrent flow is opposite to the above, and since the dried product comes into direct contact with the entering hot gases, the temperature of these gases must be such that charring, etc. will not take place. This is of course a serious limitation for the majority of materials spray dried at the present time. Entrainment of the smaller particles can also present serious problems.

High efficiencies are obtained with the mixed flow type and the flow patterns are generally rather complex. The recycling and overexposure of some of the particles with the hot gases again present a serious obstacle.

Drying chambers are usually very large and account for a considerable portion of the investment costs of a spray drying installation. It is therefore very important that they be designed properly, the greatest danger being that a portion of the spray will by-pass a section of the chamber and leave wet, while another portion of the spray will be recycled and decomposed.

The patent literature shows the continuous attempt being made to improve the chamber design (91). A high-velocity spray dryer was recently reported by Comings and Coldren (25), using hot primary air through the nozzle and a stream of secondary air to prevent recycling. High capacities for a very small unit were reported, which offers definite advantages over the conventional chamber designs.

Edeling (31) made a thorough analysis of the trajectory of particles in a cocurrent spray dryer, with tangential air inlet, in an effort to determine the necessary chamber diameter. From considerations of particle dynamics in a three-dimensional centrifugal and gravitational field Edeling (31) presented a complete solution for the particle trajectory, but some of his assumptions on the drag coefficients in the three-dimensional field are probably not correct (91). The drag coefficients of decelerating particles, such as those in the nozzle zone, are also very hard to estimate, and recent studies suggest that they are very low (52)(66). The work of Buckham (13) and of Thordarson as reported by Marshall (91) would suggest that the gas flow patterns as assumed by Edeling (31) were also oversimplified.

ii. Drying Gases

The quantity and inlet temperature of the drying gases must of course be sufficient to permit the complete drying of the liquid particles in the spray drying chamber. The theoretical quantity necessary can be easily determined from a psychrometric chart by assuming that the conditions of the gas will follow the adiabatic cooling curve. The maximum outlet humidity of the gas must be such that it will be lower than the vapour pressure of the dried product under the given conditions of temperature and humidity. A simple heat balance or material balance will then give the desired gas to feed ratio. This consideration applies to a truly cocurrent operation only, in countercurrent or mixed flow units the quantity required will be somewhat lower. Corrections for heat loss and inefficient mixing must be made in actual calculations, and the temperature driving force can not be allowed to drop to zero if a reasonable size drying chamber is desired.

The most common method of heating the drying gas is by means of oil or gas burners, and the combustion products are generally mixed directly with air to make up the gas supply. If the material to be dried is easily oxidized, the combustion can be controlled to produce gases containing little, if any, excess air. On the other hand complete combustion must be insured to prevent contamination of the product with carbon or soot. Flue gases from boilers may sometimes be used directly and a commercial installation of this type was recently described by Isenberg (68).

Under certain circumstances combustion products may be undesirable in the drying gases and heat exchangers must then be used. Electrical heaters and high pressure steam heaters have also been used, but these are rather expensive for large units.

Other gases than air may also be used. Because of its higher rate of diffusion and thermal conductivity, hydrogen would give very high rates of evaporation. Sjenitzer (130) reports that the rate of evaporation of water in hydrogen would be three to six times as great as that in air. Another gas suggested is superheated steam as witnessed by the recent patent of Leman (83). Both these gases, however, present problems of product collection and gas recirculation and have not been used in commercial installations so far.

3. PRODUCT COLLECTION

The recovery of the powdered product from the exit gases is of considerable importance from the point of view of economics as well as of air pollution. It is a problem common to many other process industries, and the separation of gases from powdered solids has therefore received considerable attention.

In many cases, at least part of the separation can be effected in the spray drying chamber itself. Special design features can be included so that the drying chamber acts as a cyclone or a settling chamber, although this becomes rather difficult in cocurrent units. Some of the possible designs were discussed by Marshall (91).

When the product and gases can leave the chamber together, then the collection equipment will depend on the particle size range and specific gravity. The volume of the gases to be treated will also be of considerable importance. In general the collection efficiency of any dust collecting equipment is a function of the pressure drop across it, and an economic balance between the additional power costs against the additional product recovered will dictate the equipment used.

Cyclones, multicones and centrifugal cyclones are commonly used because of their flexibility of operation and large capacities. Operating characteristics such as efficiency, capacity and pressure drops across cyclones have been studied in detail, so that design considerations are simplified.

For fine products or as secondary collectors after cyclones more specialized equipment can be used, such as electrical precipitators, bag filters, and wet scrubbers. Wet scrubbers are standard equipment on many dryer installations, but they are not suitable for foods because of the danger of fermentation. Electrical precipitators and bag filters are expensive, but their use is often justifiable.

After product separation the gases are commonly exhausted to the atmosphere. In certain installations, however, these gases are still warm (200°F. and higher), and economizers can be installed to preheat the feed or incoming gases.

II. EVAPORATION AND DRYING OF SPRAYS

The theory of evaporation of a liquid into a gas stream rests on the assumption that the vapour in the immediate neighbourhood of the liquid surface is saturated, or, in other words, that equilibrium conditions prevail at the interface (95). Consequently the rate of evaporation depends on the rate of removal of the vapour from the liquid surface by means of diffusion and convection. For the case of liquid droplets suspended in a gaseous medium this will involve simultaneous considerations of heat and mass transfer, because the necessary heat required for evaporation must be supplied to the droplets by means of conduction, convection and radiation through the film surrounding them. Under equilibrium conditions the temperature of the surface of the droplets and hence the vapour pressure at the surface will be such that the heat transfer and mass transfer rates are balanced.

1. HEAT AND MASS TRANSFER TO SINGLE DROPS

A large number of theoretical and experimental studies have been carried out in the field of heat and mass transfer to single drops since the beginning of this century.

Morse (97) was probably one of the first to determine experimentally that the rate of evaporation of a drop is proportional to the diameter, rather than to the surface area or to the square of the diameter. His

determinations were based on the direct measurement of the rate of evaporation from a drop of iodine placed on the flat pan of a micro-balance. His results were analyzed by Langmuir in 1918 (81), who assumed that the evaporation of small objects in air was closely related to the mechanism of heat transfer by natural convection from bodies of the same shape and presented the following equation:

$$-dm/d\theta = s \int D_v d\rho_v \dots \dots \dots (15)$$

In the above equation s is a shape factor^{*} which Langmuir defined as:

$$s = 4\pi ab/(b-a) \dots \dots \dots (16)$$

where b is the radius of the outside film of gas and a is the radius of the evaporating sphere. By assuming b to be very much larger than a , and taking D_v as practically independent of ρ_v Langmuir obtained the following equation when the vapour density was expressed in terms of its vapour pressure:

$$-dm/d\theta = 4\pi a D_v M p_s / RT \dots \dots \dots (17)$$

The rate of evaporation can also be expressed in terms of the mass transfer coefficient k_G , and when the concentration of the diffusing component is zero at a large distance from the sphere, the equation can

^{*} The list of symbols for this chapter will be found on page 153. All symbols are consistent unless otherwise defined in the text.

be written, on a molar basis:

$$-dm'/d\theta = k_G A p_s \dots\dots\dots(18)$$

Combining equations (17) and (18) the modified Nusselt number Nu' will be equal to 2 for the case of mass transfer to an evaporating sphere, at zero relative velocity between the sphere and the surrounding gas. The modified Nusselt number is defined as:

$$Nu' = (k_G M_m dp_f)/(D_v \rho) \dots\dots\dots(19)$$

Substituting the results of Morse (97) into equation (17), Langmuir found that the diffusion coefficient of iodine in air at 298°K. and atmospheric pressure should be equal to 0.053 cm.²/sec. This value was considered low due to the obstruction to air circulation by the weighing pan, and Langmuir suggested that 0.07 cm.²/sec. would probably be closer to the correct value. Later work (67) has shown that the correct value at S.T.P. is 0.097 cm.²/sec.

The validity of equation (17) has been verified by many workers (39)(46)(61)(65)(73)(89)(107)(142) and extended and corrected for certain specific conditions. Shereshefsky and Steckler (127) measured the rate of evaporation of n-butyl phthalate and revised Langmuir's equation to fit the case of a finite concentration of the diffusing component at a large distance from the sphere. Bradley et al (11) showed the limitation of Langmuir's equation at low pressures and for very small particles (below 1 micron) and presented a slightly modified equation. At very low pressures free-molecular conduction must also be considered

in heat transfer and equations for this were presented by Kyte et al (79).

Fuchs (40) made a theoretical analysis of the rate of evaporation of small droplets in a gas atmosphere, basing his derivation of the fundamental equation on the following assumptions:

1. The drop is spherical;
2. There is no motion of the drop relative to the gas atmosphere;
3. The atmosphere extends unbound in all directions;
4. The atmosphere is at uniform temperature and pressure. The temperature of the drop is not lowered by the evaporation process;
5. The evaporation process is stationary;
6. The vapour is saturated on the surface of the drop;
7. The vapour pressure of the drop is vanishingly small in comparison with the total pressure.

The equation that Fuchs obtained was the same as that presented by Langmuir (18), except for a correction for the concentration of the diffusing vapour at an infinite distance from the drop. Fuchs then proceeded to analyze his various assumptions, showing their relative importance. He stated, however, that the exact calculation of the velocity of evaporation of a droplet moving with respect to the gas medium was scarcely possible.

In 1938 Froessling (39) made a detailed study of the question of relative velocity and presented a semi-empirical solution. The velocity field was calculated from the Navier-Stokes equation, the equation of

continuity and the boundary conditions of flow; the concentration field was obtained from the equation for diffusion in a moving medium and from the boundary conditions of the vapour.

Although a complete and exact solution of this system was not possible, Froessling showed that by conversion to a dimensionless form, equation (17) would yield the following expression for the rate of mass transfer:

$$dm/d\theta = D_v(M_p'/RT)d.\Phi(Re.Sc).....(20)$$

The form of the function $\Phi(Re.Sc)$ was determined from the boundary layer theory, and the rate of evaporation before the point of separation of the laminar layer was given as:

$$dm/d\theta = 2\pi D_v(M_p'/RT)d.K_{Sc}(Re)^{1/2}.....(21)$$

where K_{Sc} is a function of the Schmidt Number.

The calculation of the rate of mass transfer after the point of separation, where turbulent vortices are formed, was rather complicated. However, experiments performed by Froessling on the evaporation of naphthalene spheres indicated that 75-80% of the total evaporation took place before the point of separation, and if the rate after the point of separation could be taken as approximately proportional to $Re^{1/2}$ (although this is probably not true), then equation (21) could be used for the whole sphere with only a slight modification of the constant in the function K_{Sc} .

Experiments subsequently performed by Froessling on the evaporation of nitrobenzene, aniline and water drops, suspended from a thin glass

rod or thermocouple permitted the semi-empirical evaluation of K_{Sc} and showed that the mass transfer equation could be written in the following form:

$$dm/d\theta = 2\pi D_v (M_p' / RT) d \left[1 + 0.276(Re)^{1/2}(Sc)^{1/3} \right] \dots(22)$$

In 1952 Ranz and Marshall (107) published the results of an investigation of the factors influencing the rate of evaporation from pure liquid drops, and liquid drops containing dissolved or suspended solids. The work was carried out under very rigid experimental conditions. The drops, which ranged in diameter from 0.06 to 0.11 cm., were suspended from a capillary and the rate of evaporation was determined by measuring the droplet diameter by means of a projection microscope. Their results verified the analogy between heat and mass transfer and the following set of equations was presented:

$$Nu = 2.0 + 0.60Re^{1/2}Pr^{1/3} \dots\dots\dots(23)$$

$$Nu' = 2.0 + 0.60Re^{1/2}Sc^{1/3} \dots\dots\dots(24)$$

$$Nu = 2.0 + 0.60Gr^{1/4}Pr^{1/3} \dots\dots\dots(25)$$

$$Nu' = 2.0 + 0.60Gr^{1/4}Sc^{1/3} \dots\dots\dots(26)$$

Equations (23) and (24) apply when finite velocities exist between the drops and the gas stream while equations (25) and (26) were proposed for natural convection. The analogy between heat transfer (23) and (25) and mass transfer (24) and (26) can be clearly seen.

The agreement between equation (24) above and equation (22) suggested by Froessling is excellent, the value of the constant of the second term

of the right hand side of equation (24) being the only difference. When written in the same form, Froessling's equation would have the value of 0.552 as compared with 0.60 above.

At zero relative velocity equation (23) would give $Nu = 2.0$, which is in agreement with Langmuir's analogous equation for mass transfer. Equations (25) and (26) were suggested as a correction for the contribution to heat and mass transfer due to free convection currents caused by density differences. These equations have been verified experimentally only to a limited degree.

Ranz and Marshall also measured the temperature of the evaporating drops and they found this to be approximately equal to the wet-bulb temperature of the air for pure liquids. Although part of their work on the temperature distribution in the drops was criticized (147), it is in general agreement with other published results (60)(69), and only the results of Langstroth (82) would appear to disagree.

Other equations have been suggested for the heat and mass transfer coefficients to drops (65)(128), but the correlations proposed by Ranz and Marshall are without doubt the most reliable equations available at the present time.

2. HEAT AND MASS TRANSFER TO CLOUDS OF PARTICLES

In spray drying the liquid feed is atomized, and the resulting spray is mixed with the hot gases and descends or ascends through the drying chamber in the form of a cloud. The rate of evaporation from such clouds

has been studied only to a very limited extent, and no reliable equations, such as those presented for single particles, are available. Although the same general theoretical considerations would apply here, the problem is complicated by the fact that the droplets are usually very small and dispersed in turbulent gas streams.

Several experimental studies have been carried out in order to determine the rate of evaporation in the nozzle zone (52)(62), particularly in the case of fuel atomization. These studies indicate that the drag coefficients of the decelerating droplets are extremely low (down to 0.01 at $Re = 100$) and a function of many variables. Although the experimental data of Ingebo (62) seem to agree well with the vaporization rates for single drops, the variations in the drag coefficient make theoretical predictions uncertain, because of the difficulty in ascertaining the instantaneous velocities.

Other experimenters have studied the rate of heat transfer to clouds of solid particles at their terminal velocity in relatively still air (72)(99) and their results also agree with the heat transfer data to single particles.

Calderbank and Korchinski (18) have shown that liquid droplets will behave as solids below a Reynolds Number of 200, that is they will not oscillate and they will have the same drag coefficients as rigid bodies. This is in agreement with other data (42)(63), and although there is little doubt that internal circulation will take place in droplets even at very low Reynolds Numbers, it does not seem to affect the drag coefficient.

From this it would appear that liquid sprays should behave in the same manner as solid sprays, providing the Reynolds Number is sufficiently small. This has been verified experimentally (71) (73), although the conditions under which these results have been obtained are outside the range of most spray drying applications.

In the case of heat and mass transfer to clouds of particles in turbulent gas streams, the problem is complicated by the fluctuations in local velocity of the gas. The velocity field was expressed by Froessling in terms of the Navier-Stokes equation (39) and this can be done only in the case of laminar flow of the gas. Consequently equation (22) is not, at least from the theoretical point of view, applicable in turbulent gas streams. In addition, the velocity fluctuations of the stream create relative velocities, apart from those average relative velocities which may exist because of gravitational forces, which make the estimation of the true Reynolds Number uncertain.

Theoretical studies of the dispersion of small particles in turbulent gas streams have been made by Liu (86), Soo (135) and others. Liu considered the forces acting on particles suspended in turbulent flow, and presented a somewhat complex equation in a one-dimensional field. The extension of this equation for a three-dimensional system in an enclosed space is rather difficult.

The statistical study of Soo (135) of the momentum transfer to particles suspended in a fluid is more promising, although the approximate solution presented neglects the effects of acceleration and deceleration of the particles. From this study it is apparent that the eddy diffusivity

of the particles is greater than that of the stream, and is a function of the intensity of turbulence $\sqrt{u'^2}$ as well as of the particle diameter and density, and of the physical properties of the fluid. The eddy diffusivities of the particles and of the gas will be almost equal for small particles and at low values of $\sqrt{u'^2}$.

Several experimental studies have also been made to clarify the question of particle diffusion (5)(75)(88), and in general these would tend to substantiate the analysis of Soo (135). Longwell and Weiss (88) studied the diffusion of particles produced by an atomizing nozzle. Although the distribution of the particles in the gas stream was a function of the type of nozzle used and of the distance from the nozzle where the sample was taken, they found that at lower gas velocities, and hence at lower values of $\sqrt{u'^2}$, an even distribution would result.

The study of Kesler (75) was somewhat more elaborate. This work also involved the measurement of the distribution of atomized sprays in turbulent air stream, and the results were expressed in terms of the dimensionless diffusion coefficient β , (defined as the ratio of the eddy diffusivity over the product of the pipe radius and the average air velocity). The experimental part of the study was carried out in a duct 5.76-in. in diameter and 44-ft. high, with air velocities ranging from 25 to 90 feet per second. Kesler found that alcohol and water sprays ranging from 14 to 30 microns in diameter had diffusion coefficients of 0.005 to 0.007, which is in apparent agreement with the data of Sherwood and Woertz (129) for the eddy diffusion of gases

in an air stream. The rate of evaporation of the alcohol droplets (25 microns in diameter and with an air velocity of 90 ft./sec.) proceeded as predicted for stagnant conditions, and from these results and the results on diffusion, Kesler concluded that the relative velocity between the droplets and the air stream was essentially zero. This means that the eddy diffusivities of the particles and turbulent gas are equal under the experimental conditions investigated.

The study of the evaporation rates of alcohol droplets carried out by Kesler was rather limited, and no data were taken on the evaporation of water droplets. Pinder (105) made an extensive study of the heat and mass transfer coefficients to water sprays in a concurrent spray dryer, and his results would indicate that the Nusselt number is equal to 0.476. This very low value is hard to explain theoretically, since an increase rather than a decrease of the heat transfer rates would be expected in turbulent gas streams. The only possible explanation would be the interfering effect of particles in close proximity, which is very unlikely because even very dense clouds in spray dryers are separated by about ten droplet diameters in all directions. Pinder probably obtained low evaporation rates because he used an external type pneumatic nozzle (Spraying Systems Co.), in an 8-in. diameter duct. The angle of spray from this type of nozzle is fairly large, and it is most likely that some of the droplets hit the dryer walls, with the resulting decrease in the total rate of evaporation.

In conclusion it can be said that there is a definite lack of reliable experimental data on the rate of heat and mass transfer to sprays in turbulent air streams. The work to date suggests that

evaporation of small particles, such as those encountered in spray drying, should proceed at the same rate as that of particles suspended or falling in stagnant gases. Such a behaviour would be expected from theoretical considerations in the field of heat and mass transfer as well as in the field of particle dynamics and the theory of turbulence, but further experimental verification of this is desirable.

3. EVAPORATION AND DRYING OF DROPS CONTAINING SOLIDS

The discussion in the previous two sections was restricted to heat and mass transfer considerations to pure liquid drops and to solid spheres. Although the complexity and extent of this field was amply demonstrated, a further variable must be taken into consideration in the case of spray drying.

The liquid atomized in a commercial spray dryer contains either dissolved or suspended solids, and even though this will not change the heat and mass transfer coefficients to the drops, it will change the rate of evaporation, and the added period of drying must be taken into account. The rate of evaporation and drying of solutions, slurries, and moist solids has been studied extensively, but few, if any, of these results are applicable to spray drying because of the size and motion of the droplets encountered in the latter case.

A liquid droplet containing suspended solids will evaporate at the same rate as if it were a pure liquid and its diameter will decrease

continually as a function of time. After most of the liquid is removed, however, a solid sphere will form which will remain constant in diameter for the remaining portion of the drying time. During this period, the rate of evaporation may decrease because the liquid on the surface of the sphere will not form a continuous film.

In the case of solutions there will be a lowering of the normal vapour pressure of the liquid because of the presence of the dissolved solids. The lowering of the vapour pressure will result in lower evaporation rates, even though the heat and mass transfer coefficients will remain the same, and it will probably be a function of the concentration of the solution. The work of Ranz and Marshall (107) would indicate, however, that the vapour pressure at the surface of the droplets will be that corresponding to a saturated solution.

Evaporation rates of solutions were determined by Ranz and Marshall by suspending droplets of the solution from a capillary, and maintaining the concentration constant by the addition of water at such a rate as to maintain the diameter constant. In particular, the evaporation rates of ammonium nitrate of 26, 46 and 50% concentration were measured, at a Reynolds Number of 66.6 and at about 29°C., the diameter of the droplet being 1.06 mm. The results suggested that the rate of evaporation was independent of the bulk concentration of the droplet, and corresponded to that of a saturated solution, about 61% solids at the temperature studied.

Although this study indicated very well the mechanism of evaporation under the given conditions, it is probably not applicable to

spray drying where the droplets are much smaller, and the Reynolds Number is probably close to zero. The droplets are also in free fall, and their diameter decreases with evaporation so that a comparison with a rigidly suspended drop, to which pure water is added continually, is difficult.

Some further evidence on the mechanism of evaporation and drying can be obtained from studies of the physical properties of the product, and their dependence on the operating conditions of the spray dryer (30). This work, as well as the work of Ranz and Marshall (107) on the heat of crystallization and solution is, however, only qualitative, and additional studies will have to be carried out before a clear picture of the whole operation can be obtained.

4. EFFECT OF HIGH EVAPORATION RATES ON THE HEAT TRANSFER COEFFICIENT

When the mass transfer rates are high, such as those that would be encountered at high air temperatures, the change in the temperature gradient in the gas film surrounding the drop will reduce the actual heat transfer coefficient to the drop surface. All the equations presented in this chapter so far refer to what might be called the apparent heat transfer coefficients, which must be corrected for the heat taken up by the vapour generated at the drop temperature if a true evaporation rate is desired. Marshall (91A) and others (44A)(106A)

(131A) have shown that the ratio of the actual Nusselt Number at the drop surface to the Nusselt Number at zero evaporation is given by the equation:

$$\text{Nu}/\text{Nu}_{E=0} = \left[E(1/R_1 - 1/R_2) \right] / \left[e^{E(1/R_1 - 1/R_2)} - 1 \right] \dots\dots(27A)$$

where E is defined by:

$$E = (dmC_{pV})/(4\pi kd\theta) \dots\dots\dots(28A)$$

In order to calculate therefore the actual rate of evaporation of a drop, equation (27A) must be used to obtain the actual Nusselt Number. This equation can be expanded in the form of a series, and if the higher powers are neglected, it can be shown that for spherical drops at zero relative velocity, that is when the apparent Nusselt Number is equal to 2, the following equation will be obtained:

$$h_{act} = h_{app} \lambda_w / \left[\lambda_w + C_{pV}(t - t_w) \right] \dots\dots\dots(29A)$$

From this it can be seen that for water drops at low air temperatures the correction will be small, but at high temperatures or for volatile liquids it may become appreciable.

B. EXPERIMENTAL SECTION

INTRODUCTION

The primary object of the experimental work covered in this investigation was to determine the rate of evaporation and drying of atomized liquids during spray drying. Since the rate of evaporation will be directly proportional to the heat and mass transfer coefficients to the droplets, the major portion of the investigation was devoted to the determination of these coefficients. Water was used in this part of the study for convenience, since the results can be easily extended to solutions and suspensions if suitable corrections are made.

The second part of the investigation was devoted to a study of the evaporation and drying of an actual solution. Lignosol - trade name of a commercial by-product of the pulp and paper industry recovered from waste sulphite liquors, and consisting essentially of calcium lignosulphonate - was selected for this investigation because of its colloidal nature, and because of the fact that it is spray dried commercially and readily available in this form.

To avoid the complex gas flow patterns commonly found in industrial spray dryers and commercially available pilot-scale units, a special drying chamber of the concurrent, vertically-downward type was designed and constructed. With a uniform air velocity distribution and little back-mixing, this type of chamber offered the great advantage of providing exact knowledge of the particle trajectory, and of permitting the measurement of the variables at various sections down the apparatus.

As is often the case in such experimental studies, the development of suitable methods of measurement for the various variables involved proved to be a major problem. To achieve the degree of accuracy desired, old techniques had to be specially adapted, and, in certain cases, new methods of determination had to be developed. The first chapter of the Experimental Section is therefore devoted to a description of these various methods of measurement.

The second chapter covers the experimental work on the heat and mass transfer coefficients to water sprays, while the third chapter deals with the rate of evaporation and drying of Lignosol solutions. A general discussion of the experimental results is also included.

I. METHODS OF MEASUREMENT

The accurate determination of the properties and variables of a liquid-gas or solid-gas system presents many difficulties, not the least of which is the sampling technique itself. In view of their obvious importance, considerable attention was devoted to these problems. More accurate methods of measuring the air temperature and air humidity were developed and adaptations for the determination of droplet or particle size, and for the measurement of their solid concentration, were worked out. Finally, in view of the complexity of the chemical structure of Lignosol and the lack of information concerning its characteristics, all the physical properties of Lignosol solutions, pertinent to the problem, had to be determined.

1. DETERMINATION OF AIR HUMIDITY

The air humidity has a direct bearing on the driving force during evaporation and drying of the droplets. Its accurate experimental determination is highly desirable in water-air contacting operations, since it permits the preparation of material and heat balances from which the heat losses - if any - can be calculated.

Apart from the doubtful accuracy of the wet and dry bulb method for the determination of air humidity under ordinary conditions (20), the method was not applicable here because it necessitates accurate determination of the air temperature, which is a variable in itself.

Other commonly available methods include the use of hair hygrometers or hair-type hygrometers employing white pine shavings (21), or nylon filaments (1), and methods based on the determination of the dew-point (118)(136). None of these methods are very accurate over a wide range of temperatures and humidities, and an attempt has been made during the past few years to utilize the change in electric properties of air with humidity as well as the change of electric properties of certain materials when in contact with humid air (23)(74) (151)(152). These methods are promising, but they require frequent and extensive calibration, and their degree of accuracy and reliability are presently limited.

Coldren and Comings (24) developed a special "Pneumatic Thermometer and Hygrometer" for use in spray dryers. This instrument consists of three orifices in series and a heater and cooler through which a sample of the air from the spray dryer is drawn. From the various readings the dry bulb temperature of the air as well as its humidity and liquid droplet content can be calculated. The large number of experimental steps and readings which are required introduce a strong possibility of error.

Gravimetric and volumetric methods offer the advantage of simplicity and good accuracy if suitable precautions are taken. They are based on the absorption or condensation of the water vapour in the air, and the weighing of this moisture or determination of the change in volume of the air. The gravimetric method requires a relatively large sample

of air, and since this was inconvenient in the present study, the volumetric method was selected.

a) Volumetric Method

Humidity determination by the volumetric method depends on the measurement of the decrease in volume of the air upon complete removal of the water vapor. The technique which was finally developed provided absorption of the latter by magnesium perchlorate, under constant temperature and pressure conditions.

i. Equipment

A photograph of the apparatus used in this study is shown in Figure 1, page 44. It consisted of a precision "mine-air" gas burette of 100-ml. capacity, made in three sections. The lower section, from 94 to 100 ml., was calibrated in 0.05-ml. subdivisions and afforded good accuracy in taking readings.

The burette was jacketed and a compensator tube, connected to the burette by means of a check valve and a levelling manometer, was also enclosed in the jacket. The air was passed from the burette through a U-tube containing magnesium perchlorate and into a mercury seal reservoir. The reservoir consisted of two chambers one above the other, and the air was forced into the lower chamber, displacing the mercury which was allowed to pass into the upper one. An electric contact was included in the reservoir so that the level of mercury in the lower chamber could be brought to the original point. The reservoir and U-tube were immersed in a constant temperature bath ($\pm 0.1^\circ\text{F.}$) and the water from this bath

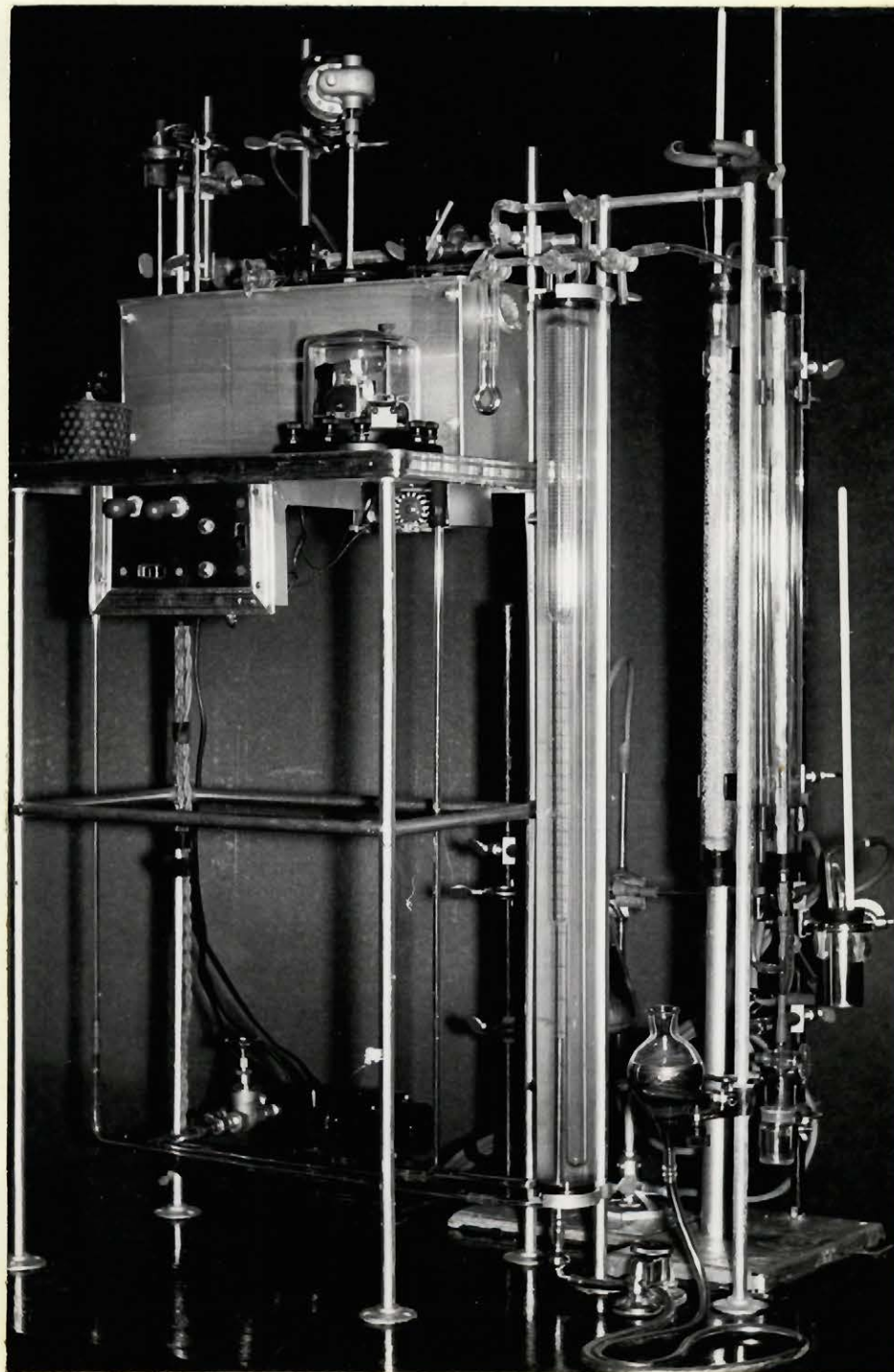


Fig. 1. Apparatus for the determination of air humidities

was also circulated through the above mentioned jacket by means of a midget centrifugal pump. The compensator tube and the use of a constant temperature bath avoided the necessity of pressure and temperature corrections.

Magnesium perchlorate was chosen as the drying agent because of the very low equilibrium water vapour pressure of this material (about 0.015 mm. of mercury at 25°C. at a water loading of 10%), and because of its high capacity. A ten-gram charge in the U-tube had a capacity of approximately one gram of water, and this is equivalent to the water content of about 500 samples of air, of 100-ml. each, under ordinary room conditions.

ii. Procedure and Calibration

The procedure consisted of first adjusting the pressure in the U-tube to that in the compensator tube, and bringing the mercury up to the point of electric contact in the reservoir. The air lying between the burette and the reservoir was thus dry and at the proper pressure. The next step was to draw a sample of air into the burette from a sampling bottle and adjusting the level of mercury in the burette so as to give a zero difference on the levelling manometer. After reading the volume of the humid air present, it was passed back and forth through the U-tube and into the reservoir until no further change in air volume was noted. When the final reading was taken, the conditions and quantity of the air between the burette and the reservoir was the same as those when the experiment was started, and consequently any change in volume

was due to the removal of water vapour. From the change in volume and the volume of the original sample, the humidity of the sample could be easily calculated.

The whole method depends on the assumption that the volume of the magnesium perchlorate will not change during a test. This assumption is undoubtedly justified, in view of the small amounts of water which are absorbed: for example, the water absorbed from a 100-ml. air sample with a humidity of 0.02 lb. water per lb. of dry air would only amount to 0.0024 gm. The validity of the assumption, and the accuracy of the method, were nevertheless tested as follows.

Samples of air of known humidity were prepared and analyzed according to the standard procedure. After careful consideration it was decided that the simplest way of preparing an air sample of a given humidity was to saturate the air at a known temperature. This was achieved by first passing the air through two bubblers and a packed column counter-currently to a stream of water, and then passing it slowly through glass wool in a water jacketed column. The temperature of the glass wool was maintained slightly lower than the temperature of the water, resulting in some condensation from the air. Entrained water mist was also separated in this column.

The results of the calibration are shown in Table I, page 47. Approximately three passes through the magnesium perchlorate U-tube were required before the volume of the sample remained constant. The results indicate the excellent accuracy of the volumetric method. The only disadvantage is the time required for an analysis - approximately

TABLE I

CALIBRATION OF AIR HUMIDITY APPARATUS

<u>H</u> mm. Hg.	<u>gl. wool t.</u> °C.	<u>pp. water</u> mm. Hg	<u>H calc.</u> lb.w./lb.d.a.	<u>H obs.</u> lb.w./lb.d.a.	<u>Deviation</u> lb.w./lb.d.a.	<u>Error</u> %
754.0	20.2	17.75	.0150	.0149	.0001	0.67
754.0	17.0	14.53	.0122	.0122	.0000	0.00
757.5	18.1	15.57	.0130	.0131	.0001	0.77
755.6	17.4	14.90	.0125	.0123	.0002	1.60
754.6	16.5	14.08	.0118	.0117	.0001	0.85

fifteen minutes - but the good accuracy and the simplicity of the apparatus more than compensate for this.

Further calibrations were carried out on this apparatus at a later date by Manning (90), who prepared dry air samples from cylinders of oxygen and nitrogen, to a known volume of which a carefully weighed amount of water was added. About thirty tests were carried out, with humidities ranging from 0.0050 to 0.0300 lb.water/lb.dry air. The results of this work confirmed the excellent accuracy of the method, the maximum error in the range investigated being 0.0004 lb.water/lb. dry air. Other drying agents than magnesium perchlorate were investigated, particularly "molecular sieves", manufactured by the Linde Air Products Company. The disadvantage of most of these materials was either the high equilibrium water vapour pressure or, as in the case of molecular sieves, their tendency to adsorb or absorb certain other gases such as carbon dioxide.

b) Sample Collection

As shall be more fully described in a later section, operation of the experimental spray dryer required the sampling of air at various locations during each run, and the determination of its humidity by the above method. The sample had to be collected in such a manner as to give a representative value of the true air humidity, and the droplets dispersed in the air had to be separated without any further evaporation or drying. Because of the latter restriction, conventional separators such as cyclones could not be used, and a special sampling device was developed.

A drawing of the sampler is shown in Figure 2B, page 50. Samples of air were drawn countercurrently to the direction of the main air flow, the superficial velocity in the first part of the sampler being below the average terminal velocity of the droplets. The air was drawn into an evacuated sampling bottle, its velocity being controlled by means of a glass orifice; an aluminium cup was attached to the sampler in order to prevent the liquid that collected on it from running inside. The efficiency of separation could be noted from the fact that when a solution was spray dried, no solid particles were found inside the sampling bottle.

2. MEASUREMENT OF AIR TEMPERATURE

The temperature of the air was one of the most important variables, and considerable attention was paid to this problem. Although the determination of the temperature of dry gases is usually quite simple, the difficulty in the case under consideration arose from the fact that the temperature measuring instrument had to be shielded from the liquid spray, which was at a substantially lower temperature than the air.

The use of thermocouples was investigated thoroughly, but satisfactory results could not be obtained. Although the tip of the thermocouples, which were usually made of copper-constantan, was protected by a curved shield, and the leads enclosed in glass tubing, conduction losses along the leads made accurate determinations impossible. It was noted that the glass tubing was completely covered with liquid due to spray impingement, and although some improvement resulted when the leads were

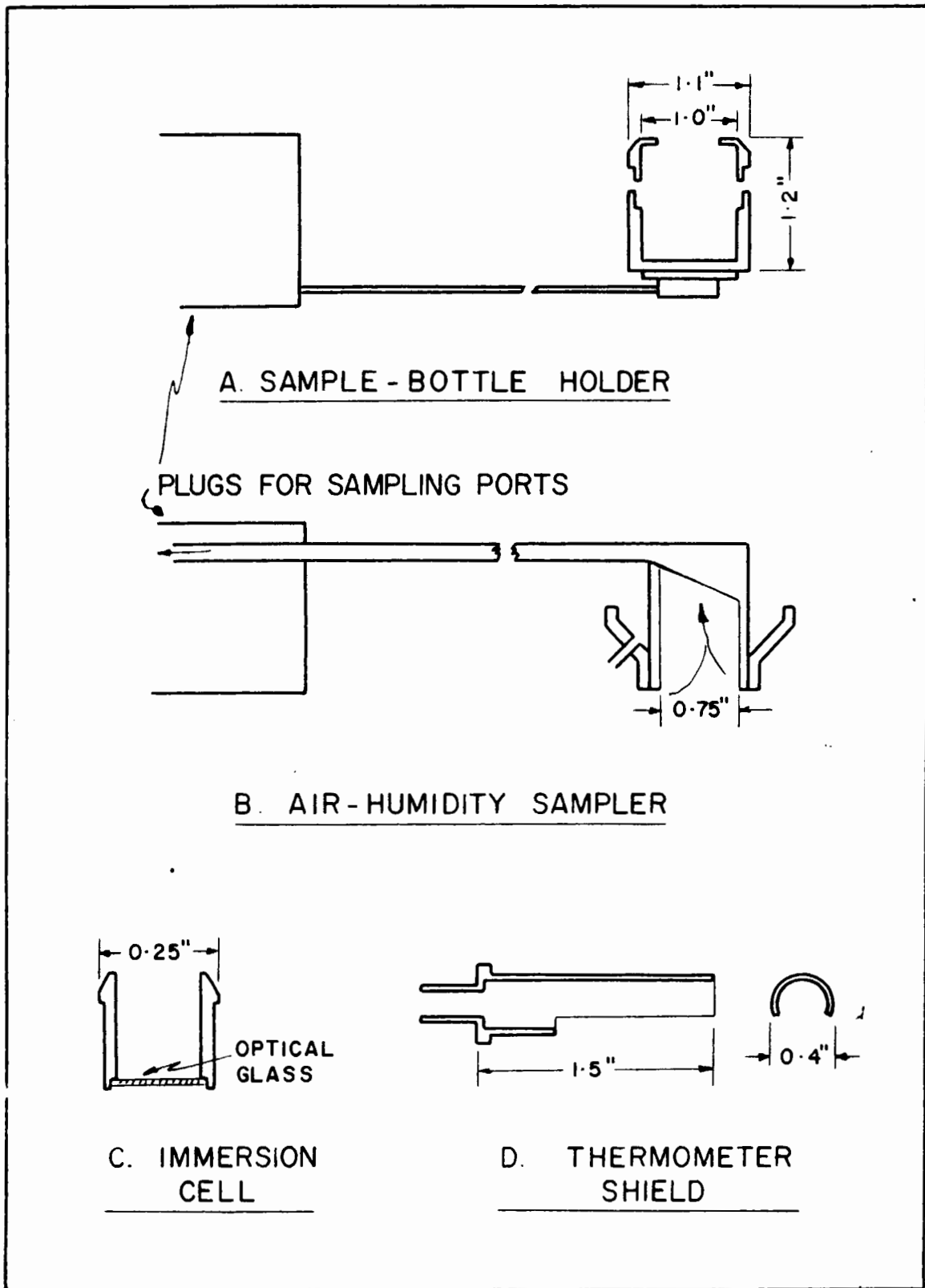


Fig. 2. Sampling Devices and the Thermometer Shield

properly insulated, reproducible results were hard to obtain and it was almost impossible to calculate the necessary temperature corrections because of the many factors involved.

Mercury thermometers were therefore used, even though they were less convenient from the operating point of view. At lower air temperatures a precision thermometer was employed, the scale being from 0 to 100°C. with 0.1°C. subdivisions. At high air temperatures a standard mercury thermometer was used (0 to 300°C., in 1°C. divisions). The whole thermometer was enclosed in a glass tube of a slightly larger diameter, with only the bulb protruding. An aluminium shield, shown in Figure 2D, page 50, was fixed to the end of the glass tube in order to protect the thermometer bulb, the purpose of the glass tube being the insulation of the thermometer stem from the cold spray.

The calculation of the necessary temperature correction was again impossible, but the following analysis could be made: the thermometer was losing heat by conduction through the stem to the outside as well as through an air gap and the walls of the insulating tube to the cold spray, and gaining heat by convection from the hot air in the dryer. The conduction loss was undoubtedly very small because of the very low thermal conductivity of glass, but the additional loss due to spray impingement on the thermometer bulb had to be considered.

The results of the heat and material balances on the spray dryer

indicated, however, that the temperature as obtained from the thermometer reading was very close to the correct temperature of the air. It was also noted that during tests carried out with Lignosol sprays only a few dried particles of the material were stuck to the thermometer bulb, indicating the efficiency of the shield.

3. PARTICLE SIZE DETERMINATION

The problem of particle size determination has applications in a wide variety of fields, and it has consequently received considerable attention (9)(10)(17)(27)(33)(36)(46)(57)(77)(131). Most of the proposed methods have been developed for solid particles, and are not readily adaptable to liquid droplets unless the droplets are first frozen as suggested by Taylor and Harmon (144). Photometric, photographic, electronic and microscopic methods are, however, suitable for solid as well as liquid particles.

Tolman and Gerke (146) reported that the intensity of a Tyndall Beam is closely proportional to the reciprocal of the particle diameter, and although this method has been used by other workers (122)(123)(132), it has the disadvantage of giving the average diameter rather than the particle size distribution which is required in spray drying studies. Photography of particles in flight can also be used (62)(137)(153), but focussing and lighting problems make this method difficult.

Geist (43) and Guyton (48) made use of the fact that particles in flight have an electrostatic charge which is a function of the particle diameter. Thin wire probes were used to intercept the particles, and this method is apparently susceptible of great accuracy because of the small disturbance of the air flow due to the probe and because of the amplification possible in an electronic circuit. This circuit is, however, complex.

Microscopic methods are the most common for the determination of particle size distributions in spray studies. Basically, the method consists of collecting a representative sample of the spray and observing or photographing the droplets through a microscope in order to make a particle count. Simplicity and accuracy are its main advantages, and the microscopic method was consequently selected for this study.

a) Sample Collection

It is obvious that the selection of the proper sampling technique prior to a microscopic count is of utmost importance in spray studies, because of the wide size distribution of the droplets. Because of the physical dimensions of the collecting device, there was always the danger that some of the smaller droplets will be deflected and that only the larger droplets will be included in the sample. The interception efficiency curves presented by Langmuir and Blodgett (103) clearly indicate the importance of using a collecting device of small size and of the proper shape.

The simplest method of collection consists of coating a slide with oil or grease and inserting it into the spray (98). Although the droplets thus collected are not spherical, the correct diameter can be determined from the angle of contact of the drop with the slide or from the focal length of the drop (60)(84)(94). The main drawbacks of this method are the danger of droplet evaporation before a photograph of the slide can be taken through a microscope - although this can be reduced by refrigeration of the slide - and the large size of the device, which results in poor target efficiency.

To minimize the problem of evaporation, coating of the slide with soot or magnesium oxide was proposed: the droplets penetrate the surface of the coating, leaving holes which can be related to the drop size (96)(108). Stoker (140) has shown that the relation between the apparent and true droplet diameter obtained by this technique is probably a function of the Weber Number ($d\rho v^2/\sigma_c$), and extensive calibration would be necessary before this method could be applied to the problem under consideration.

Another method designed to avoid evaporation is to collect the droplets under a liquid in an immersion cell. This technique was used by De Juhasz (28) and investigated in considerable detail by Rupe (121) who collected the droplets in a small cell containing Stoddard solvent. The bottom of the cell was made of optical glass which was coated with a suitable agent so that the droplets remained spherical, under which conditions Rupe showed that the error due to wetting was negligibly small.

Because of its obvious advantages, this method was selected in the present study.

The final design of the immersion cell which was found to give the best results is shown in Figure 2C, page 50. The cell was made out of aluminium, its outside diameter being 0.25 in. at the top and 0.22 in. at the bottom, while its inside diameter was 0.18 in. throughout. A circular piece of optical glass was glued into the bottom of the cell by means of Sauereisen cement, and the surface of the glass was coated with General Electric SC-87 "Dri-Film", which is strongly water repellent. The liquid used in the cell was Varsol, which is very similar to the Stoddard solvent used by Rupe.

To obtain a sample of the spray in the experimental chamber, the cell was placed into a small ring holder, 0.25 in. outside diameter and 0.23 in. inside diameter, which was attached to a 1/16 in. diameter aluminium rod. A few drops of Varsol were placed in the cell and the whole assembly was introduced into the dryer for a fraction of a second. The cell was then removed from its holder, placed on a microscope stage, and covered with a piece of optical glass after being completely filled with Varsol in order to avoid any error because of the liquid meniscus.

In order to obtain a representative sample of the spray in the dryer, a traverse was made with the cell. Since there was no danger of evaporation, the only possible sampling errors could be ascribed to the deflection of some of the small droplets by the cell, and to the coalescence of the droplets once they entered the cell. The problem

of coalescence was minimized by exposing the cell to the spray for only a very short period of time, so that the droplets collected were sufficiently far apart. The very low surface tension between water and Varsol also reduced the tendency to coalesce, and it was noted that sometimes one drop was sitting on three other drops forming a pyramid, with no coalescence taking place.

The problem of small particle deflection was more serious, but it was noted that very often particles of 1-micron diameter were collected, although all of these should have been deflected according to the curves of Langmuir and Blodgett (103) under the given operating conditions. (At an air velocity of 3.9 ft./sec. all droplets below fourteen microns in diameter should have been deflected, while at 14.8 ft./sec. this upper limit is about six and a half microns). The estimation of the target efficiency was based on the Langmuir and Blodgett curve for cylinders, and it is quite possible that the cup-like shape of the cell permitted higher collection recoveries. It should be emphasized, however, that smaller particles are of little importance in spray drying studies, as far as heat and mass transfer considerations are concerned, because they account for only a negligible fraction of the total mass of the spray. The final results of this study, - as will be shown later - have amply demonstrated that the error in sampling was very small indeed.

b) Particle Counting

In order to save time during the actual tests on the spray dryer, the sample of the spray was first photographed through a microscope,

immediately upon collection. A Bausch and Lomb microscope with a 16-mm. focal length objective and a 12.5X eyepiece was used. Use of such a low-powered objective was necessary because the depth of focus, which is inversely proportional to the numerical aperture and the magnification, had to be high when photographs were taken. Had a direct count been made, it would have been possible to refocus the microscope for each particle size and a higher magnification would have been possible.

Using visible light, the resolution of a microscope is 0.2 micron and this was more than sufficient under the given conditions. A single-lens Asahiflex reflex camera was used for taking the photographs on a 35-mm. Adox KB-14 film. This slow-speed film (16 ASA) has a resolution of 141 lines per millimeter, and since the magnification was 54.3X this corresponded to a particle resolution of 0.131 micron. The film was processed by Mitchell Photo Supply Ltd., in Montreal, who used a fine-grain developer and printed the photographs on high contrast paper.

Fine focussing was possible due to the ground-glass screen of the camera. A 200-watt microscope lamp provided the necessary parallel transmitted light, and exposures of 1/25th of a second were generally sufficient. The magnification was determined by taking photographs of a microscope stage micrometer which was calibrated in 10 and 100-micron divisions.

Several automatic counting devices have been developed recently, to avoid the tedious and slow manual procedures (2)(54)(58)(120)(121)(149). These methods are more accurate than manual methods, but the

necessary equipment is by no means simple. In the case under consideration the particle count was performed by observing the photograph prints through a low powered microscope (43X, giving an overall magnification of 2,335X) which was equipped with a micrometer eyepiece. Since all the droplets and solid particles encountered in the investigation were spherical in shape (except in one case where a count was not performed), estimates of the drop diameter presented no problem. Approximately 150 to 300 particles were measured in each sample, from which count the particle size distribution and the mean statistical diameters were computed. Regarding the former, selection of the size group was based on the average particle size. Thus, since one division on the micrometer eyepiece corresponded to 1.19 micron, size groups of 2.38 microns were used for average diameters below 30 microns, while for average diameters above this value size groups of 5.95 microns were used.

4. DETERMINATION OF SOLID CONCENTRATION

Most of the necessary information concerning drying rates and governing mechanisms of drying can be obtained from a knowledge of the change in the moisture content of the solid with time. It was therefore highly desirable to develop an accurate method for the measurement of the solid concentration of the particles as they progressively dried in the chamber.

Lignosol is a heat sensitive material (85)(154) and it begins to decompose slowly at temperatures as low as 80°C. The conventional method for the determination of moisture content by oven drying could not therefore be used. Furthermore, only a small sample of the material could be collected in the spray dryer and it had to be obtained in such a way as to avoid any further evaporation once the sample was taken. The possibility of using the Karl Fisher reagent for moisture determination was examined, but the unsaturated bonds present in the chemical structure of Lignosol would have necessitated additional extraction and filtration steps, since unsaturated bonds react with the iodine of the Fisher reagent. This method was therefore rejected.

Solutions of Lignosol have a pale yellow colour at low concentrations (of the order of 0.1% solids) and a colorimetric method obviously suggested itself. Preliminary studies soon showed that it possessed the required degree of sensitivity and it was therefore adopted for the determination of solid concentrations.

a) Sample Collection

Samples of the spray were collected in small weighing bottles at successive locations in the spray dryer during each test. To prevent further evaporation and drying of the droplets following collection, the bottles were filled with Dow Corning Silicone Fluid No. 200. This is a low viscosity (3 centistokes at 25°C.) material, immiscible with water and Lignosol solutions. Since its vapour pressure is extremely low (0.5 mm. Hg. in the range 70-100°C.), none of the silicone fluid was lost

by evaporation during collection of the sample. If therefore the weight of the weighing bottles containing the silicone fluid was determined on a semi-micro analytical balance before and after a sample was taken, the net weight of the wet sample was simply obtained by difference.

The outside of the weighing bottle was protected from the spray by means of an aluminium holder, a drawing of which is shown in Figure 2A, page 50. A period of from one to three minutes was required for sampling, depending on the concentration of the spray. Once again every effort was made to obtain a representative sample. Possible coalescence of the droplets was no longer an undesirable feature. On the other hand, some of the smaller particles were undoubtedly deflected away from the collecting device, but as in the previous case, their loss represented such a small fraction of the total mass of the spray that it could be neglected without introducing any appreciable error.

b) Analysis for Concentration

The samples of Lignosol collected by the above procedure ranged from 25 to 150 milligrams, and their concentration varied from 20 to 100% solids. Since the colorimeter was effective only in the range from 0 to 0.25% Lignosol, the samples were first diluted in volumetric flasks to approximately 0.1%, using distilled water. Most of the silicone fluid separated and floated to the top of the solution, but because of the diluting procedure some of it became dispersed in the solution. Since this interfered with the colorimeter readings, the solution was first filtered to coalesce the dispersed silicone droplets.

A Fisher Neffluoro-Photometer was used in the colorimetric work, with an incandescent light source and a 425-millimicron filter, which is in the preferred absorption band for lignin, one of the main constituents of Lignosol. The Fisher instrument had both a measuring and a reference phototube, and it was adjusted to zero light absorption for distilled water which was used as a standard in all readings.

The instrument was calibrated by means of standard solutions, carefully prepared in the laboratory from Lignosol of almost zero moisture content obtained by drying to constant weight in a vacuum desiccator for approximately one week. The calibration curves are given in Figure 3, page 62. As expected from the Beer-Lambert Law, a straight line relationship was obtained between the logarithm of the light absorption and the Lignosol concentration. It is observed that, in the range from 0 to 2.2 mg. Lignosol per millilitre, two curves are given: the lower one represents the behaviour with no silicone added, while the upper one refers to calibrating solutions prepared according to exactly the same procedure as that used for the determination on the actual samples. No reasonable explanation can be offered for the higher absorption in the case of solutions of low concentrations prepared from weighed amounts of Lignosol in the presence of silicone, diluted and subsequently filtered. By diluting the samples to give a final solution concentration between 0.5 and 1.5 mg./ml. (in other words, using the upper calibration curve), the analytical results were found to be perfectly reproducible and completely independent of the relative amount of silicone added to the sampling bottle. All samples - once diluted - were analyzed immediately, as fungus growth was observed to occur after six hours or more of standing.

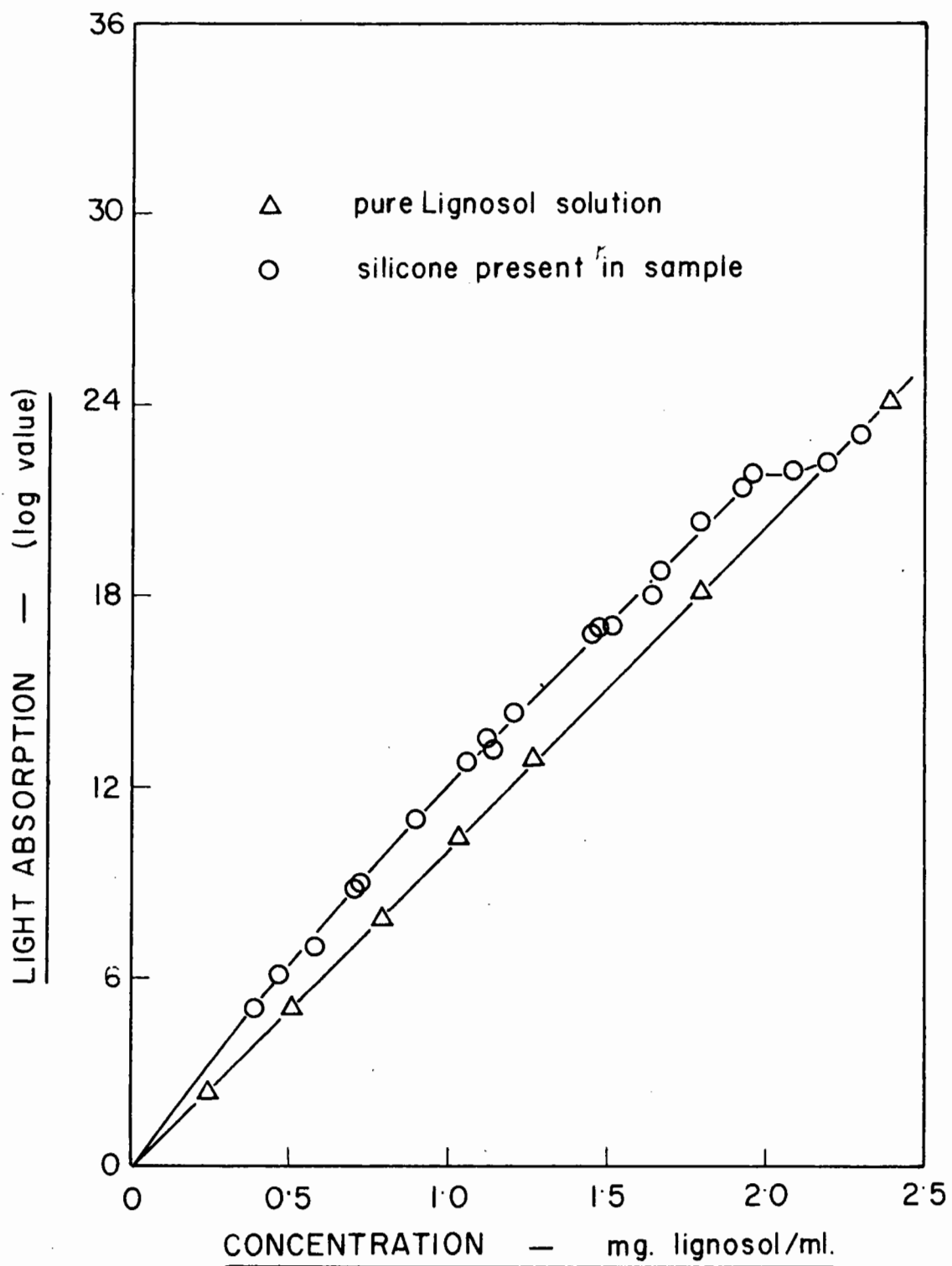


Fig. 3. Calibration Curve for the Fisher Neffluoro-Photometer

5. PHYSICAL PROPERTIES OF LIGNOSOL SOLUTIONS

In order to analyze the operation of the spray dryer, certain pertinent basic properties of Lignosol solutions were required. These included the density, heat of solution, specific heat and vapour pressure.

a) Density

The densities of solutions containing 26.1, 49.9, 60.5 and 99.0% Lignosol were determined at room temperature. For the liquid solutions a standard 25-ml. pycnometer was used, while for the solid particles (99.0% spray dried material) the absolute density was determined in a pycnometer using varsol to find the absolute volume of the weighed sample.

The following straight line relationship was found between the density and concentration:

$$\rho_s = 1.0 + 0.4c \dots\dots\dots(27)$$

where ρ_s is the density in gm./ml.*

The variation of density with temperature was found to be so small that equation (27) could be used in the range 20 to 50°C. without appreciable error. This temperature range was sufficient in the case under consideration.

* The list of symbols for this chapter will be found on page 153. All symbols are consistent unless otherwise defined in the text.

b) Heat of Solution

Lignosol does not crystallize when it is spray-dried, hence the heat of crystallization was not involved in the falling-rate period of drying. However, the possibility of the existence of a heat of solution required consideration.

The enthalpy of a solution may be expressed by the following equation, on the basis of one pound of solid:

$$h' = \Delta h' + h'_1 + Xh'_2 \dots\dots\dots(28)$$

where h' - enthalpy of the solution, (B.t.u.)/(lb. solid);

$\Delta h'$ - heat of solution, (B.t.u.)/(lb.);

h'_1 - enthalpy of the solid, (B.t.u.)/(lb.);

h'_2 - enthalpy of water, (B.t.u.)/(lb.);

X - concentration, (lb. water)/(lb. solid).

The enthalpies h'_1 and h'_2 are functions of the temperature only. The heat of solution h' is a function of the concentration of the solution as well as of the temperature.

The heat of solution of Lignosol was investigated experimentally by slowly adding 8 gm. of the solid to 25 ml. of distilled water in a well insulated beaker. Both materials were at exactly 25°C. before mixing, and the water in the beaker was stirred by means of a magnetic stirrer. Since no change in the temperature of the solution could be observed with a precision thermometer, it was concluded that the heat of solution

was negligibly small.

c) Specific Heat

Equation (28) indicates that in the absence of any heat of solution, the enthalpy of a solution can be calculated from the temperature level and the specific heats of the two components.

Because it is more convenient to determine the specific heat of a liquid than of a powdered solid, the specific heat of a 26.1% Lignosol solution was carefully determined experimentally, from which the specific heat of the dry material was then calculated.

A Dewar flask was used, the water equivalent weight of which was first determined experimentally to be 4.0 gm. A known quantity of water (app. 100 gm.) was then heated up to about 100°F. and introduced into the flask. The temperature of this water was measured accurately with a mercury thermometer (0.1°F. subdivisions) and a known quantity of the Lignosol solution, at approximately room temperature, was added, its temperature being also measured to the same degree of accuracy. From the final temperature of the mixture, the specific heat of the Lignosol solution could be easily determined.

From the results of five trials under slightly different conditions (the ratio of water to Lignosol solution ranging from 0.5 to 2.0 and the temperatures ranging from 75 to 105°F.) specific heats of $0.84 \pm 0.3\%$ for the 26.1% solution and 0.39 for the dry solid were found, which can be taken as the average value in the temperature range 75 to 105°F.

d) Vapour Pressure

At low concentrations, Lignosol forms a colloidal solution with water, and the vapour pressure of the solution is equal to that of pure water at the same temperature. At higher concentrations, however, a departure from colloidal behaviour occurs with a resulting decrease in the vapour pressure which must be determined experimentally.

i. Equipment and Procedure

The vapour pressure was determined by the dew-point method (44). The apparatus consisted of a chromium-plated tube inserted into a beaker through a rubber stopper, as shown on the photograph in Figure 4, page 67. Thermometers were placed in both the tube and the beaker. The latter was submerged in a constant temperature water bath and maintained within 0.1°F. of the desired temperature. Another constant temperature bath supplied the water that was circulated through the chromium-plated tube by means of a small gear pump, and a cooling coil was inserted into this bath.

Solutions of Lignosol of known concentrations were added to the beaker, and the temperature of the solution was brought to the desired level. When equilibrium conditions were established, that is when the temperature of the vapour space in the beaker was the same as that of the liquid, circulation of the water through the dew-point tube was started. The temperature of the circulating water was at first slightly above the expected dew-point, but was then slowly decreased until the first traces of dew were observed on the chromium plating, at which point all temperatures were noted. The

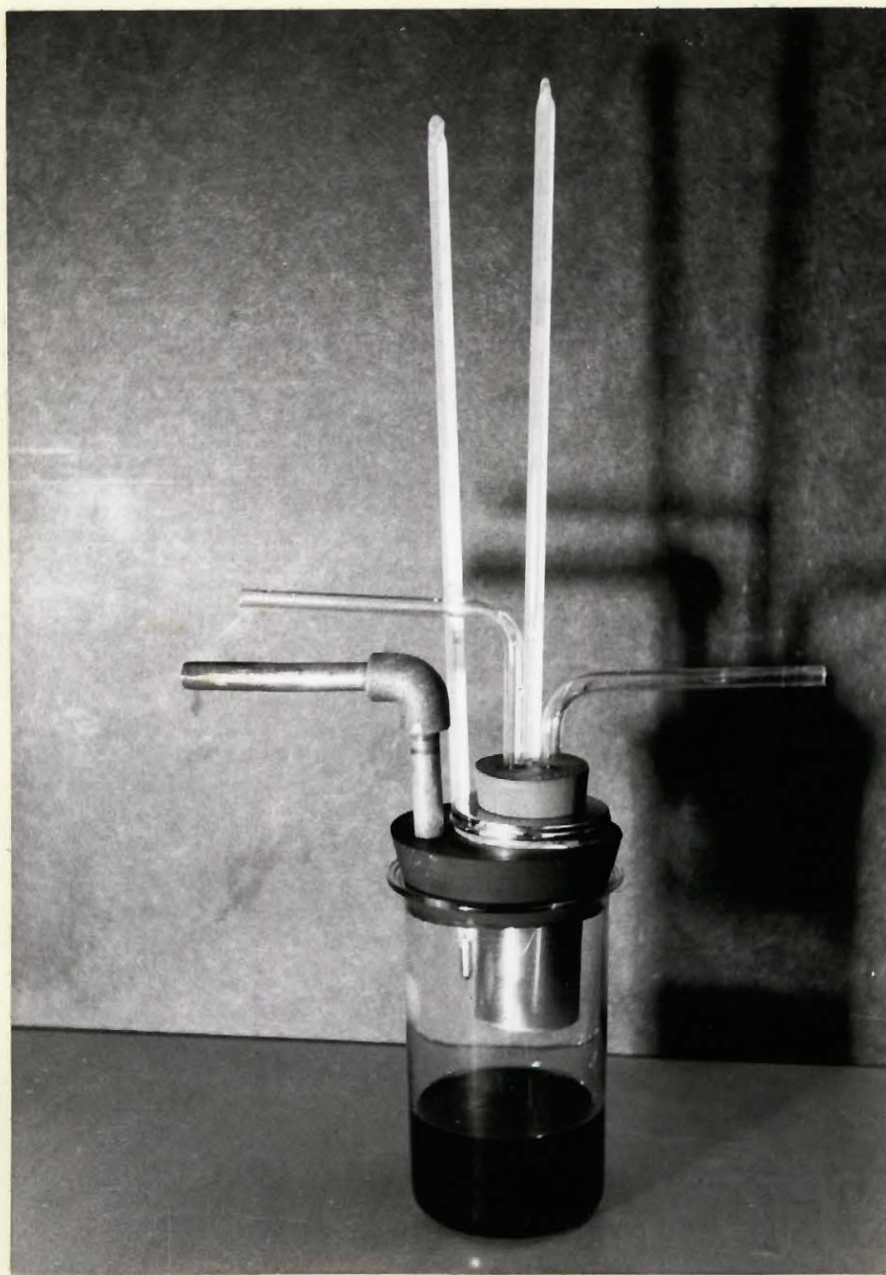


Fig. 4. Dew-Point Apparatus

circulating water was then slowly heated until the dew disappeared, when the temperatures were again noted. The rate of heating and cooling was adjusted so that the difference in temperature between the point when the dew was first observed and that when it disappeared was not more than 0.5°C . From the average temperature the dew-point of the vapour was calculated, and hence the equilibrium humidity of the solution determined.

The accuracy of this method depends largely on the determination of the exact instant when the fogging of the chromium-plated tube first occurs. In order to facilitate the observation of this point, the apparatus was lighted with a standard desk lamp and a low-powered telescope was installed at approximately sixty degrees, in the horizontal plane, to the light. It was noted that the fogging first took place in small patches, probably more active centers on the chromium plating. The appearance and disappearance of these patches of dew was very sudden and no difficulty was encountered in determining the exact temperature at this point. Several readings were taken under each set of conditions, and the results were averaged. Calibration tests with distilled water indicated that the accuracy in determining the dew-point was within 0.1°C .

ii. Results

Solutions containing 20, 40, 60, 80 and 90% Lignosol were prepared. Lignosol is extremely soluble in water, even though the solutions containing 80 and 90% solids are very viscous and do not flow at room temperature. No difficulty was encountered in preparing solutions of up to 60% in

concentration, but the 80% solution had to be prepared at about 60°C. while the 90% solution was obtained by evaporation.

The dew-points of these solutions were determined at various temperatures and the vapour pressure data, with the corresponding saturated air humidities, are shown in Table II, page 70. A graph of the variation in water vapour pressure with temperature is shown in Figure 5, page 71.

From Table II and from Figure 5, the saturation humidities of Lignosol solutions up to 20% in concentration are observed to be the same as those of pure water. A definite lowering of the water vapour pressure is noticed at higher concentrations, but there was no sharp break that would indicate a limit in the solubility of Lignosol in water.

TABLE IISATURATION HUMIDITIES OF LIGNOSOL SOLUTIONS

<u>Concentration</u> wt. %	<u>Temperature</u> t. °F.	<u>Dew Point</u> °F.	<u>Humidity</u> lb.w./lb.d.a.
20	100.0	99.9	0.0431
	120.0	120.0	0.0815
	130.0	129.8	0.1110
	140.0	139.9	0.1529
40	86.0	84.6	0.0261
	105.2	103.8	0.0488
	120.7	118.4	0.0775
	139.5	135.5	0.1429
60	86.0	82.6	0.0244
	103.1	99.1	0.0420
	120.7	115.4	0.0705
	141.0	135.7	0.1337
80	86.5	79.7	0.0221
	102.9	93.0	0.0344
	120.4	109.2	0.0580
	138.4	124.4	0.0936
90	86.7	75.9	0.0184
	104.4	85.5	0.0269
	120.6	100.5	0.0439
	139.3	113.0	0.0654

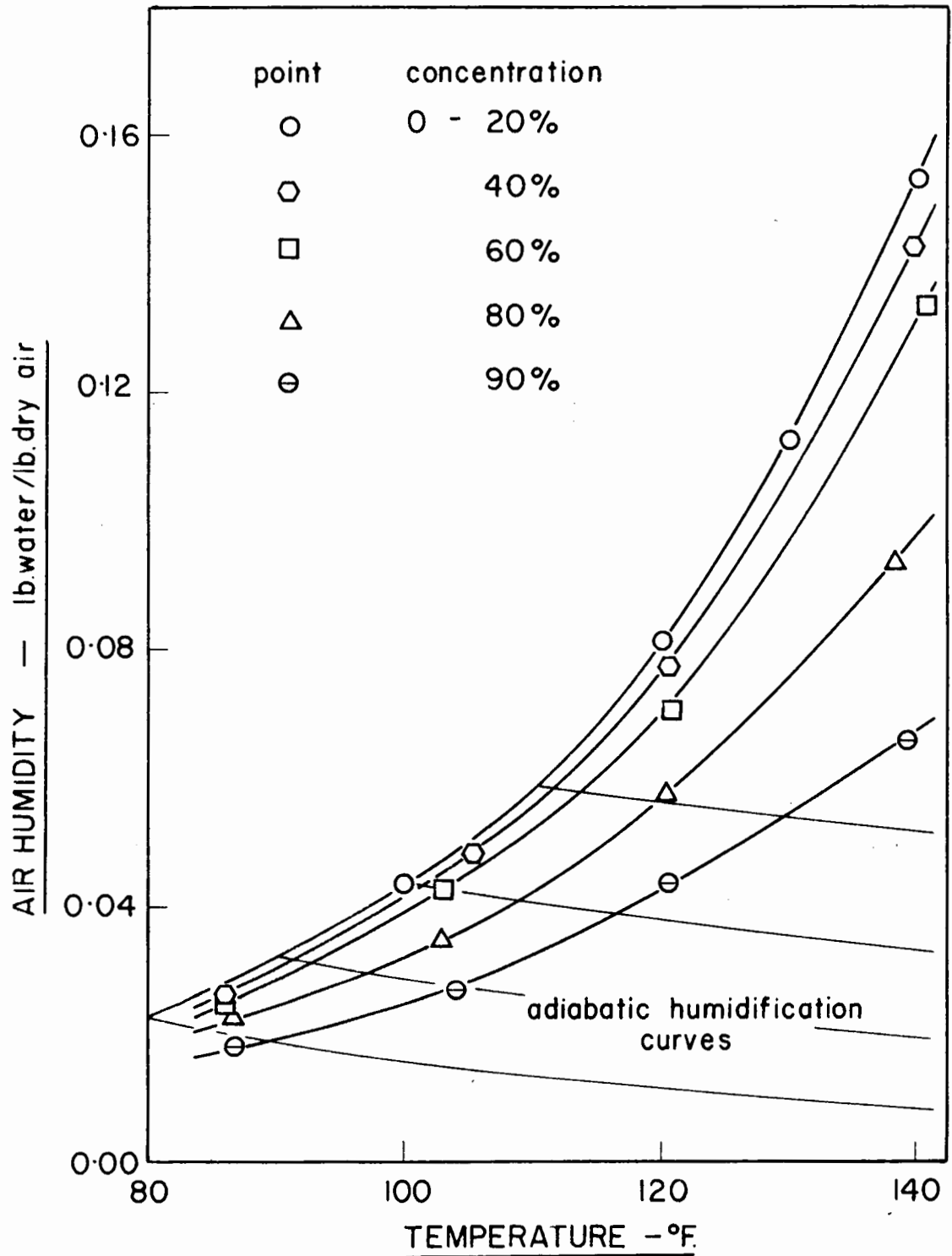


Fig. 5. Saturation Humidities of Lignosol Solutions

II. HEAT AND MASS TRANSFER COEFFICIENTS

As shown in the Historical Review, most of the previous studies on heat and mass transfer from liquid drops to air have been carried out on single stationary spheres with diameters of the order of one millimeter or more. In spray drying, on the other hand, the droplets range in size from 200 microns down, and they are, moreover, dispersed in a turbulent air stream and transported with it. Experimental studies in a system of this type have been limited, owing principally to the complexity of the air flow patterns and particle trajectories that are encountered in conventional spray dryers, with the accompanying difficulties in determining the rate of evaporation of the droplets. The concurrent spray dryer designed in the present study provided complete control over the particle trajectory, once passed the nozzle zone, which in turn permitted the measurement of the droplet evaporation as it proceeded down the drying chamber, as well as the measurement of the corresponding droplet size, air temperature and air humidity. It was thus possible to calculate the local heat and mass transfer coefficients throughout the chamber.

1. EQUIPMENT

The experimental spray dryer consisted of the same basic units as an industrial installation except that no device for product collection was provided. A photograph of the apparatus is given in Figure 6, page 73,

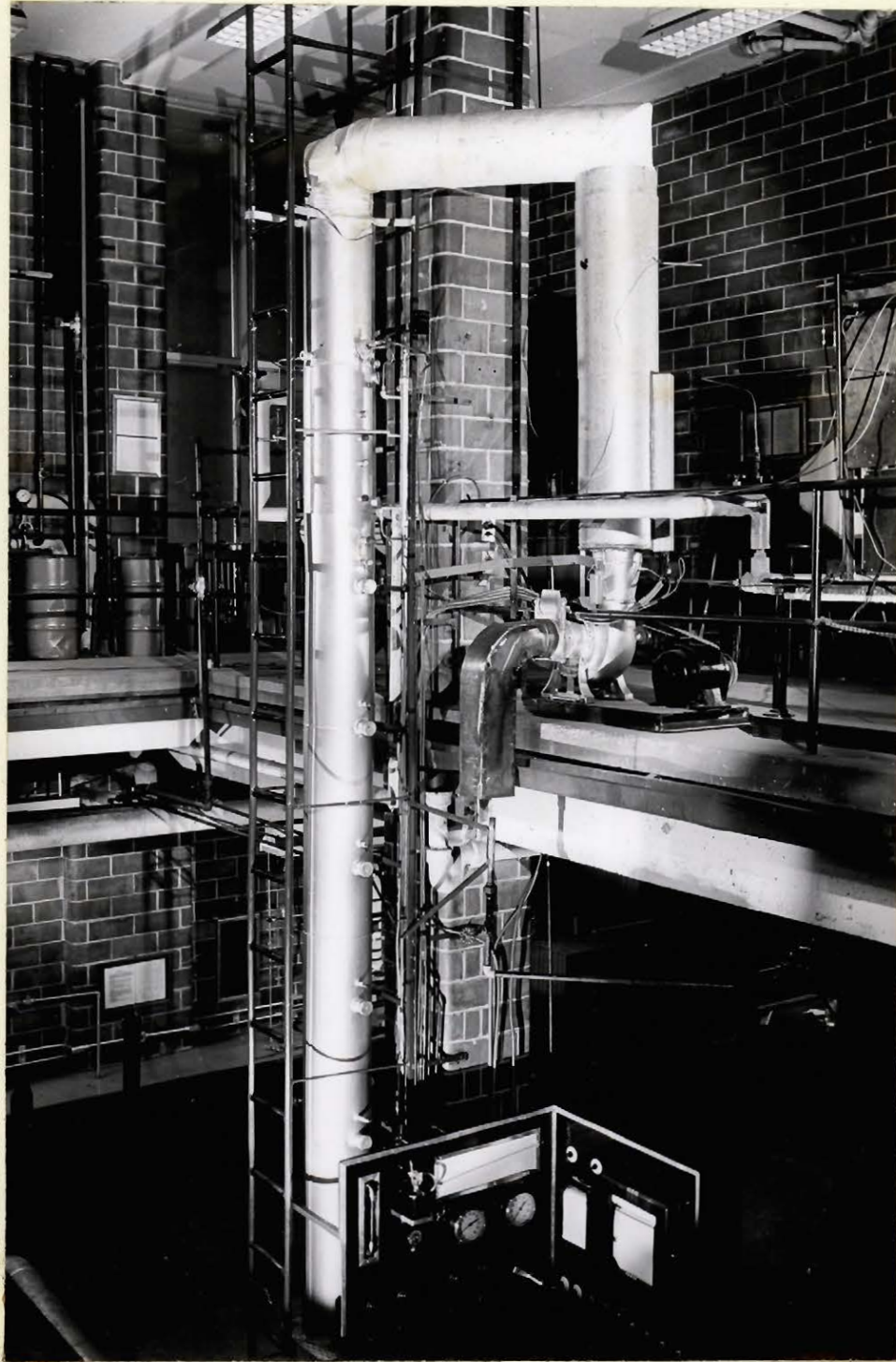


Fig. 6. Spray Drying Apparatus

showing the air blower and heater section on the right and the drying chamber on the left. A schematic drawing of the apparatus is also given in Figure 7, page 75. In order to facilitate the operation of the equipment, all the various controls and instruments necessary were accommodated on a central control panel which is shown in Figure 8, page 76. The left hand side of the panel included the controls for the atomizer, and the feed and air supply to the dryer, while the right hand side carried all the electrical instruments and recorders. The photograph also shows the arrangement for taking photomicrographs and the Fisher Neffluoro-Photometer, mentioned in the previous section.

a) Air Supply

The drying air was supplied by a fifteen-inch, No. 22, Canadian Blower and Forge Co. blower, V-belt driven at approximately 3000 r.p.m. by a 1-H.P. Electric Tamper motor. The air flow was controlled by means of a 6-in. slide valve located at the blower inlet, the valve being operated from the central control panel (Figure 8). A 4-in. diameter orifice was installed above the blower to meter the air flow, and its pressure taps were connected to an inclined manometer with a slope of 1:10, mounted on the panel. Because of its close proximity to the blower and to other sources of disturbance in the line, this orifice was calibrated by means of a standard 4-in. orifice which was temporarily installed at the end of the drying chamber. The calibration curve is shown in Figure 9, page 77.

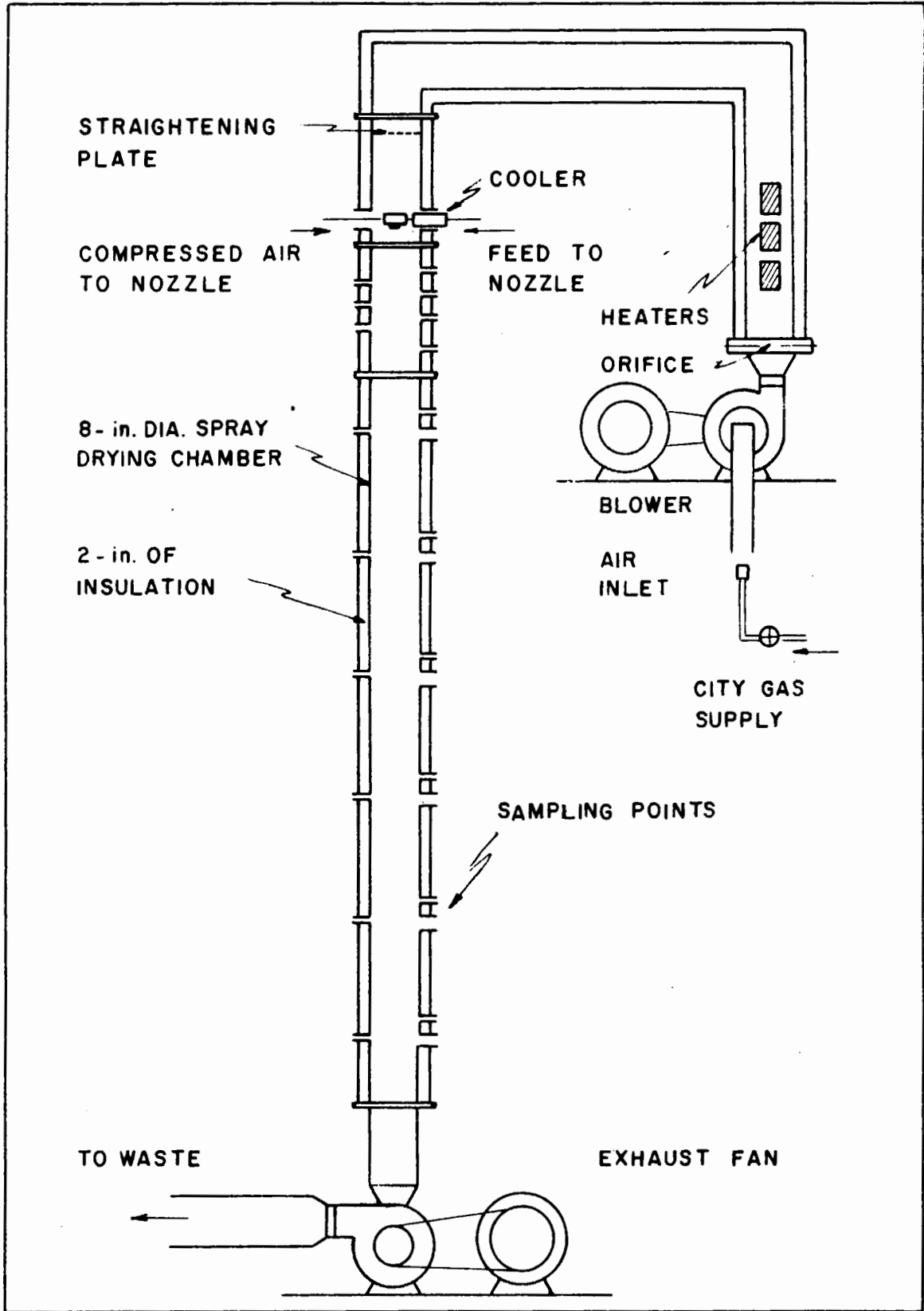


Fig. 7. Schematic Arrangement of the Spray Drying Apparatus.

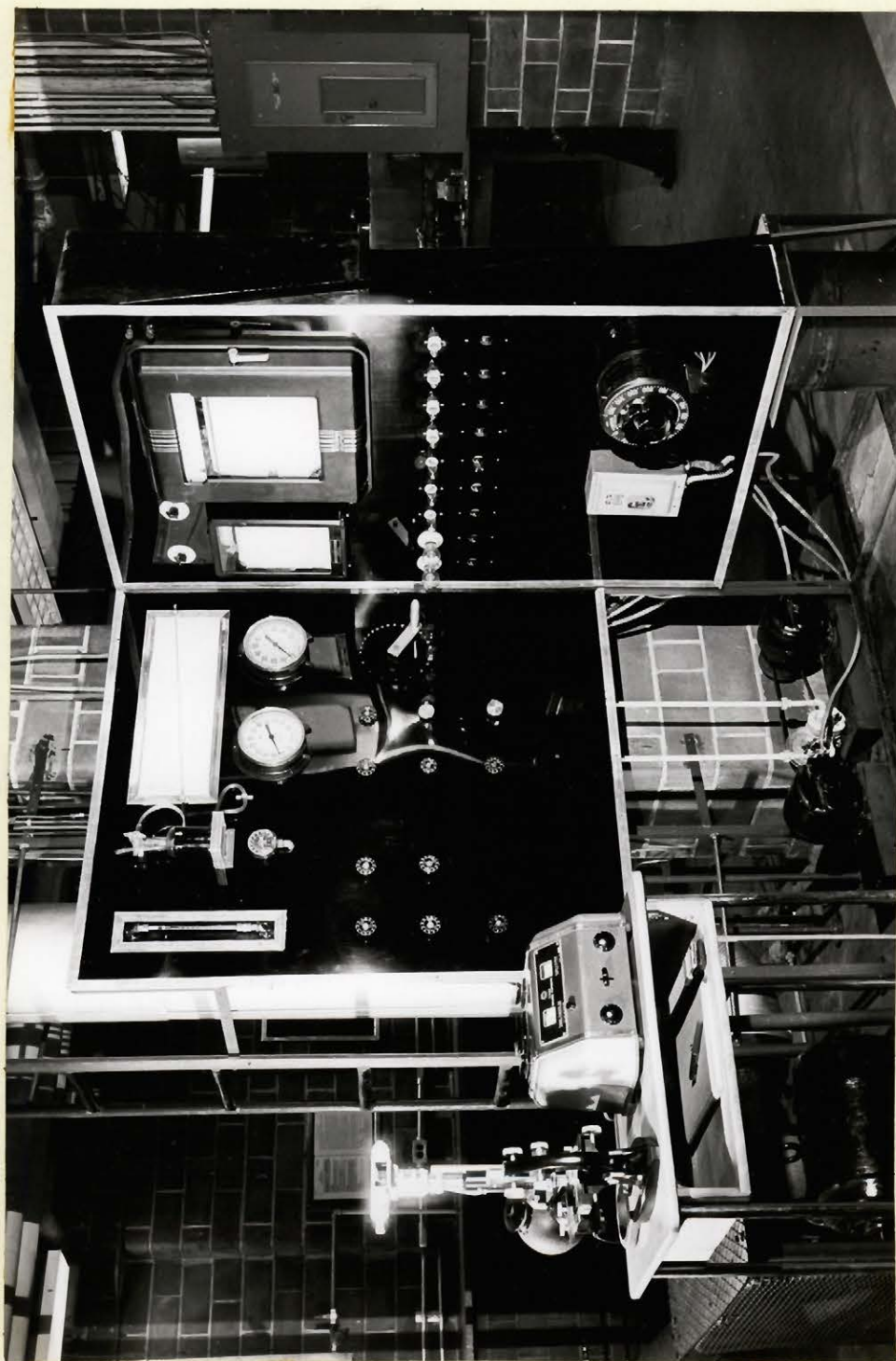


Fig. 8. Control Panel

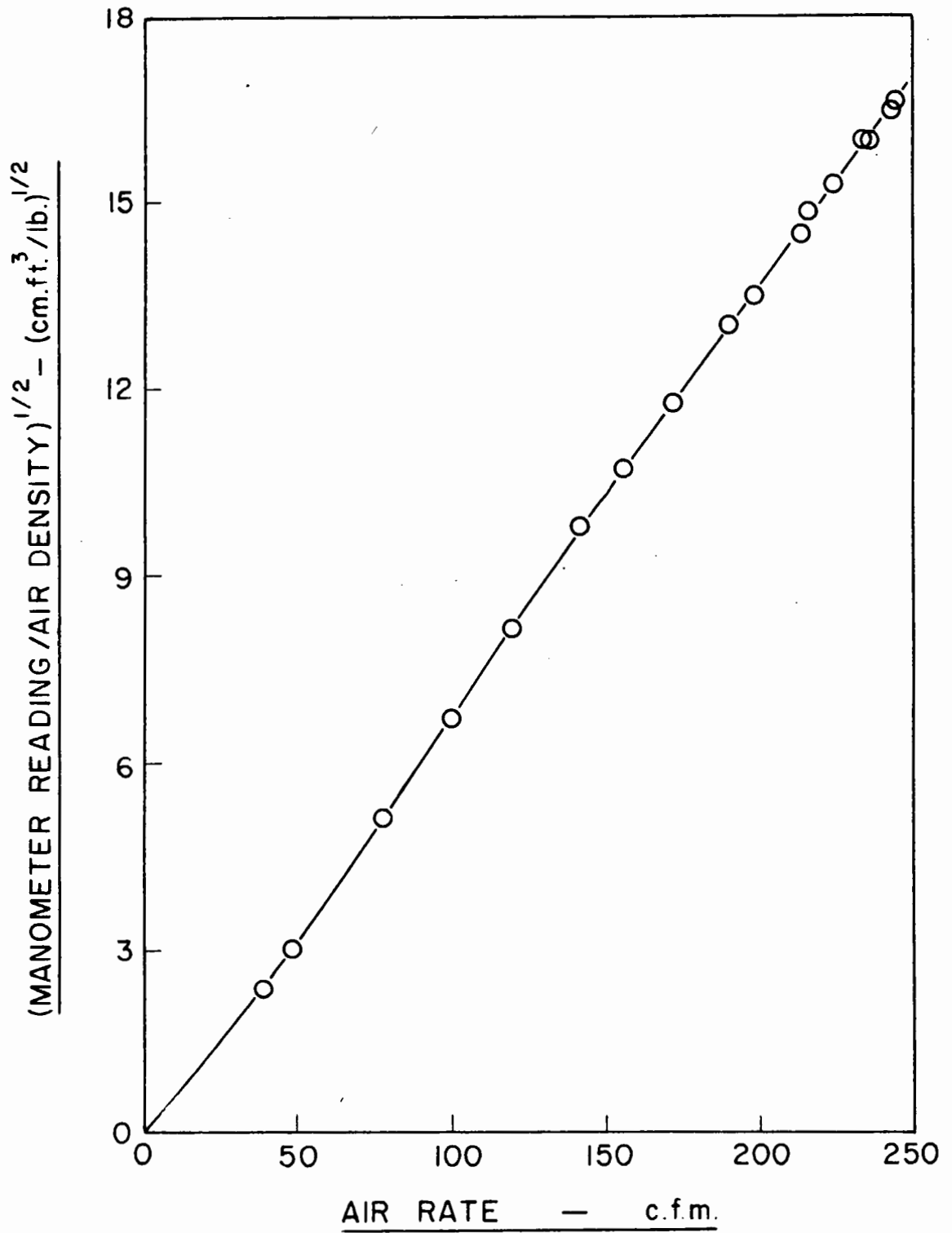


Fig. 9. Blower Orifice Calibration Curve

b) Air Heating

Provision for heating the drying air consisted of three electric heaters, located in the 8-in. diameter galvanized iron duct connected to the blower, and of a gas burner, which was used only when high air temperatures were required, and which was located in the intake duct of the blower (Figure 7). City gas was used in the gas burner and its flow rate was controlled by means of a standard 1/2-in. globe valve.

The three electric heaters (No. 1, 2 and 3) were rated at 3.25, 2.0 and 1.0-kilowatt each, respectively, at a voltage input of 220 Volts; the switches and pilot lights for the heaters were installed on the central control panel. The air temperature was maintained at the desired level by means of an Aminco bimetallic thermoregulator which was located at the entrance to the drying chamber, and which was connected to heater number 3 through a mercury relay. In order to provide temperature control over the whole range, heater number 2 was connected in series with a General Radio Company Variac and the power input to it was recorded on an Esterline-Angus registering wattmeter.

The temperature of the air was measured right after the heater section and at the point where the thermoregulator was installed by means of copper-constantan thermocouples which were connected to a 12-point Speedomax Recording Potentiometer. A selector switch and a Leeds and Northrup millivoltmeter type 8662 were also provided, to permit a check on the readings. It was noted that with proper adjustment of the power to heater number 2 the air temperature could be controlled to within 0.5°C. The heater section as well as the duct

leading to the drying chamber were insulated with a 2-inch layer of 85% magnesia to reduce heat losses.

c) Drying Chamber

No definite expanded section of the equipment - comparable to the drying chamber of an industrial installation - was provided in the experimental apparatus, but rather the air heater section, the nozzle section, the drying chamber and the air exhaust system were all contained in one continuous duct, eight inches in diameter (Figure 7). This design was adopted to minimize back-mixing in the air flow pattern.

The heated air first passed through a straightening plate, to insure a uniform velocity distribution, and then through the nozzle section which was made of galvanized iron, 2-feet long and insulated with a 2-inch layer of magnesia. Two 1/2-inch diameter observation ports, made of Herculite high temperature glass, were provided at the level of the nozzle to permit observation of the spray.

The drying chamber itself - which was constructed through the kind co-operation of the Pulp and Paper Research Institute of Canada - was made in two sections: the first was 2-feet long, made of galvanized iron, and surrounded with a 1-foot diameter galvanized iron jacket, the annular space being filled with vermiculite; the second was 12-feet long and welded in one piece from 16-gauge cold rolled steel, also insulated with a 2-inch layer of vermiculite. A ladder, running along the full height of the chamber, was installed to provide access to the various parts of the chamber, and to supply the necessary structural support. To minimize corrosion, the inside of the chamber and the outer jacket were painted with high-temperature aluminum paint. The temperature of the chamber wall was measured by

means of copper-constantan thermocouples, which were welded to the wall at 2-foot intervals, and connected to the Speedomax Recorder.

Sampling points, shown in Figures 6 and 7, were installed along the whole length of the chamber, so that the evaporation of the water droplets could be followed and the conditions under which they were evaporating measured. They were made out of either 1/2, 3/4 or 2-inch standard steel nipples (4 inches long), welded to the chamber, the various sizes being necessary to accommodate the various sampling and measuring devices used in the experiments. The locations of the sampling points in terms of their distance from the nozzle are given in Table III, page 81. When not in use, they were closed with plugs made out of Transite and wood which fitted flush with the inside walls of the chamber.

d) Atomization and Feed Supply

Pneumatic nozzles of the internal mixing type (Model 1/4 J, made by Spraying Systems Co. in Chicago) were used for the atomization of the water feed. Two different sizes were employed (No. 12 and 22B), depending on the liquid feed rate and on the particle size desired.

The feed to the nozzle was ordinary tap water, its rate being controlled by means of a 1/4-inch stainless steel needle valve and metered by a Emil Greiner Co. flowmeter (type G-9144 B) with a stainless steel and a sapphire float. Provision was made in the piping to allow calibration of the flowmeter. All the lines were made out of brass piping or copper tubing to avoid corrosion, and a strainer was introduced

TABLE IIILOCATION OF SAMPLING POINTS

<u>No.</u>	<u>Dist. from nozzle, ft.</u>	<u>Size in.</u>
1	0	2.0
2	0.79	1/2
3	0.96	3/4
4	1.12	1/2
5	1.29	3/4
6	1.46	1/2
7	1.79	2.0
8	1.96	1/2
9	2.54	3/4
10	2.86	1/2
11	3.19	3/4 and 2.0
12	4.86	1/2
13	5.19	3/4 and 2.0
14	6.86	1/2
15	7.19	3/4 and 2.0
16	8.86	1/2
17	9.19	3/4 and 2.0
18	10.86	1/2
19	11.19	3/4 and 2.0
20	12.86	1/2
21	13.19	3/4 and 2.0

into the line to filter out any loose dirt which would have blocked the small openings in the nozzle. A thermocouple was located in the latter to measure the temperature of the feed, which was preheated by means of two heat exchangers through which water was circulated from a constant temperature water bath by means of a small gear pump. One of the heat exchangers was outside the chamber and the other was inside, extending right up to the nozzle. The pressure of the feed was measured on a 0 to 60 p.s.i.g. Bourdon gauge.

An Ingersoll Rand compressor (Type 30) supplied the necessary air for atomization. A Taylor pressure reducing valve controlled the pressure of the air which was measured by a 0 to 100 p.s.i.g. Bourdon gauge, and a filter was also installed in the line in order to obtain absolutely clean air.

2. PROCEDURE

A series of ten runs was made in order to determine the rate of evaporation of the water droplets under various experimental conditions. During all these tests, a rigidly standardized operating procedure was followed.

The equipment was started by adjusting the air rate from the blower to the desired value by means of the slide valve, and by turning on the electric heaters at full capacity. When the temperature of the air reached approximately the desired level, the automatic control to the heaters was turned on. Approximately one hour was then allowed for the

equipment to heat up to equilibrium conditions.

The compressed air to the nozzle was then adjusted at the desired pressure and the circulating water for the feed heat exchangers was started. The small stream of cold air from the nozzle as well as the cool water in the heat exchanger reduced the air temperature by one or two degrees, and when this effect became steady, a temperature traverse along the length of the drying chamber was made with a mercury thermometer. The traverse indicated invariably that the heat losses were negligibly small, the temperature difference between the inlet and outlet conditions being usually about 1°C . and never exceeding 4°C . The temperature reading that was obtained 1.96-feet downstream from the nozzle under these conditions was considered to be the corrected inlet air temperature, and will be designated by the symbol t_0 in all subsequent equations.

The feed to the nozzle was then turned on and its rate was adjusted by means of the needle valve to give the desired reading on the rotameter. Great care had to be exercised in adjusting the compressed air pressure and the liquid feed rate to prevent the spray from hitting the chamber walls. Although the internal type of mixing nozzles used had quite a small angle of spray under proper operating conditions (12 to 20°), this angle increased rapidly when an excessive feed rate was employed in combination with a high atomizing pressure and a low drying air rate. Visual observation was adequate to reveal the wetting of the walls when this effect was large, but when it was small, detection was prevented

by the rapid evaporation of the droplets on the walls. On the other hand, this evaporation cooled the walls sufficiently to alter the distribution of the wall temperature throughout the chamber; in other words, the Speedomax recording of the wall temperature indicated a lower temperature at the top than at the bottom: a distribution of this kind was therefore avoided by reducing the feed rate.

Approximately one half to one hour was required for conditions to become steady once the feed was introduced, steady conditions being assumed to be attained when all the temperatures remained constant for ten minutes. When this condition was reached, all the necessary readings and samples were taken, namely

1. WATER FEED
 - flowmeter reading and hence L_f ;
 - temperature in the nozzle, t_f ;
 - pressure at the nozzle;
2. ATOMIZING AIR - pressure at the nozzle;
3. DRYING AIR
 - temperature at the blower orifice;
 - orifice manometer reading and hence w ;
 - inlet air humidity, H_0 ;
 - inlet air temperature, t_0 ;
4. CONDITIONS AT VARIOUS LOCATIONS ALONG THE CHAMBER
 - air temperature, t ;
 - sample of air and hence H ;
 - sample of spray and hence d_{vs} .

3. CALCULATIONS

a) Determination of the Rate of Evaporation

The rate of evaporation was calculated from a heat balance based on the air temperature drop through the drying chamber, as well as from a material balance based on the humidity increase of the air. No correction was necessary for heat losses since they were negligibly small as described in the procedure, at least at the temperature levels used in this investigation.

A complete heat balance between the inlet conditions (designated by the subscript "o" for the air and by the subscript "f" for the feed) and the conditions at any given point in the drying chamber (designated by the subscript "n") gave the following equation, based on a datum of 32°F., liquid water:

$$\begin{aligned} w \int_{32}^{t_o} C_{p_a} dt + w H_o [\lambda_{32} + \int_{32}^{t_o} C_{p_v} dt] + L_f \int_{32}^{t_f} C_{p_w} dt = \\ = w \int_{32}^{t_n} C_{p_a} dt + w H_n [\lambda_{32} + \int_{32}^{t_n} C_{p_v} dt] + L_n \int_{32}^{t_{wn}} C_{p_w} dt \dots (29) \end{aligned}$$

Similarly, a material balance between the same two points will give:

$$L_f - L_n = w(H_n - H_o) \dots \dots \dots (30)$$

Equation (29) was based on the assumption that the drop remained at the wet bulb temperature of the air throughout its flight in the chamber, an assumption which was undoubtedly justified in the light of existing experimental evidence. Average specific heats can be used in equation (29),

and by substituting into it equation (30), the following simplified expression will be obtained:

$$\begin{aligned} (L_f - L_n) [\lambda_{32} + C_{p_v}(t_n - 32) - C_{p_w}(t_{wn} - 32)] = \\ = w(C_{p_a} + H_0 C_{p_v})(t_o - t_n) + L_f C_{p_w}(t_f - t_{wn}) \dots \dots \dots (31) \end{aligned}$$

The vaporization was calculated both from equation (30), which was based on the measurement of the air humidity H_n , and from equation (31), which was based on the measurement of the air temperature t_n , thus affording a check on the accuracy of the experimental readings.

b) Calculation of the heat transfer coefficient and the Nusselt Number

In order to permit the accurate calculation of the heat transfer coefficients, an equation had to be derived on a differential basis because of the continuous variation in the value of the variables involved in the system. Considering a length dx of the chamber, the following heat balance equation will be obtained, based on equation (29):

$$-w(C_{p_a} + H C_{p_v})dt = wdH [\lambda_w + C_{p_v}(t - t_w)] \dots \dots \dots (32)$$

The rate of heat transfer to the drops located in the differential volume of the chamber of length dx will be given by:

$$wdH \lambda_w = hdA(t - t_w) \dots \dots \dots (33)$$

where dA is the surface area of the droplets, and it can be expressed as follows:

$$dA = (S_w L/v + v_T)dx \dots \dots \dots (34)$$

Combining equations (34), (33) and (32) an expression for the calculation of the heat transfer coefficient is obtained, after suitable rearrangement:

$$h = \left\{ -ws(v+v_T) \lambda_w \right\} / \left\{ S_w L (t-t_w) [\lambda_w + C_{p_v}(t-t_w)] \right\} (dt/dx) \dots (35)$$

The values of all the variables involved in equation (35) were either determined experimentally or calculated from the local conditions at the point under consideration: w and v were obtained from the air rate, air temperature t and air humidity H , s is the humid heat and t_w and λ_w correspond to the wet bulb temperature of the air; S_w is the surface area of the droplets per pound of liquid water, and it was obtained from the particle count by substitution into the following expression:

$$S_w = 6 \sum nd^2 / \rho \sum nd^3 \dots (36)$$

L refers to the pounds of liquid droplets passing per hour through the section dx of the chamber, and it was calculated from the rate of evaporation as described previously; the value of (dt/dx) was obtained from a graph of the air temperature distribution along the drying chamber, while v_T corresponds to the terminal velocity of the droplets.

The Nusselt Number was calculated from its definition

$$Nu = hd_{vs}/k \dots (37)$$

where k refers to the thermal conductivity of air at the arithmetic average temperature between the air and the surface of the droplets, or the wet bulb temperature.

c) Calculation of the Mass Transfer Coefficient and the Modified Nusselt Number

The rate of mass transfer can be expressed by an equation which is similar to equation (33):

$$wdH = k'_g dA (H_w - H) \dots\dots\dots(38)$$

and dividing this equation by (33), the following result will be obtained:

$$\lambda_w k'_g / h = (t - t_w) / (H_w - H) \dots\dots\dots(39)$$

Owing to the analogy between heat and mass transfer and to the physical properties of the system air-water, it has been found experimentally that the adiabatic humidification curves and the constant wet bulb temperature curves coincide when the contribution from convection to heat transfer is large compared to the contribution from radiation. The constant wet bulb temperature curve is given by equation (39) above, while the adiabatic humidification curve is given by equation (32), which can be integrated to give the following:

$$\lambda_w / s = (t - t_w) / (H_w - H) \dots\dots\dots(40)$$

Since equations (39) and (40) apply to the same curve, it follows that:

$$\lambda_w k'_g / h = \lambda_w / s \quad \text{or} \quad k'_g / h = s \quad \dots\dots\dots(41)$$

Consequently the mass transfer coefficient can be calculated very simply from the heat transfer coefficient for the system air-water. Similarly the modified Nusselt Number Nu' can be obtained directly from the Nusselt Number Nu , or from the heat transfer coefficient h as follows:

$$Nu' = (hd_{vs}/\rho_a s D_v) \dots\dots\dots(42)$$

4. RESULTS

A total of ten runs were made under different conditions of inlet air temperature (135.2 to 229.7°F.), air velocity (3.9 to 14.8 ft./sec.) and droplet size (11.5 to 38.5 μ). The initial droplet size was varied either by changing the atomizing air pressure or by using a different nozzle. All runs were carried out under atmospheric pressure conditions, and no effort was made to control the inlet air humidity.

The observed values of the experimental variables as well as the calculated results are shown in Tables IV to XIII. The experimental values include the air rate w , air velocity v , feed rate L_f and feed temperature t_f which remained constant throughout each run, and the air temperature t , air humidity H and mean Sauter diameter of the droplets d_{vs} , along the chamber. The calculated results presented are: the wet bulb temperature of the air t_w , as obtained from the psychrometric chart; the amount of liquid water

TABLE IVHEAT AND MASS TRANSFER TO WATER DROPLETSAT HIGH AIR VELOCITYRUN NO. 1

Nozzle No. 22B Atom. air pressure = 20 p.s.i.g. Feed temp. = 89°F.
 Feed rate = 5.62 lb./hr Drying air rate = 1048 lb.d.a./hr.
 Average air velocity = 12.4 ft./sec.

OBSERVED					CALCULATED					
\bar{x}	\bar{t}	$\frac{H}{\text{lb.w.}}$	$\frac{d_{vs}}{\mu}$	$\frac{t_w}{^\circ\text{F.}}$	$\frac{L_{hb}}{\text{lb.}}$	$\frac{L_{mb}}{\text{lb.}}$	$\frac{dt/dx}{\text{ft.}}$	$\frac{h}{\text{hr.ft.}^2\text{.}^\circ\text{F.}}$	$\frac{Nu}{-}$	$\frac{Nu^t}{-}$
ft.	°F.	lb.d.a.		°F.	hr.	hr.				
0	141.2	0.0054			5.62	5.62				
1.13	139.0				5.10					
3.19	129.9	0.0079	24.8	77	3.00	3.00	-6.6	396	2.02	1.84
5.20	121.6	0.0098	24.4	77	1.02	1.00	-2.0	406	2.05	1.86
7.19	119.4		26.0	77	0.45		-0.8	397	2.14	1.94
9.18	118.8				0.32					

TABLE VHEAT AND MASS TRANSFER TO WATER DROPLETSAT HIGH AIR VELOCITYRUN NO. 2

Nozzle No. 22B Atom. air pressure = 20 p.s.i.g. Feed temp. = 90°F.
 Feed rate = 6.42 lb./hr. Drying air rate = 1000 lb.d.a./hr.
 Average air velocity = 11.6 ft./sec.

OBSERVED					CALCULATED					
\underline{x}	\underline{t}	$\frac{H}{\text{lb.w.}}$	$\frac{d_{vs}}{\mu}$	$\underline{t_w}$	$\frac{L_{hb}}{\text{lb.}}$	$\frac{L_{mb}}{\text{lb.}}$	$\frac{dt/dx}{\text{ft.}}$	$\frac{h}{\text{hr.ft.}^2\text{.}^\circ\text{F.}}$	$\frac{Nu}{-}$	$\frac{Nu'}{-}$
ft.	°F.	lb.d.a.		°F.	hr.	hr.				
0	135.2	0.0057			6.42	6.42				
1.13	132.2				5.75					
3.19	117.0	0.0097	26.1	76	2.30	2.42	-4.0	381	2.07	1.84
5.20	111.4	0.0113	24.8	76	0.80	0.82	-1.3	391	2.08	1.79
7.19	109.1	0.0116	25.0	76	0.28	0.52	-0.4	381	2.00	1.75
9.18	108.7				0.25					

TABLE VI

HEAT AND MASS TRANSFER TO WATER DROPLETSAT LOW AIR VELOCITYRUN NO. 3

Nozzle No. 22B Atom. air pressure = 20 p.s.i.g. Feed temp. = 90°F.

Feed rate = 6.42 lb./hr. Drying air rate = 449 lb.d.a./hr.

Average air velocity = 5.6 ft./sec.

OBSERVED					CALCULATED					
\underline{x}	\underline{t}	\underline{H}	\underline{d}_{vs}	\underline{t}_w	\underline{L}_{hb}	\underline{L}_{mb}	$\underline{dt/dx}$	\underline{h}	\underline{Nu}	\underline{Nu}'
ft.	°F.	$\frac{\text{lb.w.}}{\text{lb.d.a.}}$	μ	°F.	$\frac{\text{lb.}}{\text{hr.}}$	$\frac{\text{lb.}}{\text{hr.}}$	$\frac{\text{F.}}{\text{ft.}}$	$\frac{\text{B.t.u.}}{\text{hr.ft.}^2 \text{°F.}}$	-	-
0	187.7	0.0094			6.42	6.42				
0.79	163.8				3.95					
0.96	153.8		23.3	91	2.80		-6.4	447	2.08	1.91
1.13	146.4		22.9	91	2.31		-5.3	452	2.08	1.91
1.29	141.6		21.9	91	1.56		-3.6	486	2.15	1.96
1.46	138.0		20.5	91	1.22		-2.8	486	2.02	1.85
1.96	133.5				0.77					
2.54	132.2				0.62					

TABLE VIIHEAT AND MASS TRANSFER TO WATER DROPLETSAT LOW AIR TEMPERATURERUN NO. 4

Nozzle No. 22B Atom. air pressure = 20 p.s.i.g. Feed temp. = 90°F.

Feed rate = 4.87 lb./hr. Drying air rate = 429 lb.d.a./hr.

Average air velocity = 5.1 ft./sec.

OBSERVED					CALCULATED					
\bar{x}	\bar{t}	\bar{H}	$\frac{d_{vs}}$	\bar{t}_w	$\frac{L_{hb}}$	$\frac{L_{mb}}$	$\frac{dt}{dx}$	$\frac{h}{h}$	$\frac{Nu}{Nu}$	$\frac{Nu'}{Nu'}$
ft.	°F.	$\frac{\text{lb.w.}}{\text{lb.d.a.}}$	μ	°F.	$\frac{\text{lb.}}{\text{hr.}}$	$\frac{\text{lb.}}{\text{hr.}}$	$\frac{\text{F.}}{\text{ft.}}$	$\frac{\text{B.t.u.}}{\text{hr.ft.}^2\text{°F.}}$	-	-
0	142.0	0.0094			4.87	4.87				
0.79	123.0				3.02					
0.96	115.4		18.8	82	2.27		-35.8	576	2.25	2.02
1.13	110.1		17.3	82	1.73		-24.9	572	2.07	1.86
1.29	106.6		17.3	82	1.39		-17.8	580	2.09	1.86
1.79	100.2	.0191	16.9	82	0.74	0.71	- 7.4	593	2.11	1.85
1.96	99.1				0.66					
2.54	97.0				0.45					
2.86	96.7				0.43					

TABLE VIII

HEAT AND MASS TRANSFER TO WATER DROPLETSAT HIGH AIR VELOCITYRUN NO. 5

Nozzle No. 22B Atom. air pressure = 20 p.s.i.g. Feed temp. = 90°F.

Feed rate = 7.91 lb./hr. Drying air rate = 1239 lb.d.a./hr.

Average air velocity = 14.7 ft./sec.

OBSERVED					CALCULATED					
\underline{x}	\underline{t}	\underline{H}	$\underline{d_{vs}}$	$\underline{t_w}$	$\underline{L_{hb}}$	$\underline{L_{mb}}$	$\underline{dt/dx}$	\underline{h}	Nu	Nu'
ft.	°F.	$\frac{\text{lb.w.}}{\text{lb.d.a.}}$	μ	°F.	$\frac{\text{lb.}}{\text{hr.}}$	$\frac{\text{lb.}}{\text{hr.}}$	$\frac{\text{F.}}{\text{ft.}}$	$\frac{\text{B.t.u.}}{\text{hr.ft.}^2\text{°F.}}$	-	-
0	136.6	0.0102			7.91	7.91				
0.79	133.9				7.15					
1.13	133.0				6.90					
1.46	131.9				6.60					
1.96	129.9				6.03					
2.54	125.3		19.4	81	4.69		-10.0	507	2.03	1.84
2.86	123.0		18.6	81	4.07		- 8.5	510	1.96	1.78
3.19	120.3	0.0141	18.4	81	3.26	3.08	- 6.9	536	2.05	1.85
4.87	112.4		16.7	81	1.06		- 2.3	617	2.15	1.93
6.86	109.4		16.4	81	0.20		- 0.4	602	2.06	1.84

TABLE IX

HEAT AND MASS TRANSFER TO WATER DROPLETSAT HIGH AIR TEMPERATURERUN NO. 6

Nozzle No. 22B Atom. air pressure = 20 p.s.i.g. Feed temp. = 85°F.

Feed rate = 7.91 lb./hr. Drying air rate = 429 lb.d.a./hr.

Average air velocity = 5.8 ft./sec.

OBSERVED					CALCULATED					
\bar{x}	\bar{t}	$\frac{H}{\text{lb.w.}}$	$\frac{d_{vs}}{\mu}$	$\frac{t_w}{^\circ\text{F.}}$	$\frac{L_{hb}}{\text{lb.}}$	$\frac{L_{mb}}{\text{lb.}}$	$\frac{dt/dx}{\text{ft.}}$	$\frac{h}{\text{hr.ft.}^2\text{.}^\circ\text{F.}}$	Nu	Nu'
ft.	°F.	lb.d.a.		°F.	hr.	hr.	ft.		-	-
0	229.7	0.0123			7.91	7.91				
0.79	194.2				4.45					
0.96	179.7		23.8	100	3.02		-59.9	431	2.02	1.87
1.13	171.5		22.2	100	2.20		-44.3	441	1.93	1.78
1.29	166.0		22.9	100	1.61		-28.4	457	2.07	1.91
1.46	161.8		23.0	100	1.22		-21.5	474	2.17	1.99
1.79	156.5	0.0290	21.9	100	0.71	0.75	-11.5	471	2.05	1.88
1.96	154.6				0.52					
2.86	149.5				0.02					

TABLE X

HEAT AND MASS TRANSFER TO WATER DROPLETS
OF LARGE AVERAGE DIAMETER

RUN NO. 7

Nozzle No. 22B Atom. air pressure = 15 p.s.i.g. Feed temp. = 95°F.

Feed rate = 6.42 lb./hr. Drying air rate = 309 lb.d.a./hr.

Average air velocity = 3.9 ft./sec.

OBSERVED					CALCULATED					
\underline{x}	\underline{t}	\underline{H}	\underline{dvs}	$\underline{t_w}$	$\underline{L_{hb}}$	$\underline{L_{mb}}$	$\underline{dt/dx}$	\underline{h}	\underline{Nu}	$\underline{Nu'}$
ft.	°F.	$\frac{\text{lb.w.}}{\text{lb.d.a.}}$	μ	°F.	$\frac{\text{lb.}}{\text{hr.}}$	$\frac{\text{lb.}}{\text{hr.}}$	$\frac{\text{F.}}{\text{ft.}}$	$\frac{\text{B.t.u.}}{\text{hr.ft.}^2\text{°F.}}$	-	-
0	213.6	.0087			6.42	6.42				
0.79	168.0		38.5	95	3.22		-46.2	270	2.05	1.91
0.96	160.5		38.0	95	2.67		-36.1	243	2.21	2.04
1.13	154.7		36.9	95	2.33		-31.0	299	2.20	2.01
1.29	149.8		33.7	95	1.93		-27.0	314	2.13	1.95
1.46	145.5		32.3	95	1.62		-23.0	328	2.13	1.94
1.79	138.3	0.0255	30.8	95	1.07	1.23	-14.0	343	2.14	1.94
1.96	135.7				0.97					
2.86	130.0				0.58					

TABLE XI

HEAT AND MASS TRANSFER TO WATER DROPLETS
OF LARGE AVERAGE DIAMETER

RUN NO. 8

Nozzle No. 22B Atom. air pressure = 15 p.s.i.g. Feed temp. = 90°F.

Feed rate = 7.91 lb./hr. Drying air rate = 580 lb.d.a./hr.

Average air velocity = 7.4 ft./sec.

OBSERVED					CALCULATED					
\bar{x}	\bar{t}	$\frac{H}{\text{lb.w.}}$	$\frac{d_{vs}}{\mu}$	$\frac{t_w}{\text{°F.}}$	$\frac{L_{hb}}{\text{lb.}}$	$\frac{L_{mb}}{\text{lb.}}$	$\frac{dt/dx}{\text{F.}}$	$\frac{h}{\text{hr.ft.}^2\text{°F.}}$	Nu	Nu'
ft.	°F.	lb.d.a.	μ	°F.	hr.	hr.	ft.		-	-
0	190.3	0.0087			7.91	7.91				
0.79	178.8				6.37					
0.96	173.0		33.5	91	5.64		-32.5	300	2.00	1.87
1.13	167.6		31.9	91	4.92		-28.9	310	1.96	1.84
1.29	162.6		31.4	91	4.27		-27.0	350	2.19	2.02
1.46	158.2		29.4	91	3.66		-24.5	370	2.17	2.01
1.79	150.7	0.0179	26.7	91	2.66	2.58	-18.0	380	2.04	1.87
1.96	148.1				2.32					
2.54	141.7		30.8	91	1.47		- 7.0	361	2.25	2.04
2.86	140.2				1.30					

TABLE XII

HEAT AND MASS TRANSFER TO WATER DROPLETS
OF SMALL AVERAGE DIAMETER

RUN NO. 9

Nozzle No. 22B Atom. air pressure = 35 p.s.i.g. Feed temp. = 90°F.

Feed rate = 7.91 lb./hr. Drying air rate = 586 lb.d.a./hr.

Average air velocity = 7.5 ft./sec.

OBSERVED					CALCULATED					
\bar{x}	\bar{t}	$\frac{H}{\text{lb.w.}}$	$\frac{dvs}{\mu}$	$\frac{tw}{\text{°F.}}$	$\frac{L_{hb}}{\text{lb.}}$	$\frac{L_{mb}}{\text{lb.}}$	$\frac{dt/dx}{\text{F.}}$	$\frac{h}{\text{hr.ft.}^2\text{°F.}}$	Nu	Nu'
ft.	°F.	lb.d.a.		°F.	hr.	hr.	ft.		-	-
0	190.3	0.0087			7.91	7.91				
0.79	159.6		17.6	91	3.81		-62.0	548	1.93	1.78
0.96	151.5		16.4	91	2.75		-47.0	609	2.01	1.84
1.13	145.5		15.8	91	1.87		-31.0	630	2.02	1.84
1.29	141.2		14.8	91	1.26		-21.5	654	1.96	1.78
1.46	138.3				0.90					
1.79	135.4	0.0211	18.3	91	0.56	0.65	- 5.5	526	1.95	1.77
1.96	134.7				0.42					
2.54	133.2				0.32					
2.86	133.0				0.20					

TABLE XIII

HEAT AND MASS TRANSFER TO WATER DROPLETS
OF SMALL AVERAGE DIAMETER

RUN NO. 10

Nozzle No. 12 Atom. air pressure = 44 p.s.i.g. Feed Temp. = 85°F.

Feed rate = 4.86 lb./hr. Drying air rate = 860 lb.d.a./hr.

Average air velocity = 10.7 ft./sec.

OBSERVED					CALCULATED					
\bar{x}	\bar{t}	$\frac{H}{\text{lb.w.}}$	$\frac{d_{vs}}{\mu}$	$\frac{t_w}{\text{°F.}}$	$\frac{L_{hb}}{\text{lb.}}$	$\frac{L_{mb}}{\text{lb.}}$	$\frac{dt/dx}{\text{ft.}}$	$\frac{h}{\text{hr.ft.}^2\text{°F.}}$	Nu	Nu'
ft.	°F.	lb.d.a.		°F.	hr.	hr.			-	-
0	161.2	0.0097			4.86	4.86				
0.96	154.0		18.3	86	3.35		25.7	560	2.06	1.92
1.13	150.3		17.5	86	2.71		21.1	571	2.03	1.88
1.29	147.1		16.9	86	2.11		17.3	610	2.09	1.92
1.46	144.2		15.7	86	1.52		13.8	660	2.09	1.94
1.79	140.5	0.0143	13.6	86	0.82	0.90	9.0	737	2.04	1.86
1.96	139.2		12.6	86	0.53		6.3	760	1.96	1.79
2.54	137.0		11.5	86	0.12		1.7	863	2.02	1.85
2.86	136.6				0.05					

remaining at any point in the chamber calculated from the heat balance (L_{hb} , obtained from equation 31) as well as from the material balance (L_{mb} , obtained from equation 30); the slope dt/dx of the temperature distribution curve; and the heat transfer coefficient h , Nusselt Number Nu and modified Nusselt Number Nu' which were obtained from equations (35), (37), and (42) respectively.

The temperature distribution along the drying chamber was plotted against the distance from the nozzle, these curves being shown in Figures 9, 10 and 11. They give a direct indication of the rate of vaporization and their slope at any given point is equal to dt/dx . The fraction of vaporization is also shown in Figures 12, 13 and 14 as a function of time.

As mentioned previously, the particle size was obtained from photomicrographs of the spray samples by observation through a microscope. Two typical photomicrographs are shown in Figures 16 (large drops from Run No. 7) and 17 (small drops from Run No. 10).

5. DISCUSSION

The experimental procedure followed in this investigation was carefully planned to permit a detailed analysis of the process of evaporation from water droplets suspended in a turbulent air stream

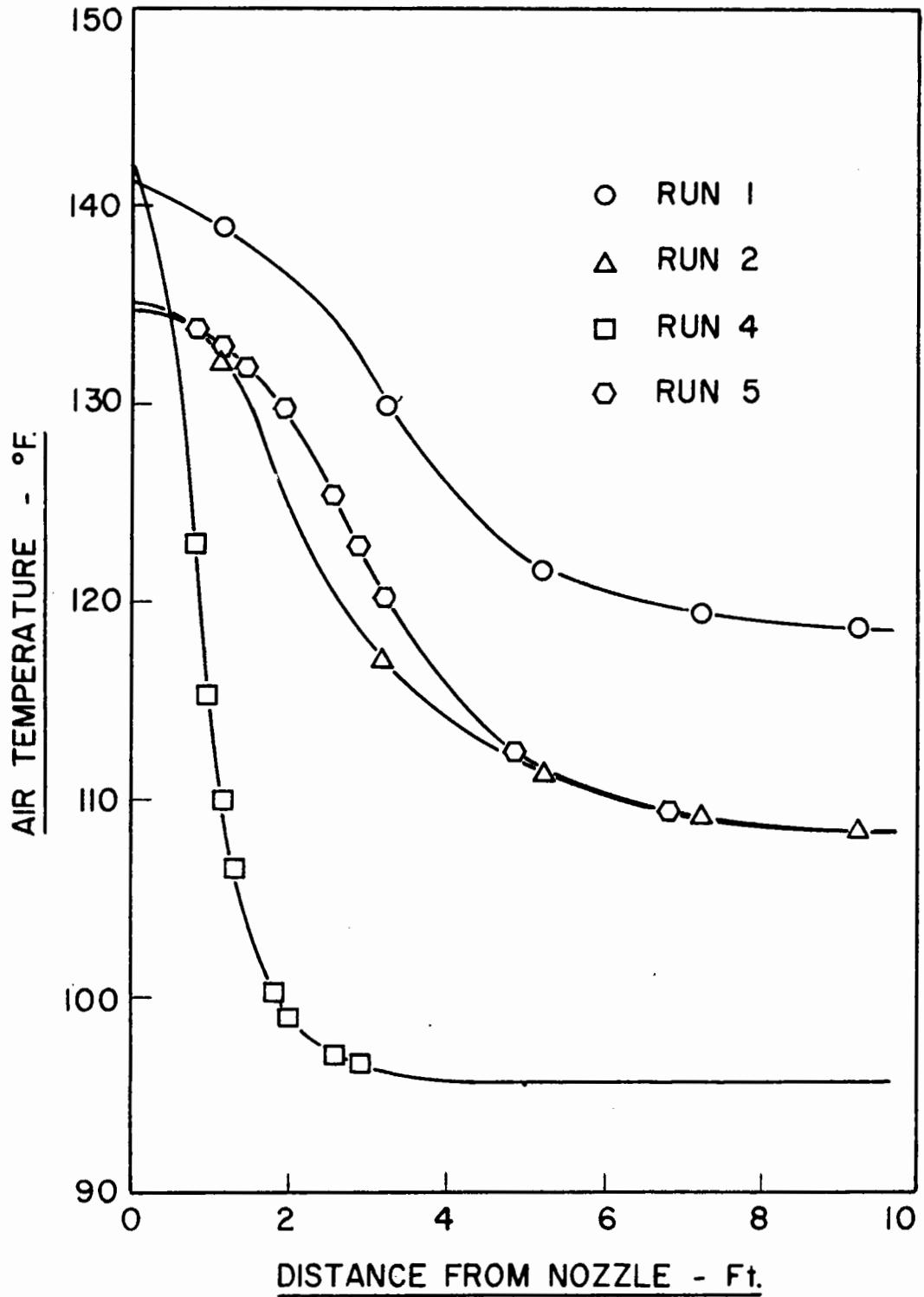


Fig. 10. Temperature Distribution along the Drying Chamber at Different Air Velocities

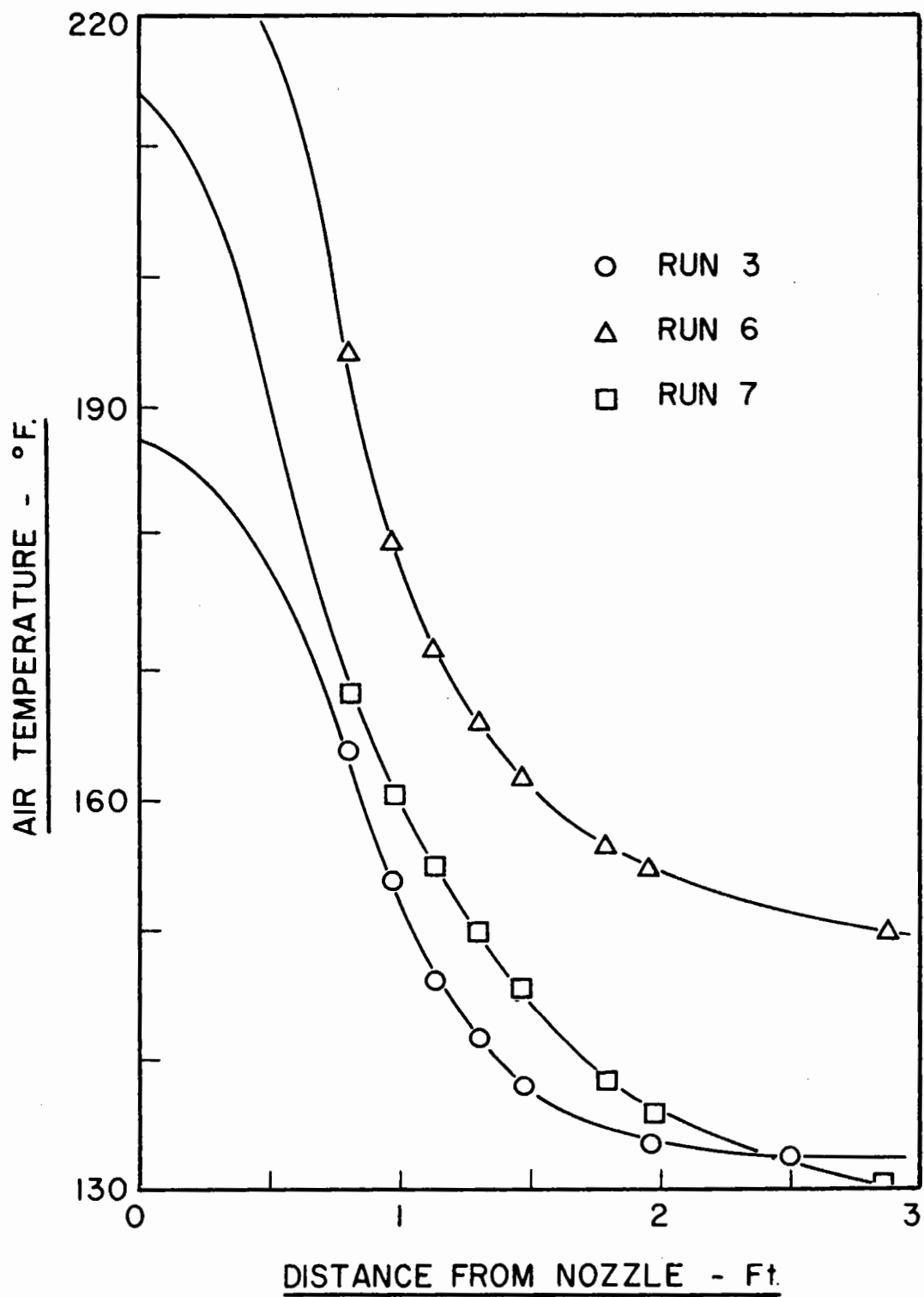


Fig. 11. Temperature Distribution along the Drying Chamber at High Inlet Air Temperatures

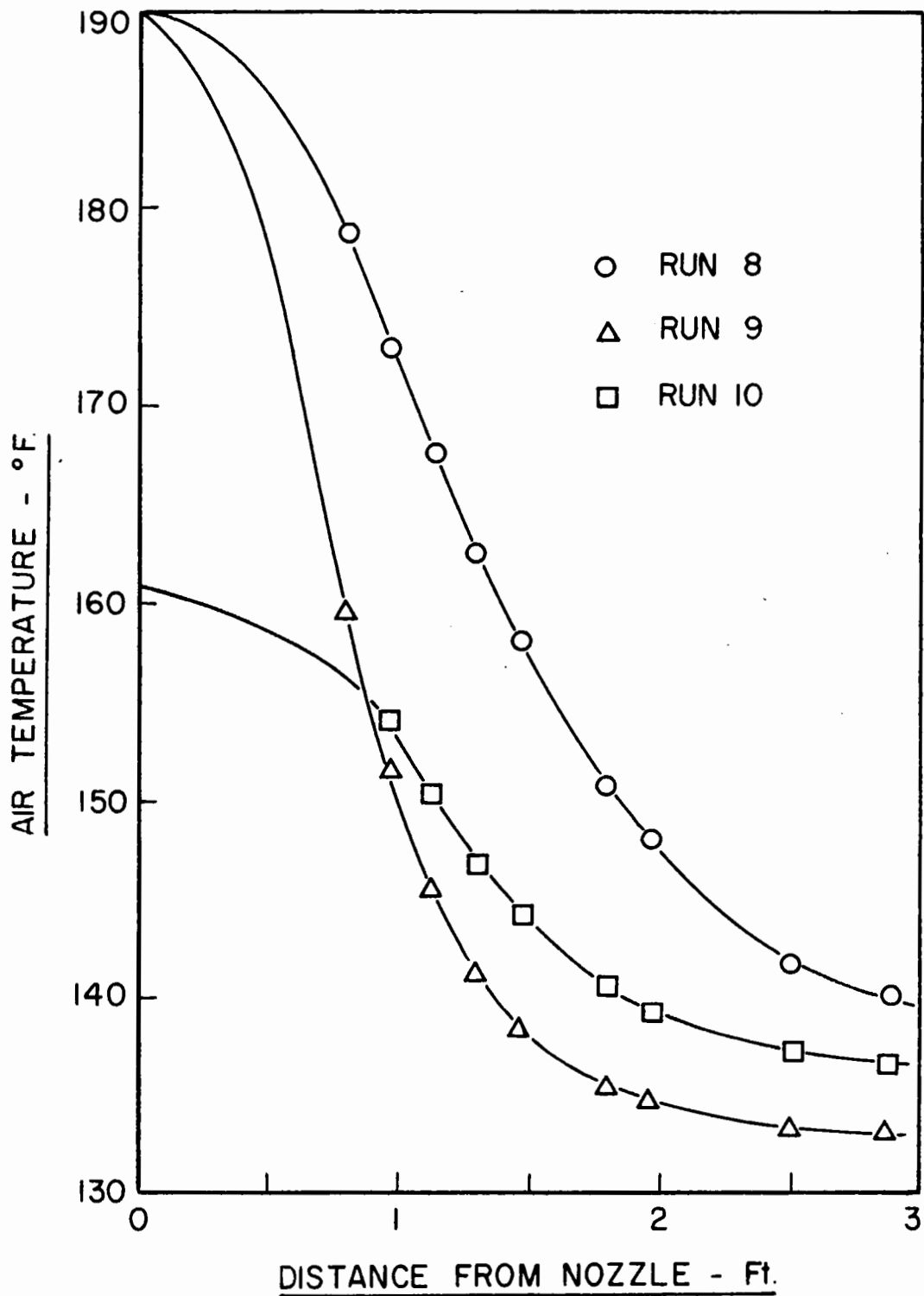


Fig. 12. Temperature Distribution along the Drying Chamber at Various Average Droplet Diameters

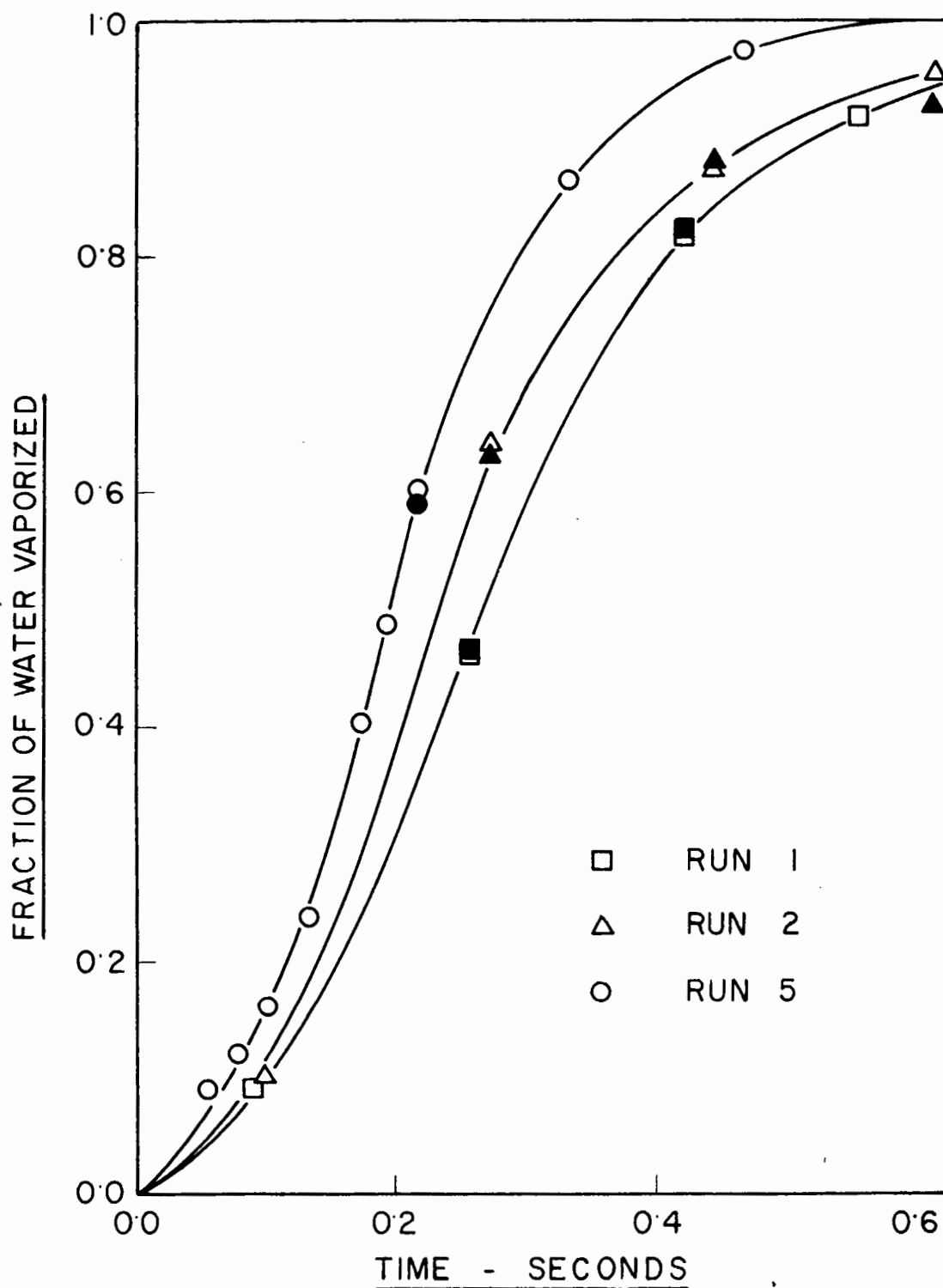


Fig. 13. Dependence of the water Vaporization on the Average Droplet Diameter and Inlet Air Temperature (Open symbols - heat balance; black symbols - material balance)

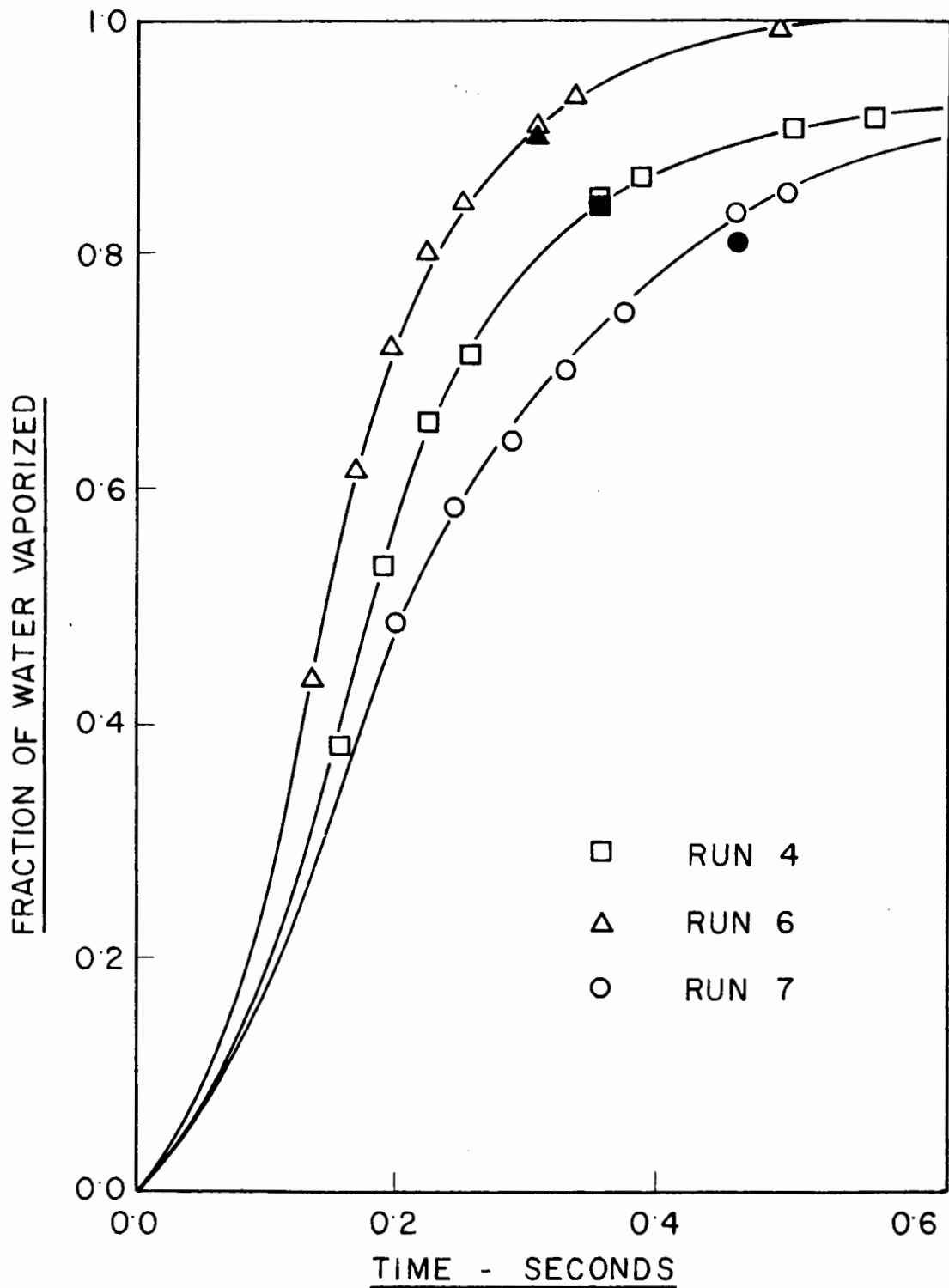


Fig. 14. Dependence of the Water Vaporization on the Average Droplet Diameter and Inlet Air Temperature (Open symbols - heat balance; black symbols - material balance)

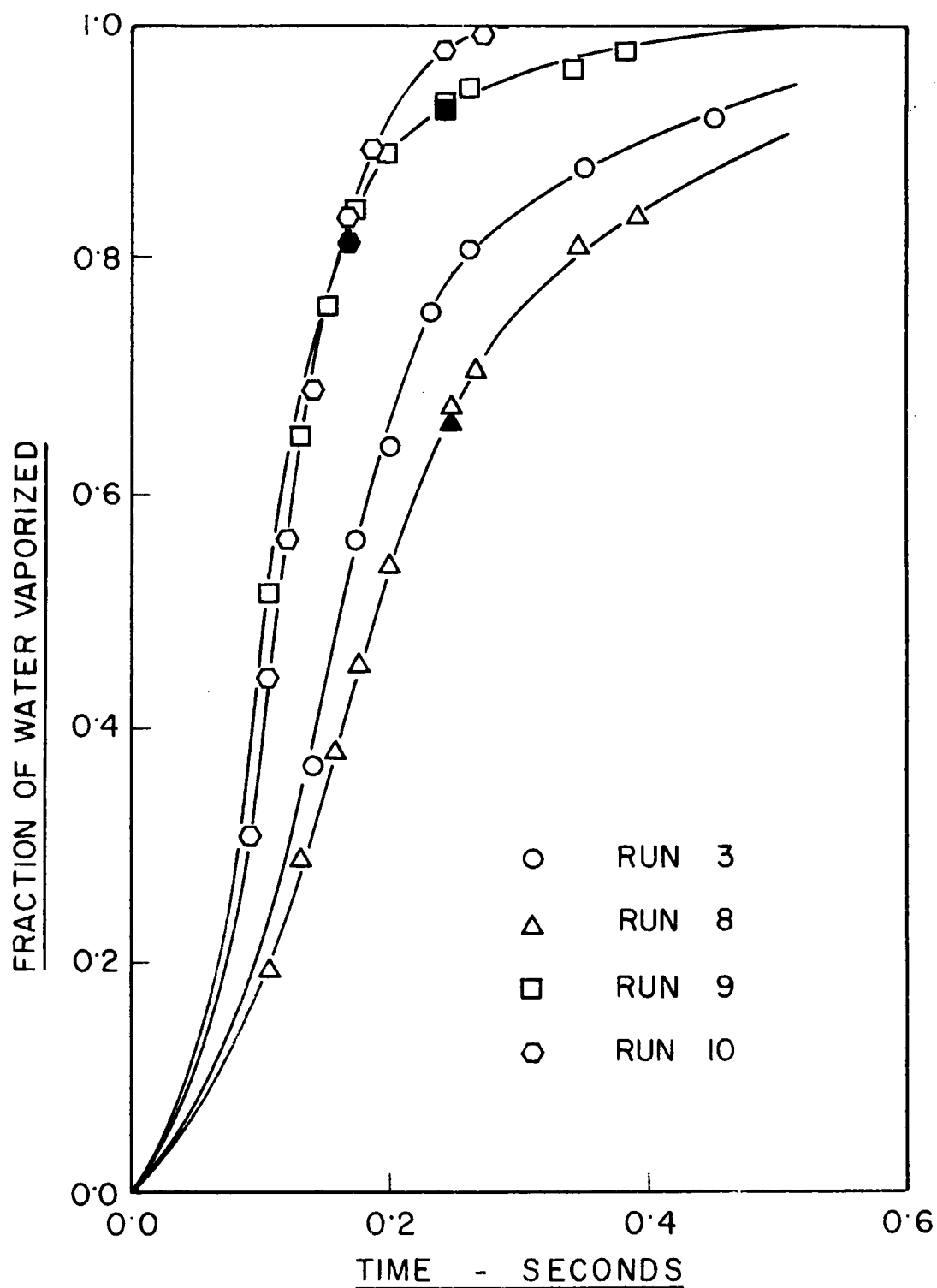


Fig. 15. Dependence of the Water Vaporization on the Average Droplet Diameter and Inlet Air Temperature (Open symbols - heat balance; black symbols - material balance)

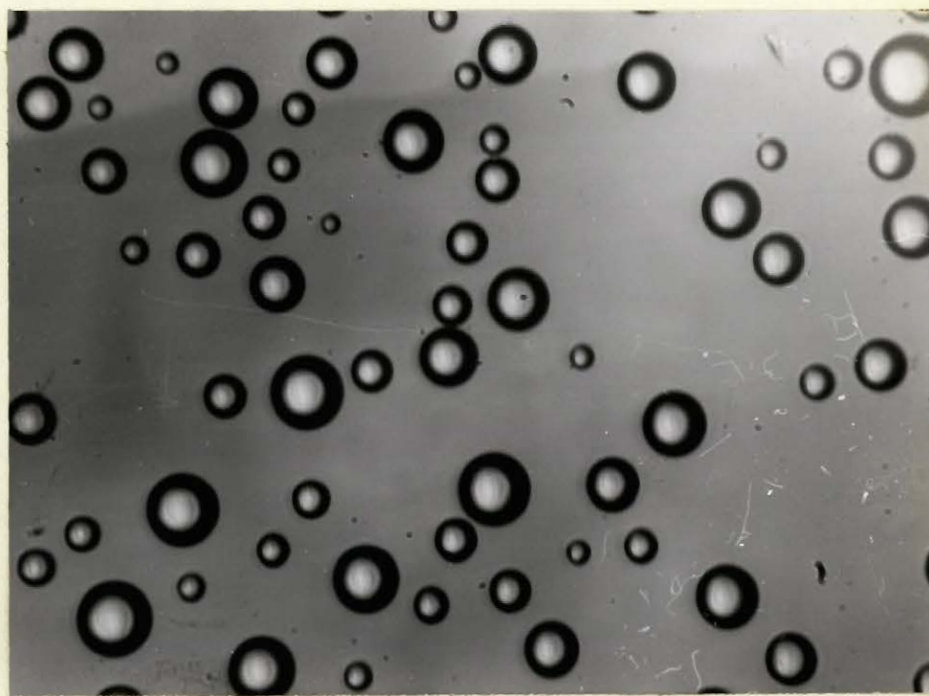


Fig. 16. Photomicrograph of Large Water Droplets
(220 X)

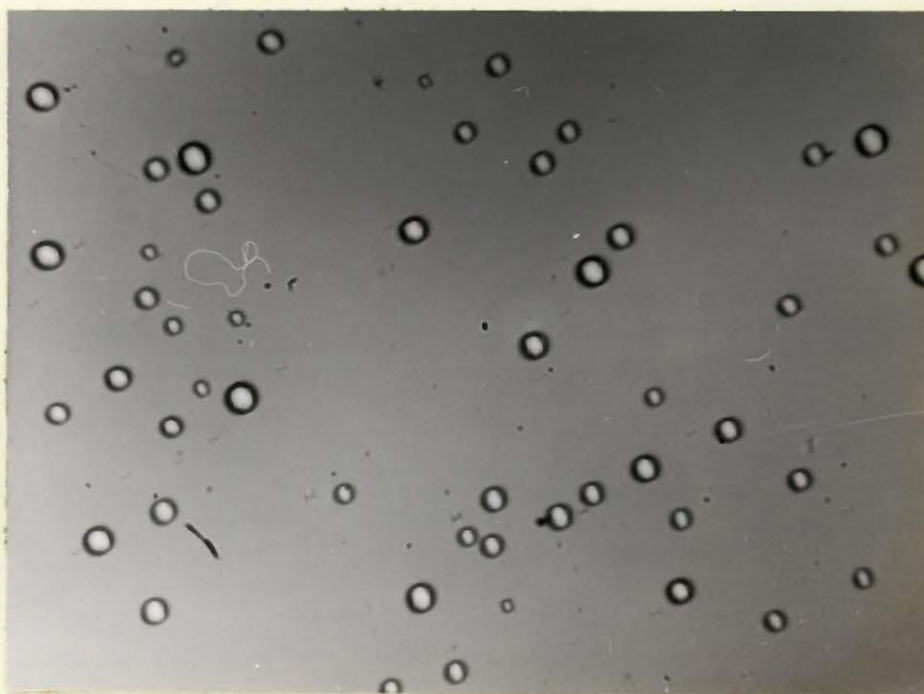


Fig. 17. Photomicrograph of Large Water Droplets
(220 X)

as they proceed along a spray drying chamber. Owing to the large number of factors present however, the relationship between the rate of evaporation and the variables involved may not be always readily apparent. Fortunately, the special design of the drying chamber facilitates the separation of these variables and the assessment of their respective effects on the rate of evaporation.

a) Temperature Distribution

The evaporation of the water droplets proceeding along the drying chamber is perhaps best illustrated by the temperature distribution curves shown in Fig. 9, 10 and 11, since they are a direct function of the amount of water evaporated. The grouping of the runs into three families of curves was done mainly to improve and facilitate the physical presentation. However, Fig. 9 shows principally the effect of air velocity, Fig. 10 the effect of inlet air temperature and Fig. 11 that of droplet size. Although of widely different point values, these curves represent, however, a common pattern of behaviour: starting with a gentle slope in the immediate vicinity of the nozzle, which slowly increases to a maximum, all curves exhibit an inflection point beyond which they fall exponentially until their slope is nearly zero. Although a detailed study of the nozzle range was outside the scope of the present investigation, it is interesting to note that the temperature distribution data seem to indicate that the amount of water evaporated in

the first few inches from the nozzle is relatively small. This inference - which incidentally is contrary to the findings of another investigator (105) - receives strong support from the following line of reasoning. The velocity of the droplets in the nozzle range is undoubtedly quite high. (Some droplet velocity measurements were carried out in a lucite column with a Fastax high speed camera - 7,500 frames per second - using the same type of nozzle as in the spray dryer, but with no drying air. Two inches below the nozzle, values of 170 feet per second on the average were obtained, while 6 inches below, velocities of 30 feet per second were still observed. These results, although not directly comparable, show that the liquid is atomized into droplets very close to the nozzle, and that the initial droplet velocity is very high). The equations presented by Ranz and Marshall (equations 23 and 24, page 49) predict that the heat transfer coefficient is proportional to the square root of the relative velocity and very high evaporation rates can be expected in the nozzle zone. On the other hand, the droplet residence time in this region is inversely proportional to the droplet velocity. Consequently, the quantity of water evaporated will be inversely proportional to the square root of the relative velocity and should therefore be small.

Once the droplets reach their terminal velocity, they will be transported with the air along the chamber, their absolute velocity

being the sum of the air velocity and the terminal velocity. If the droplets were settling in still air, the latter would be of the order of 0.05 feet per second which is negligible when compared to the air velocity (3.9 to 14.8 feet per second); owing to the fact that the effect of the air turbulence on the terminal velocity is not known, it may be assumed that the relative velocity between the droplets and the air is negligible.

b) Heat and Material Balance

The accuracy of the determination of the rate of evaporation depended mainly on the precision of the experimental measurements of the air temperature and air humidity. That the latter was more than adequate is amply demonstrated by Figures 12, 13 and 14, which show the fraction of water evaporated as a function of time, calculated from heat balances (based on temperature measurements, open symbols) as well as from material balances (based on humidity measurements, black symbols). The excellent agreement between the points indicates the general accuracy of the results. Some of the curves, particularly for Runs No. 4, 7 and 8, show that not all the water was evaporated in the time interval given (0.65 second). This apparent discrepancy is due to the formation of some very large droplets at low atomizing pressures, requiring a long time for complete evaporation.

The general agreement between the material balance and the heat balance also indicates that the heat losses were very small. Verifi-

cation of this was obtained by a simple calculation: for example, taking the run with the highest inlet air temperature (Run No. 6) the heat loss in the first 2.87-ft. amounted to approximately 150 B.t.u./hr., using a value of 0.05 B.t.u./(hr.)(°F.)(ft.) for the thermal conductivity of vermiculite. The heat transfer coefficient for the inside film was calculated from the Dittus-Boelter equation, while the heat transfer coefficient for the outside film was calculated from the equation:

$$h = 0.5(\Delta t/D')^{0.25}$$

where Δt - temperature difference between the outside walls of the drying chamber and the room air, °F.;

D' - outside diameter, in.

The total amount of heat required to evaporate the water droplets in the same section was about 8,200 B.t.u./hr., compared to which the heat loss was consequently negligible.

c) Droplet Mean Statistical Diameter

In the derivation of equation (35) on page 87, it was shown that the definition of the term S_w dictated the use of the Sauter diameter, d_{vs} , as the mean statistical diameter of the droplets. The latter was therefore calculated for all the spray samples collected in this study. In this connection, it has already been mentioned that

deflection of some of the smaller droplets during collection might possibly constitute a serious source of error in these determinations. The nature of the mean Sauter diameter is such, however, that its value is almost completely governed by the large droplets in the distribution. This is rather strikingly demonstrated by considering an arbitrary particle size distribution consisting, as an extreme example, of 100 droplets 20 microns in diameter and of 100 droplets 5 microns in diameter. The true mean Sauter diameter of this sample is 19.1 microns. If it is now assumed that all the small droplets are deflected during collection, the mean Sauter diameter of the sample becomes 20 microns. In practice, deflection of more than a fraction of the smaller droplets would be unusual.

Examination of the results presented in Tables IV to XIII shows that the mean Sauter diameter of the spray decreased at first only slightly with distance from the nozzle, and that in certain runs it even increased to a small extent. A behaviour of this nature can be expected where a wide particle size distribution exists: the small droplets will disappear faster than the large droplets will decrease in diameter. In Run No. 10 (Table XIII) where a high atomizing air pressure was used, the particle size distribution was more uniform and consequently the diameter decreased steadily throughout the chamber.

The possibility of predicting accurately the changes in the droplet size distribution of a spray as evaporation proceeds is

obviously of great importance in spray dryer design. To show the feasibility of such an approach - once a representative frequency curve is available at a convenient reference plane - the size distribution at a distance of 5.2-feet from the nozzle was calculated for Run No. 2 (Table V) from the size distribution experimentally determined at a point 3.19-feet from the nozzle. A Nusselt Number of 2.05 was used (this being the average value obtained for the run) and the decrease in diameter of each size group was calculated. The results were then compared with the experimentally determined size distribution and excellent agreement was obtained, as shown in Figure 18, page 113.

d) Heat Transfer Coefficients

The heat transfer coefficients calculated from the experimental results ranged from 270 to 863 B.t.u./hr.)(°F.)(ft.²). The relationship obtained between h and d_{vs} in this study is shown in Figure 19, page 114. A good indication of the accuracy of the experimental work can be obtained from the relatively small scatter of the points about the average curve. To obtain a correlation in terms of the Nusselt Number, the heat transfer coefficients were also plotted against the ratio of the thermal conductivity of the air and the mean Sauter diameter (Figure 20, page 115). The equation of the straight line shown on the graphs is given by:

$$hd_{vs}/k = 2.0$$

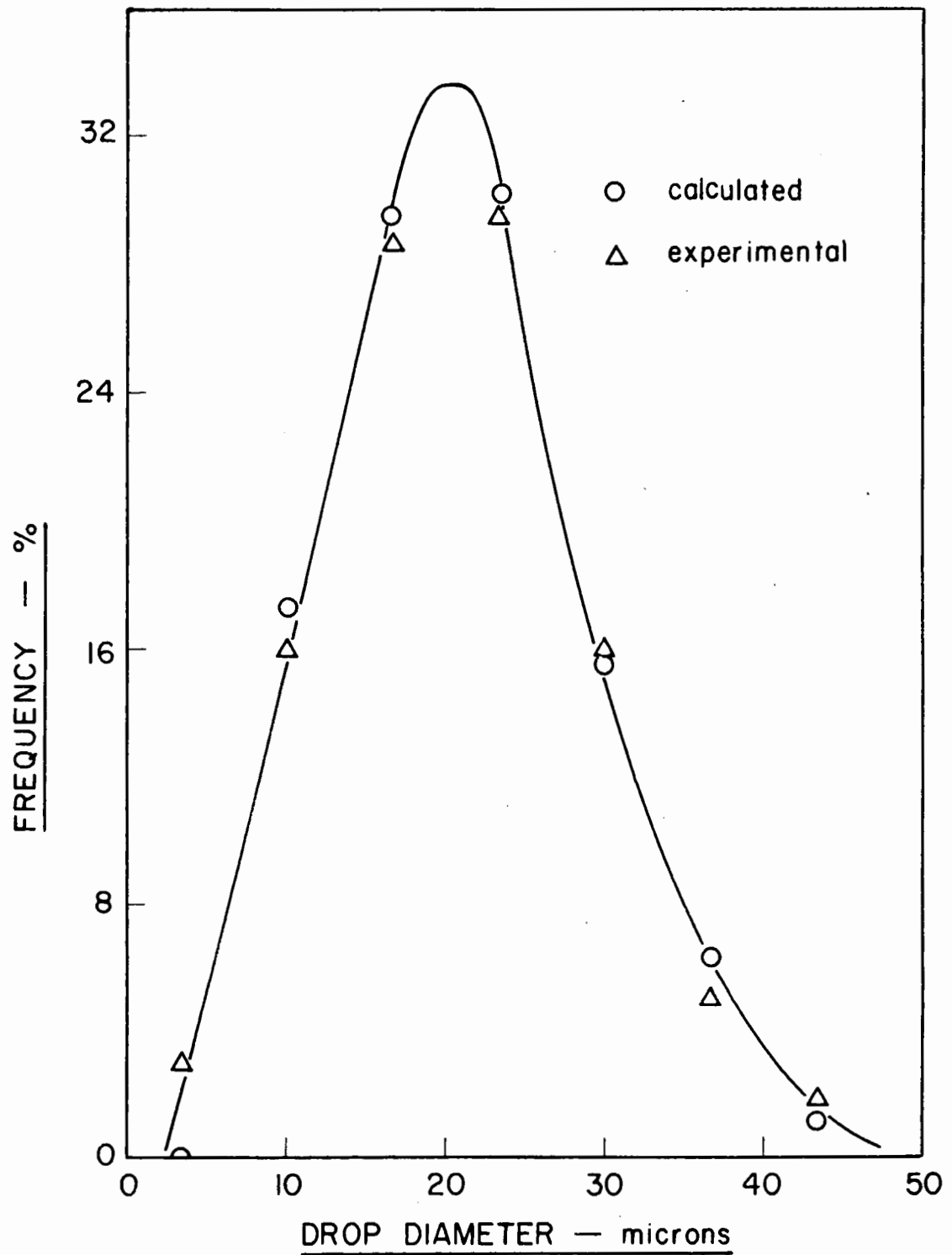


Fig. 18. Calculated and Experimentally Determined Particle Size Distribution (Run No. 2, $x = 5.2$ feet)

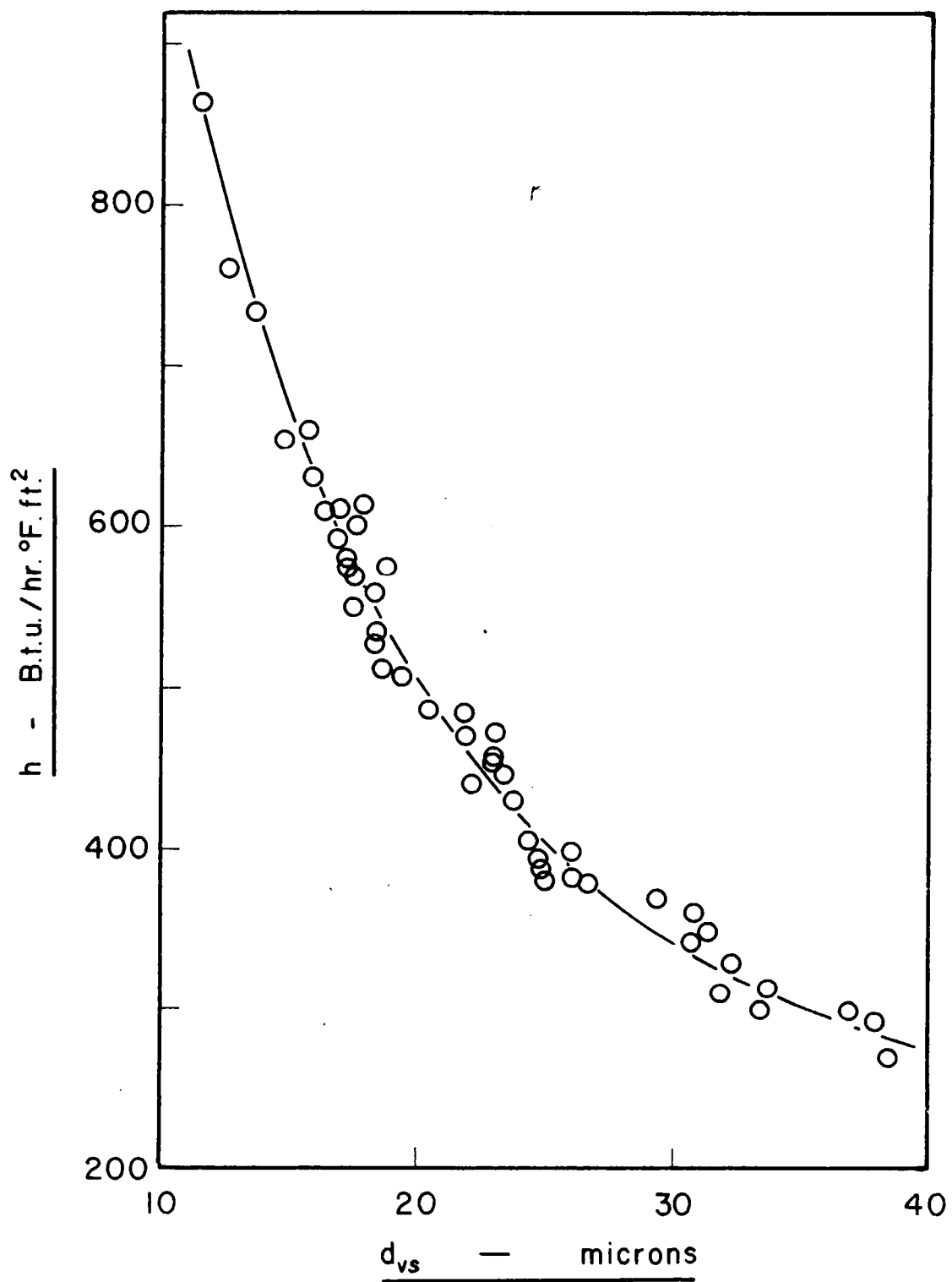


Fig. 19. Variation of the Actual Heat Transfer Coefficient with the Droplet Diameter

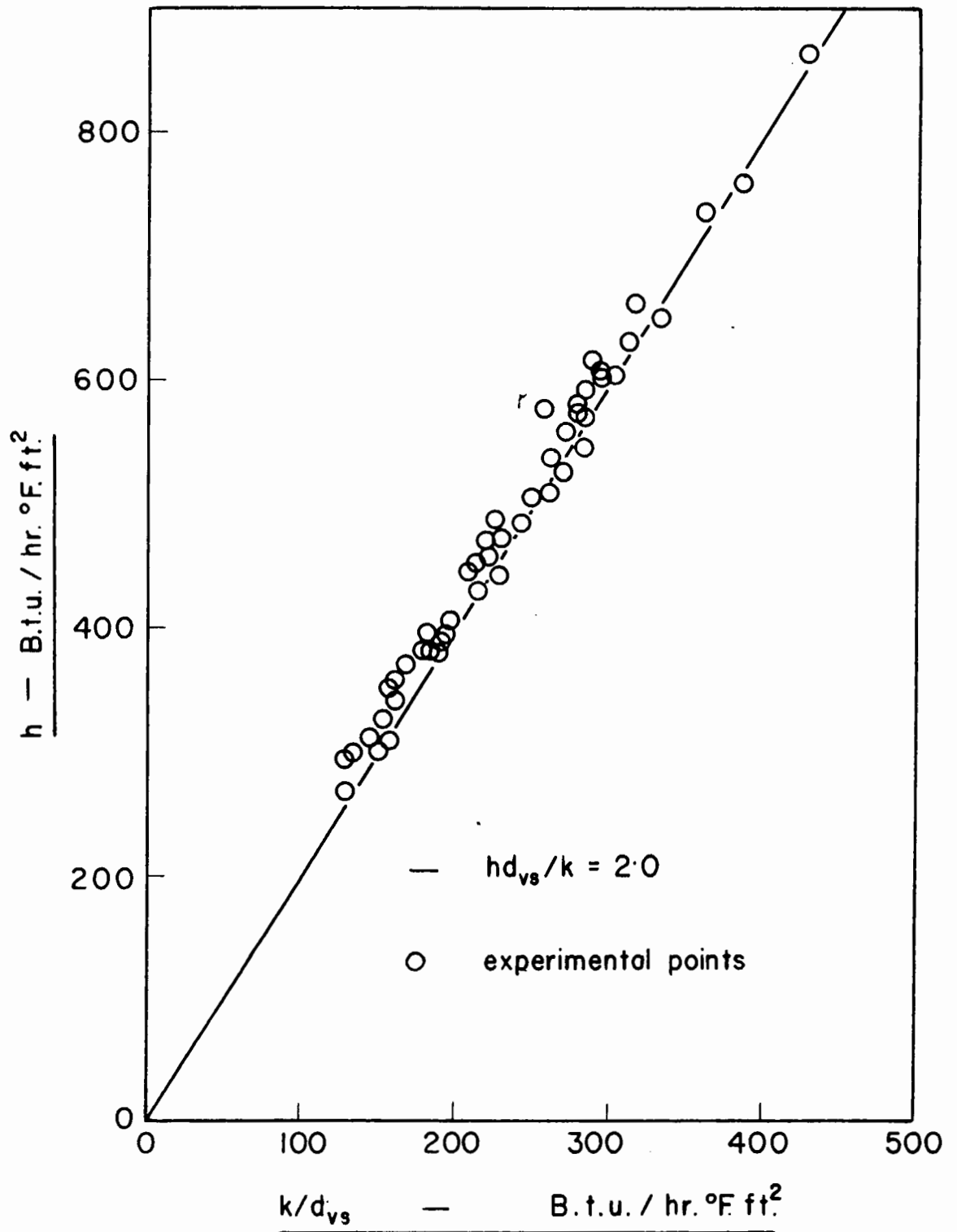


Fig. 20. Correlation of the Actual Heat Transfer Coefficient in Terms of the Nusselt Number

while the average value of the Nusselt Number experimentally obtained was 2.07 ± 0.06 . The average value of the modified Nusselt Number was found to be 1.89 ± 0.06 .

As previously mentioned, the heat transfer coefficients were calculated by substitution of the experimental results into equation (35), and from the derivation of this equation it is obvious that these calculated coefficients are the actual values, since only the latent heat of vaporization at the droplet temperature was included (Equation 33). On the other hand, since the temperature of the air in all runs was rather low, the correction given in equation (29A) on page 38 would be small and could be neglected, and the values of h obtained can be compared directly with the theoretical equations presented in the Historical Section.

III. EVAPORATION AND DRYING OF LIGNOSOL SPRAYS

Water vaporizes from a liquid solution or suspension in very much the same way as it evaporates from a free water surface, except for possible depression of the vapor pressure, in the case of solutions. As the concentration of the solids increases, however, the latter will separate out and at a certain moisture content the drying rate will decrease markedly. Thus two different periods of drying may be recognized, namely the constant rate period and the falling rate period. Many theoretical as well as experimental studies have been carried out to determine the mechanism of drying under conventional conditions but none of the results can be applied directly to spray drying problems owing to the size and motion of the particles involved.

The experimental concurrent spray dryer, described in the previous chapter, was ideally suited for the study of evaporation and drying of atomized solutions, because the appearance and concentration of the solids could be determined as the particles proceeded along the chamber.

1. EQUIPMENT

Only slight modifications were necessary in the original spray

drying apparatus which was described on page 72. A stainless steel feed tank of one-cubic foot capacity was installed for the storage of the Lignosol solution. To obtain very steady flow rates, the feed tank was maintained under pressure with compressed air, thus eliminating the need for a pump. The feed rate was controlled by adjusting the pressure in the tank as well as by means of a 1/4-inch stainless steel needle valve. The rotameter, strainer and preheater in the feed line were used as before. Additional water lines were installed to facilitate flushing and cleaning of all parts of the system.

2. PROCEDURE

The procedure used for the study of the rate of evaporation and drying of Lignosol solutions was identical to that followed in the water runs (page 82 et seq.), except for the additional determination of the solid concentration. Samples of the spray were taken as described on page 58, and the concentration was measured colorimetrically.

Lignosol, as mentioned previously, consists essentially of calcium lignosulphonate, and is more specifically referred to as Lignosol BD. A very similar material is Lignosol TS, in which the calcium ion has been replaced by an ammonium ion. It is also spray dried commercially,

but it has been reported that the normal capacity of the industrial installation, based on Lignosol BD production, is cut approximately in half when Lignosol TS is dried (85). This apparent anomaly could not be explained on the basis of the physical properties of the Lignosol TS solution and consequently the drying rates of these two solutions were compared qualitatively in the experimental spray dryer under identical operating conditions.

A further test was carried out in a laboratory tray dryer, which consisted of a 9x6x1/2-in. transite tray suspended from a trip scale. The tray had a 5x5x1/8-in. depression in the center into which the solution was placed, and with heated air of known temperature and humidity passing over the tray, the rate of evaporation and drying of Lignosol BD and Lignosol TS could be followed under identical constant conditions.

3. CALCULATIONS

The rate of evaporation was calculated from a heat balance as well as from a material balance, using equations similar to those previously given. The heat balance equation becomes, in the absence of any heat of solution:

$$Z(X_f - X_n) \left[\lambda_{wn} + C_{p_v}(t_n - t_{wn}) \right] = \\ = w(C_{p_a} + H_0 C_{p_v})(t_0 - t_n) + Z(C_{p_z} + X_f C_{p_w})(t_f - t_{wn}) \dots (43)$$

where Z is the rate of feed of bone dry Lignosol in pounds per hour and

the subscript z refers to the physical properties of bone dry Lignosol.

The material balance equation is:

$$(X_f - X_n) = w(H_n - H_o)/Z \dots\dots\dots(44)$$

The concentration of the solution was also obtained directly from the reading of the Fisher Neffluoro-Photometer.

4. RESULTS

The experimental tests carried out on the evaporation and drying of Lignosol solutions can be divided into three sections, namely: spray drying of Lignosol BD, spray drying of Lignosol TS, and tray drying of both solutions.

a) Spray Drying of Lignosol BD

All the runs were made under approximately the same conditions of air velocity (about 10 ft./sec.), feed rate (about 5.7 lb. solution per hour), feed concentration (about 20%), and atomizing pressure. The only factor that was varied was the inlet air temperature t_o , ranging from 106.0°F to 419.0°F. Altogether four runs were carried out and the results obtained are presented in Tables XIV to XVII, which include all the constant operating conditions that were presented for the water runs, with the additional value of the feed concentration.

TABLE XIV

SPRAY DRYING OF LIGNOSOL BDRUN NO. 20

Nozzle No. 22B Atom. air pressure = 20 p.s.i.g. Feed temp. = 86°F.

Feed rate = 5.68 lb./hr. Feed concentration = 0.182 lb.Lig./lb.sol.

Air rate = 891 lb.d.a./hr. Average air velocity = 10.5 ft./sec.

OBSERVED					CALCULATED			
\bar{x}	\bar{t}	$\frac{H}{\text{lb.w.}}$	$\frac{X}{\text{lb.w.}}$	$\frac{d_{vs}}{\mu}$	$\frac{X_{hb}}{\text{lb.w.}}$	$\frac{X_{mb}}{\text{lb.w.}}$	$\frac{H_{hb}}{\text{lb.w.}}$	$\frac{H_{mb}}{\text{lb.w.}}$
ft.	°F.	lb.d.a.	lb.Lig.		lb.Lig.	lb.Lig.	lb.d.a.	lb.d.a.
0	147.0	0.0031	4.49		4.49	4.49	0.0031	0.0031
1.46	134.0				2.00		0.0060	
1.79		0.0064	1.86	28.9		1.65		0.0063
1.96	129.9				1.22		0.0069	
2.86	126.5				0.45		0.0078	
3.19		0.0079	0.42	21.1		0.36		0.0078
4.86	125.3				0.19		0.0081	
5.19		0.0082	0.02	16.1		0.10		0.0083
6.86	125.2				0.10		0.0082	
7.19		0.0083	0.02	16.9		0.01		0.0083
8.86	125.1				0.10		0.0082	
9.19		0.0084	0.01	15.8		0.00		0.0083
11.19			0.01	15.0				0.0083

TABLE XV

SPRAY DRYING OF LIGNOSOL BDRUN NO. 21

Nozzle No. 22B Atom. air pressure = 20 p.s.i.g. Feed temp. = 80°F.

Feed rate = 5.66 lb./hr. Feed concentration = 0.194 lb. Lig./lb.sol.

Air rate = 891 lb.d.a./hr. Average air velocity = 10.0 ft./sec.

OBSERVED					CALCULATED			
\bar{x}	\bar{t}	$\frac{H}{\text{lb.w.}}$	$\frac{X}{\text{lb.w.}}$	$\frac{d_{vs}}{\mu}$	$\frac{X_{hb}}{\text{lb.w.}}$	$\frac{X_{mb}}{\text{lb.w.}}$	$\frac{H_{hb}}{\text{lb.w.}}$	$\frac{H_{mb}}{\text{lb.w.}}$
ft.	°F.	lb.d.a.	lb.Lig.		lb.Lig.	lb.Lig.	lb.d.a.	lb.d.a.
0	117.0	0.0060	4.15		4.15	4.15	0.0060	0.0060
1.12	112.0				3.18		0.0072	
1.46	108.3				2.53		0.0080	
1.79		0.0085	2.18	22.8		2.12		0.0085
1.96	103.5				1.64		0.0091	
2.86	98.6				0.75		0.0102	
3.19		0.0103	0.613	18.1		0.66		0.0104
4.86	96.0				0.26		0.0108	
5.19		0.0108	0.370	16.5		0.26		0.0107
6.86	95.7				0.26		0.0108	
7.19			0.250	15.6				0.0108
8.86	95.5				0.18		0.0109	
11.19			0.111	15.2				0.0110

SPRAY DRYING OF LIGNOSOL BDRUN NO. 22

Nozzle No. 22B Atom. air pressure = 20 p.s.i.g. Feed temp. = 80°F.

Feed rate = 5.66 lb./hr. Feed concentration = 0.194 lb.Lig./lb.sol.

Air rate = 891 lb.d.a./hr. Average air velocity = 9.9 ft./sec.

OBSERVED					CALCULATED			
\bar{x}	\bar{t}	$\frac{H}{\text{lb.w.}}$	$\frac{X}{\text{lb.w.}}$	dvs	$\frac{X_{hb}}{\text{lb.w.}}$	$\frac{X_{mb}}{\text{lb.w.}}$	$\frac{H_{hb}}{\text{lb.w.}}$	$\frac{H_{mb}}{\text{lb.w.}}$
ft.	°F.	lb.d.a.	lb.Lig.	μ	lb.Lig.	lb.Lig.	lb.d.a.	lb.d.a.
0	106.0	0.0028	4.15		4.15	4.15	0.0028	0.0028
1.12	101.8				3.34		0.0038	
1.46	98.5				2.77		0.0045	
1.79		0.0052	2.42	27.4		2.20		0.0050
1.96	94.2				1.96		0.0055	
2.86	89.7				1.07		0.0066	
3.19		0.0067	0.89			0.99		0.0068
4.86	85.7				0.42		0.0074	
5.19			0.47	17.4				0.0074
6.86	85.2				0.26		0.0076	
7.19			0.30					0.0076
8.86	84.8				0.18		0.0077	
9.19		0.0075	0.20			0.34		0.0077
12.86	84.0				0.01		0.0079	
13.19			0.03	15.5				0.0079

TABLE XVII

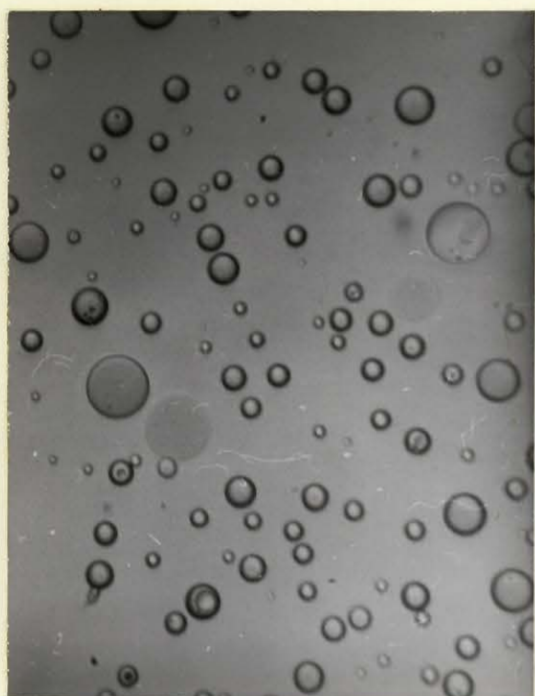
SPRAY DRYING OF LIGNOSOL BD AND LIGNOSOL TSRUN NO. 23

Nozzle No. 22B Atom. air pressure = 20 p.s.i.g. Feed temp. = 96°F.
 Feed rate = 5.70 lb./hr. Feed concentration = 0.182 lb.Lig./lb.sol.
 Air rate = 530 lb.d.a./hr. Average air velocity = 9.46 ft./sec.

LIGNOSOL BD						LIGNOSOL TS	
\bar{x}	\bar{t}	$\frac{H}{\text{lb.w.}}$	$\frac{X_{hb}}{\text{lb.w.}}$	$\frac{X_{mb}}{\text{lb.w.}}$	$\frac{H_{hb}}{\text{lb.w.}}$	\bar{t}_{TS}	$\frac{H}{\text{lb.w.}}$
ft.	°F.	lb.d.a.	lb.Lig.	lb.Lig.	lb.d.a.	°F.	lb.d.a.
0	419.0	0.0261	4.50	4.50	0.0261	419.0	0.0261
0.79	406.0		3.10		0.0288	406.0	
1.12	385.5		0.85		0.0331	385.0	
1.46	379.5		0.19		0.0345	379.1	
1.79		0.0347		0.00			0.0346
1.96	377.8		0.00		0.0347	377.5	
2.86	377.8		0.00		0.0347	377.5	
3.19		0.0348		0.00			0.0348

The experimental observations along the drying chamber at various distances from the nozzle are the temperature of the air t , humidity of the air H , the moisture content of the Lignosol particles X and their mean Sauter diameter d_{vs} . The calculated results consist of the particle moisture content at any point obtained from the heat balance, X_{hb} , and from the material balance, X_{mb} , as given by equations (43) and (44) respectively, and the calculated air humidities H_{hb} and H_{mb} which were obtained from the same two equations. In the high temperature run (Table XVII), no experimental value is shown for the particle moisture content because the Silicone fluid, under which a sample was normally collected, decomposed under these conditions. The diameter of the hollow particles obtained in this run was likewise not determined, but the photomicrographs of the spray samples obtained at 0.96, 1.29, 1.79 and 3.19-ft. from the nozzle are shown in Figure 21, page 126. A photomicrograph of the dried product obtained at a low air temperature (Run No. 20) is shown in Figure 22, page 127.

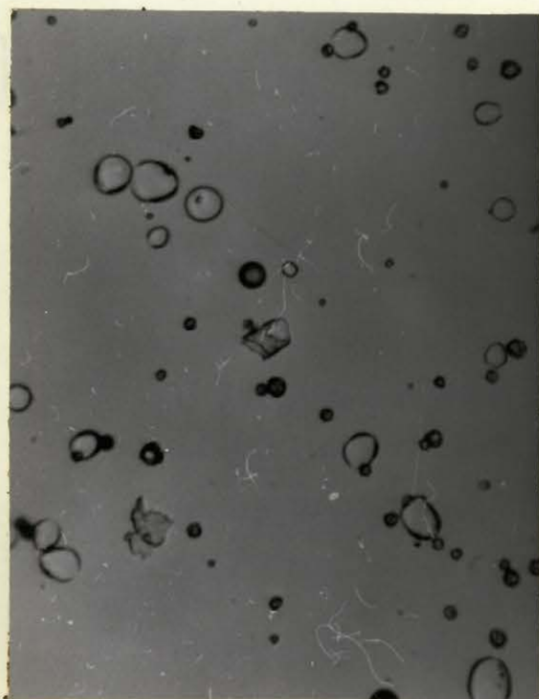
The temperature and humidity changes in the drying chamber as a function of time are plotted in Figures 23 to 26, the time factor being computed from the average velocity of the air and from the distance x for each of the points under consideration. Since in the nozzle zone the droplet velocity is not equal to the air velocity, this time basis is not truly representative of the droplet residence



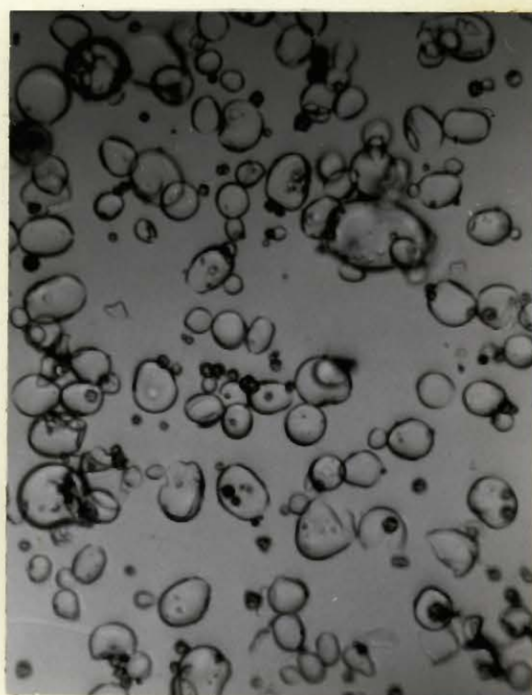
$x = 0.96\text{-ft.}$



$x = 1.29\text{-ft.}$



$x = 1.79\text{-ft.}$



$x = 3.19\text{-ft.}$

Fig. 21. Photomicrographs of Lignosol Particles, Run No. 23 (220X)

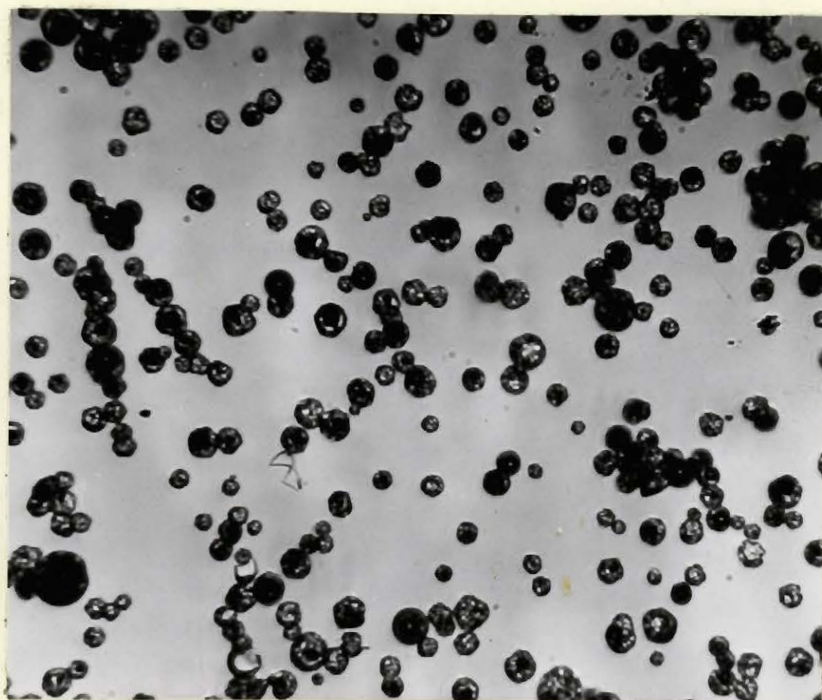


Fig. 22. Photomicrograph of Lignosol Particles, Run No. 20 (220X)

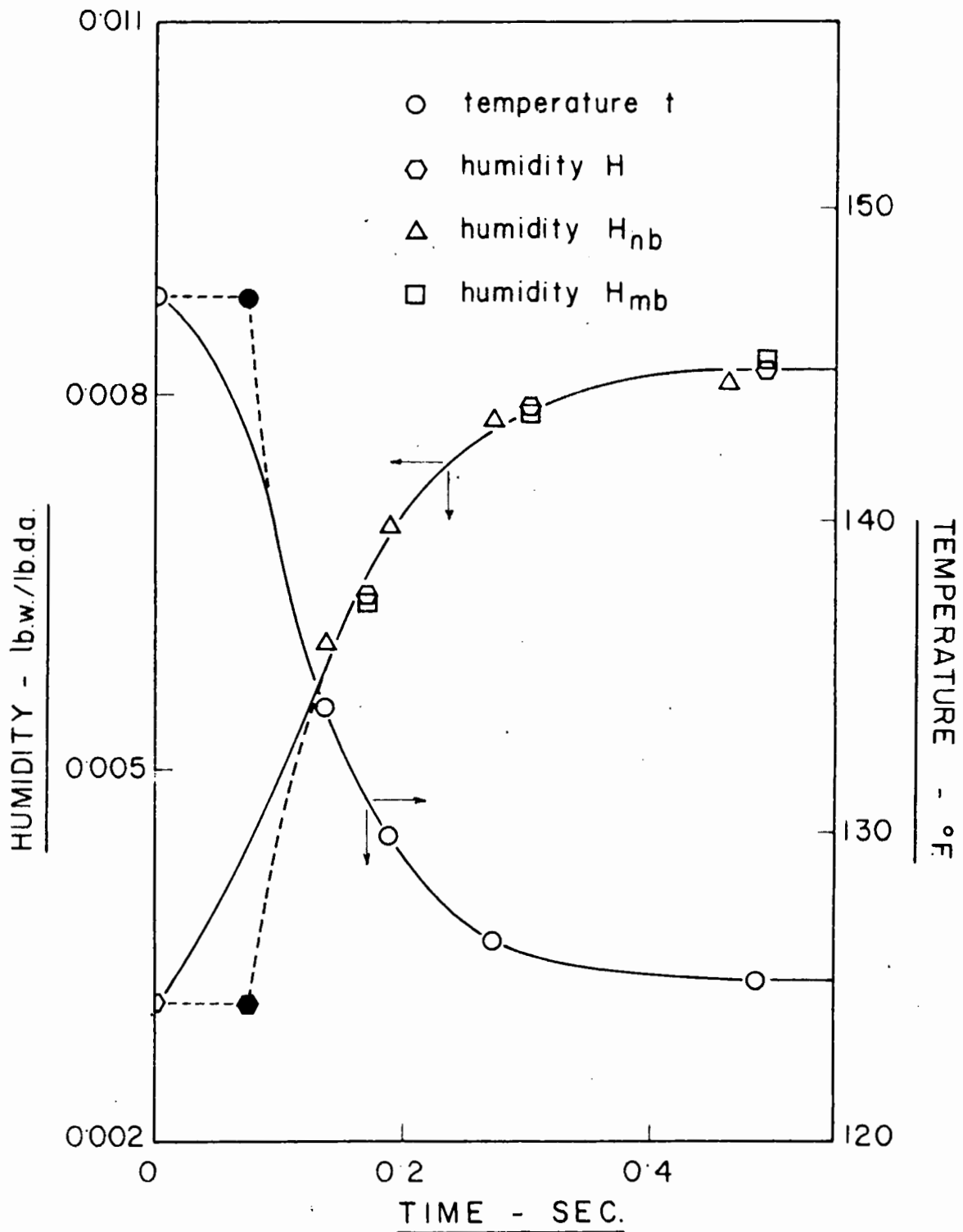


Fig. 23. Temperature and Humidity Distribution in the Spray Dryer, Run No. 20

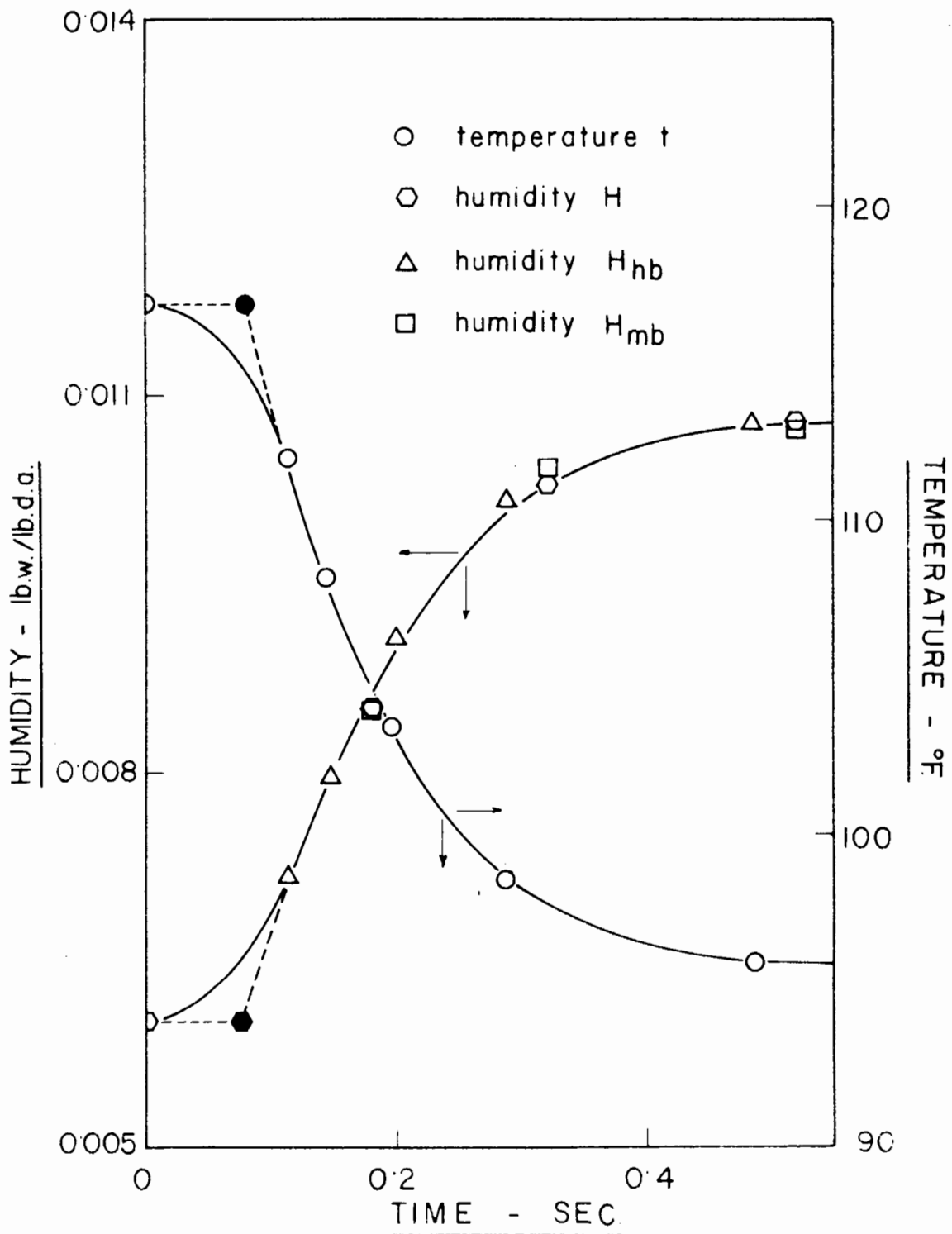


Fig. 24. Temperature and Humidity Distribution in the Spray Dryer, Run No. 21

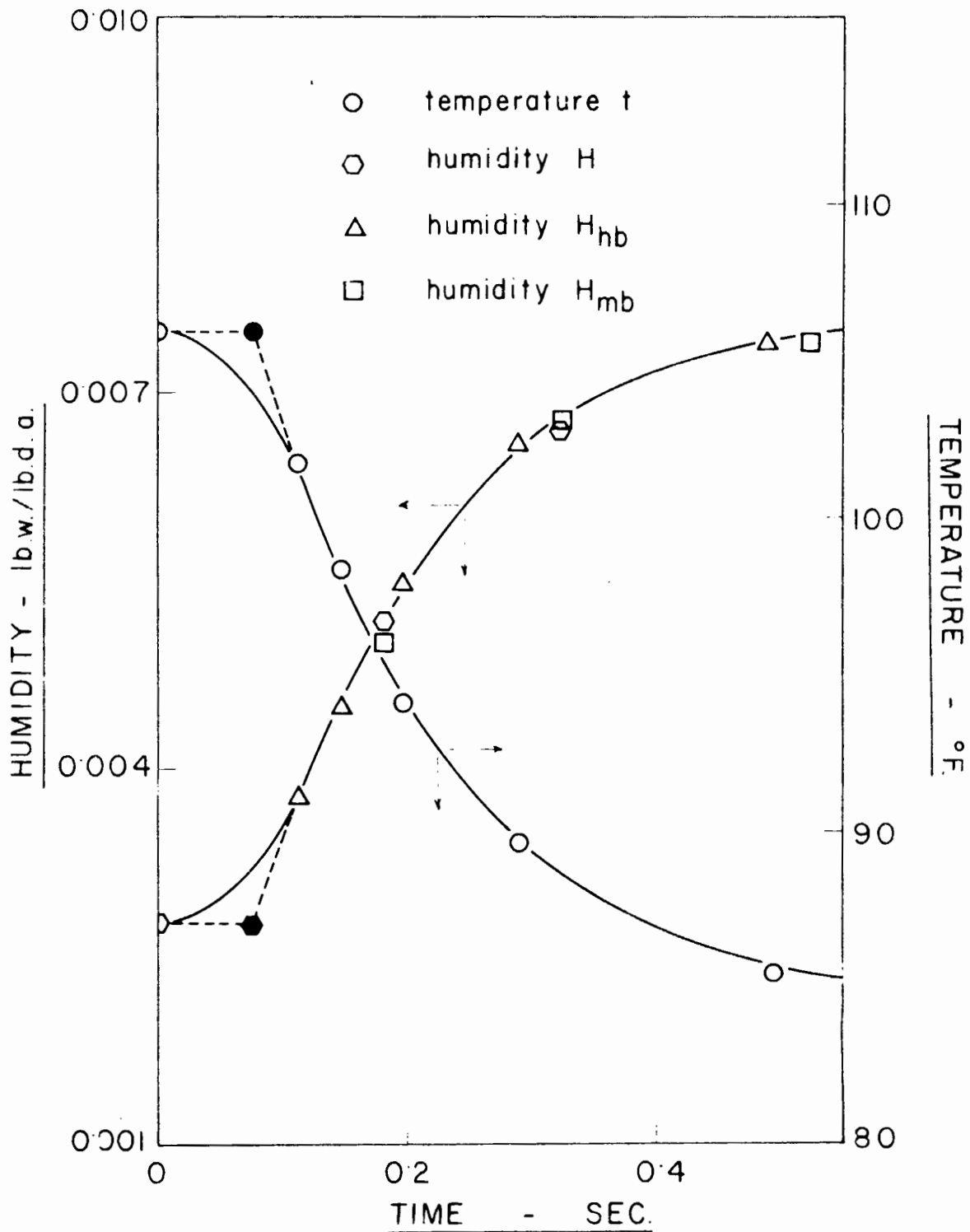


Fig. 25. Temperature and Humidity Distribution in the Spray Dryer, Run No. 22

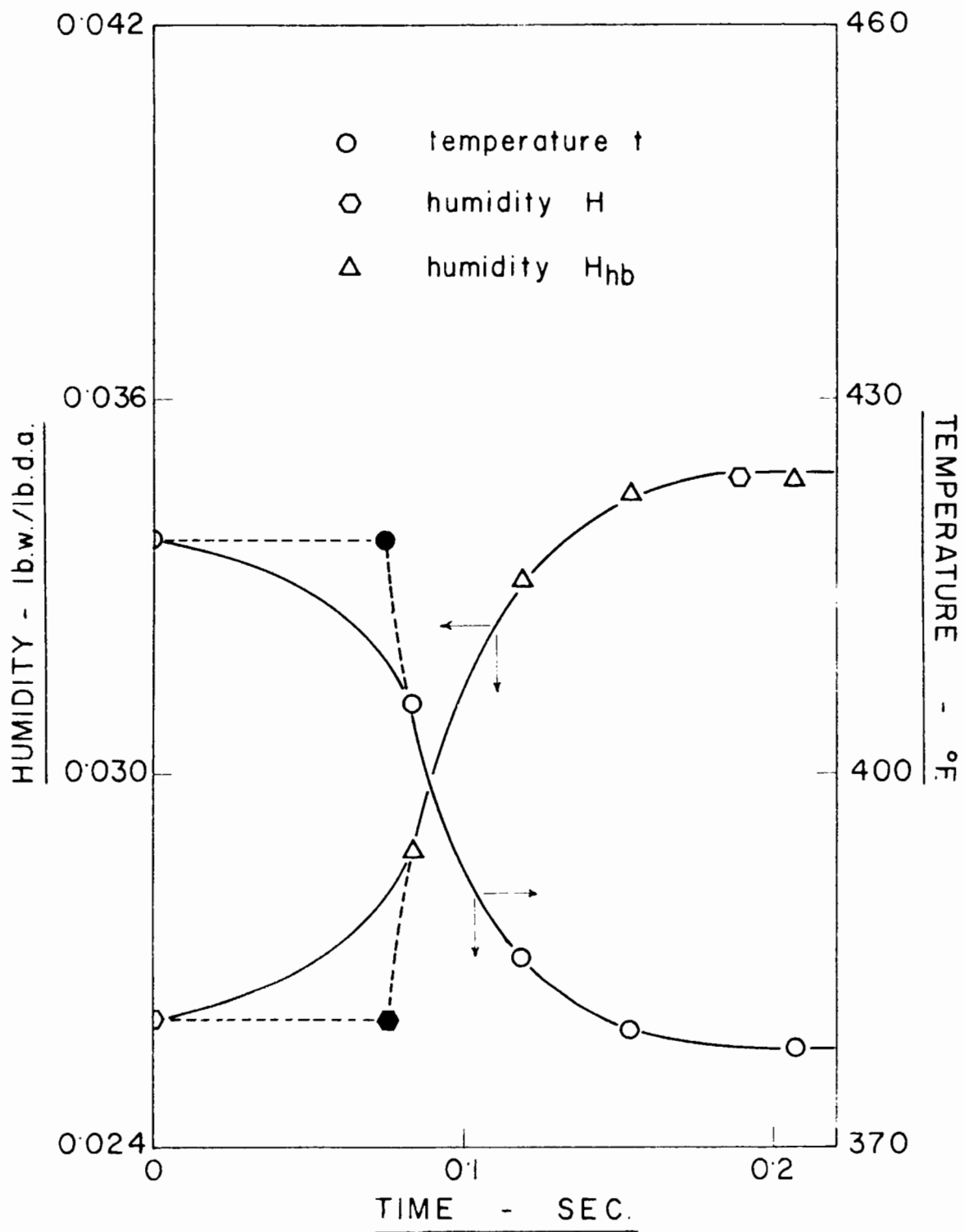


Fig. 26. Temperature and Humidity Distribution in the Spray Dryer, Run No. 23

time in that range, although it is quite accurate when the droplet has reached its terminal velocity. To obtain an arbitrary value of the time at which the latter has been reached, the temperature and humidity curves were extrapolated to their respective initial values. It should be emphasized that the time thus obtained is based on the assumption of zero evaporation in the nozzle zone.

The changes in moisture content with time for the four runs are plotted in Figures 27 and 28, zero time being taken as the arbitrary value derived from the extrapolated curves, and the experimental points as well as the points calculated from heat balances and from material balances are shown.

b) Spray Drying of Lignosol TS

To permit a fully quantitative approach to the spray drying of Lignosol TS - similar to that used with Lignosol BD - would have necessitated the complete determination of its physical properties. Since the drying of this material is only of secondary interest, it was decided that a qualitative test would be sufficient. This test was carried out under identical conditions to those used in Run No. 23 with Lignosol BD, and the temperature distribution obtained along the drying chamber is shown together with results of this run in Table XVII. Although the temperature distribution was almost identical, the final appearance of the dried particles was quite different, as shown by the photomicrograph given in Figure 29, page 135.

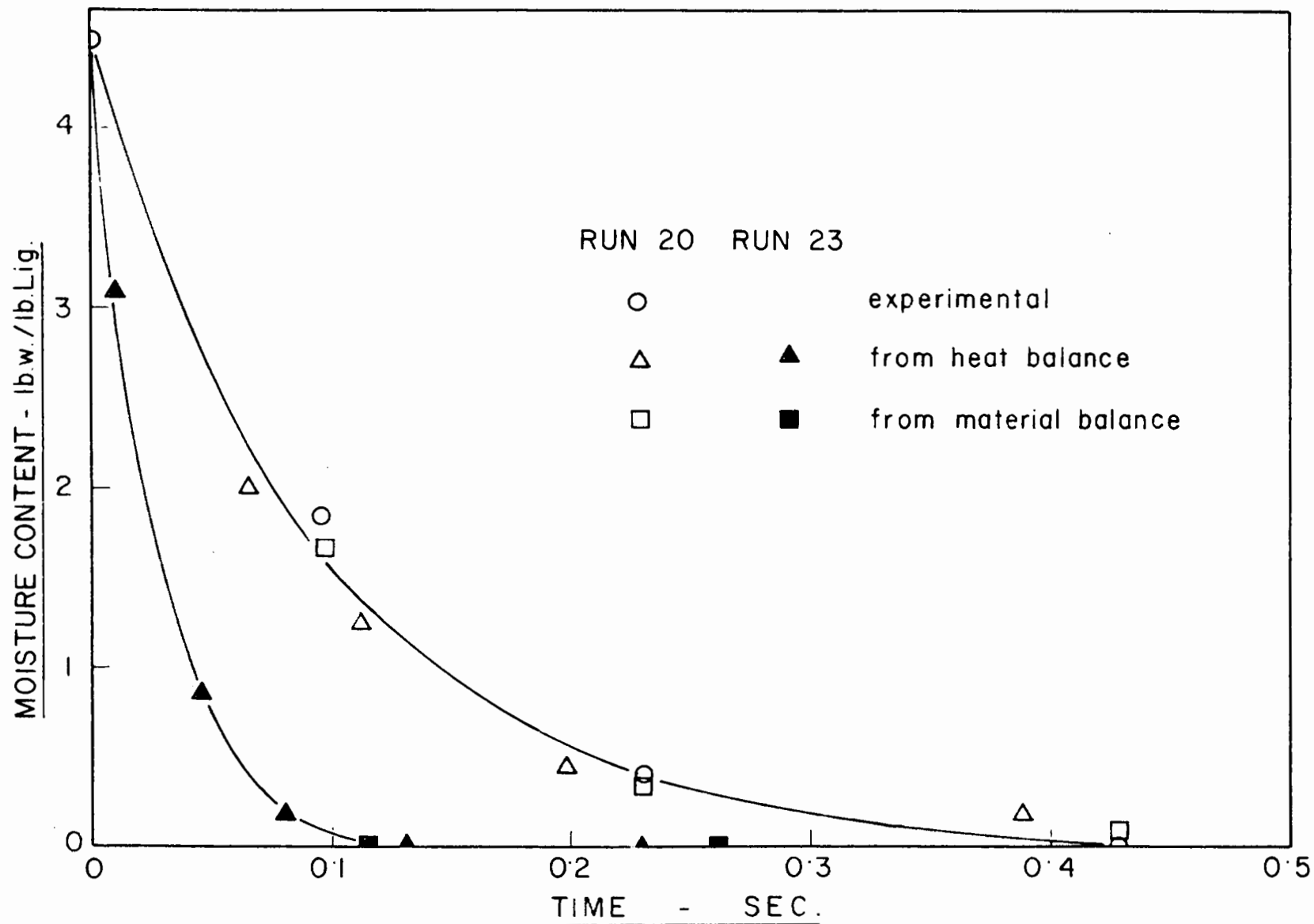


Fig. 27. Drying of Lignosol Sprays

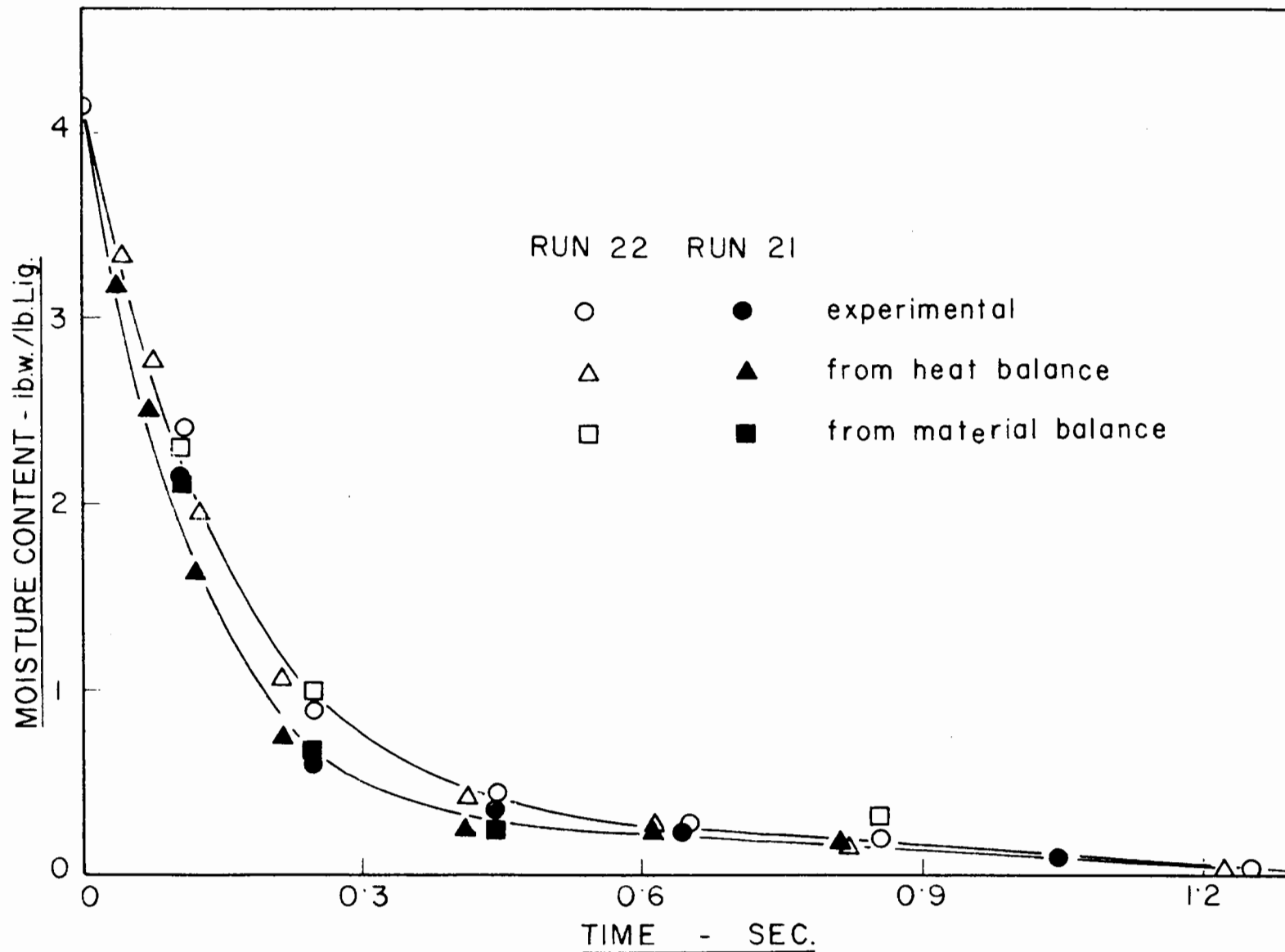


Fig. 28. Drying of Lignosol Sprays



Fig. 29. Photomicrograph of Spray Dried Lignosol TS (220X)

c) Tray Drying

The rate of evaporation of Lignosol BD and Lignosol TS were compared in a laboratory scale tray dryer under identical constant drying conditions. The air temperature and humidity were 118.5°F. and 0.003 pound of water per pound of dry air, respectively. The initial concentration of both the solutions was 20%, and the results obtained are shown in Figure 30, page 137.

5. DISCUSSION

a) Spray Drying of Lignosol BD

The progressive evaporation and drying of the Lignosol particles down the spray drying chamber appear to be faithfully represented by the temperature and humidity distribution curves shown in Figure 22 to 25. The humidity data are particularly significant, because of the close agreement between the experimental values and those calculated by mass and heat balances. Since all four runs were carried out under approximately the same operating conditions, with the exception of the inlet air temperature, the effect of this variable can be assessed directly from the curves: thus at a t_0 of 419°F., the total drying time required was 0.12 second, while at t_0 of 106°F., approximately 1.3 second was necessary.

It is extremely interesting to note that extrapolation of the temperature and humidity distribution curves to the original inlet

McLENNAN LIBRARY
 XEROX/MICROFILM SERVICES
 Name *Hofmann*
 Dept. *History*
 Status *Professor*
 Date *14 Nov 72*
 Material to be copied:
maps

Signature *P. Hofmann*
 Meter Nos.: *2000*
 Charges *10*
 Verified by: *704*
 Cash Cheque Req. M.O.

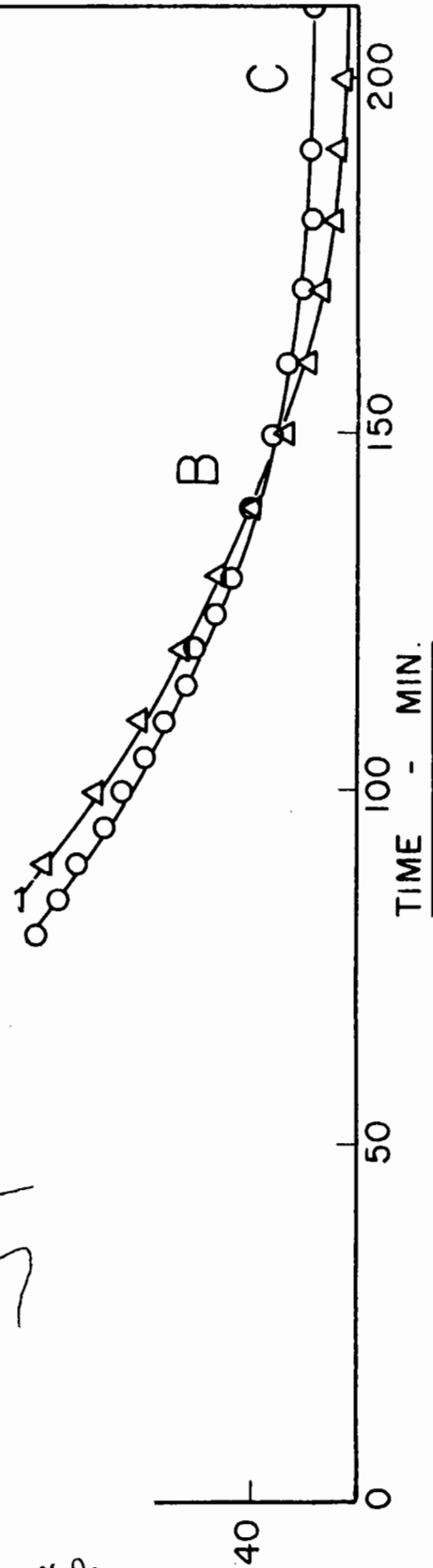


Fig. 30. Tray Drying

conditions in all four cases gave the identical residence time of 0.075 second. At an average air velocity of 10-feet per second, this corresponds to a particle trajectory of 0.75 foot, which may be interpreted as the distance from the nozzle at which terminal velocity is reached, on the assumption that no evaporation has occurred. In Figures 23 to 26 the broken lines indicate the process as assumed above, while actually a certain amount of evaporation does take place in the nozzle zone - which extends beyond the 0.75 foot distance - as shown by the full lines.

The change in the average moisture content of the particles with time is given in Figures 26 and 27, which also show very good agreement between the experimentally-determined values and moisture contents calculated by heat balances and by material balances. Besides affecting the drying time required to attain a specified residual moisture content, the inlet air temperature appears to have a profound influence on the appearance of the product. Thus, from the photomicrograph in Figure 29 it can be seen that the dried particles were solid at an inlet air temperature of 147°F., while at an inlet air temperature of 419°F. the particles expanded to hollow, nearly-spherical shapes in the last stages of drying (Figure 28).

Throughout this study, emphasis has been placed on the accurate determination of the mean droplet or particle diameter and of the size distribution data. No experimental check on this aspect of the work

could be obtained with water droplets, since they obviously disappear gradually from the system. With Lignosol particles, however, size distribution data should remain constant down the chamber, once moisture removal is complete. Thus in Run No. 20 (Table XIV) all the particles were completely dry at a distance of 5.19 feet from the nozzle, and consequently their size distribution at all points beyond this should remain constant. This is clearly verified by the experimentally-determined size distribution data at distances of 5.19, 7.19, 9.19 and 11.19 feet from the nozzle, as shown by Figure 31, page 140. An even more exacting verification can be obtained by calculating the mean volume diameter (not the mean Sauter diameter) of the spray. Providing there was no agglomeration of the particles and the latter were solid, the mean volume diameter of the particle suspension should be a function of the average concentration only, as shown by the equation:

$$(\pi d_v^3 \rho) / (6) = (Z) / (c) \dots\dots\dots(45)$$

Equation (45) can therefore be used to calculate d_v at any point where the concentration is known. Table XVIII gives a comparison between the experimentally-determined mean volume diameters at various points down the chamber and the corresponding calculated values, starting at a distance of 1.79 foot from the nozzle. The results indicate that the method used for the particle size determination was

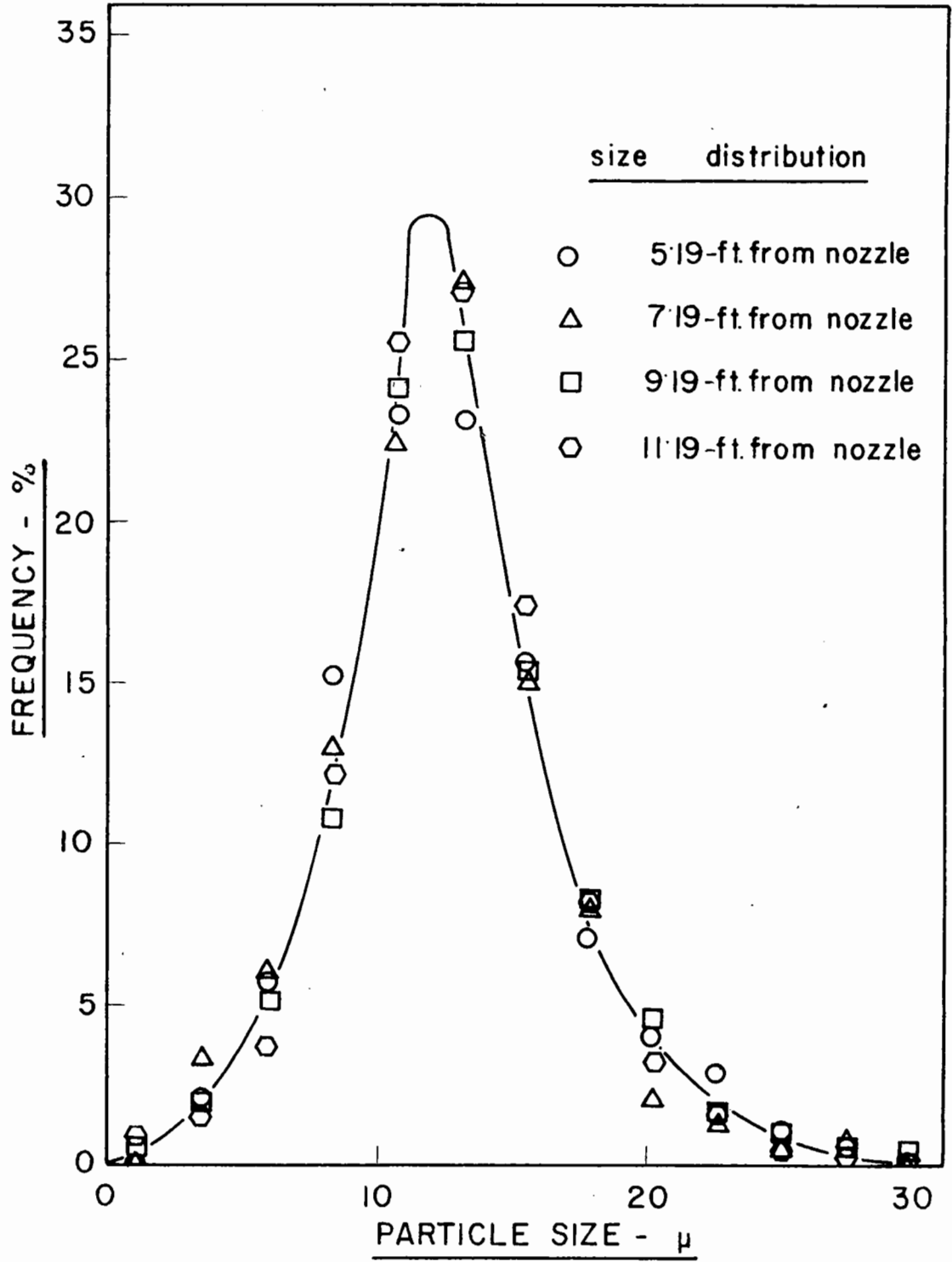


Fig. 31. Particle Size Distribution, Run No. 20

TABLE XVIIIMEAN VOLUME DIAMETERS

(Experimental value and the value calculated from
the mean volume diameter 1.79-ft. from the nozzle)

<u>x</u> ft.	<u>RUN 20</u>		<u>RUN 21</u>		<u>RUN 22</u>	
	EXP.	CONV.	EXP.	CONV.	EXP.	CONV.
1.79	21.6	21.6	20.3	20.3	22.2	22.2
3.19	17.7	16.9	16.6	15.7		
5.19	14.9	15.1	15.2	14.7	15.8	16.0
7.19	14.4	14.6	14.3	14.2		
9.19	14.3	14.5				
11.19	13.9	14.5	13.7	13.9		
13.19					13.9	13.9

very reliable indeed, because in the case of the mean volume diameter, the small particles are no longer unimportant, in direct contrast with the mean Sauter diameter, as clearly shown by the respective definitions of the two diameters:

$$d_{vs} = \frac{\sum nd^3}{\sum nd^2}, \quad d_v = (\frac{\sum nd^3}{\sum n})^{1/3}$$

b) Drying of Lignosol TS

The results presented in Table XVII show that the temperature distribution in the drying chamber was practically the same when Lignosol TS and Lignosol BD were spray dried under identical conditions, and consequently the drying rates of these two materials must be nearly identical. A microscopic examination of the commercial product, as obtained from Lignosol Chemicals Co., revealed that the particles of the TS material were considerably larger than those of BD, while the product obtained in the laboratory spray dryer showed little difference in size. A difference of this kind would explain the lowered capacity reported (85), and it can be seen from equations (9) and (13) that the particle size from a pneumatic nozzle will be affected by the physical properties of the solution to a different degree from that observed from a disk atomizer of the type used by Lignosol Chemicals.

The tray drying experiment also confirmed the similarity in drying rates of Lignosol BD and Lignosol TS (Figure 30). The drying rate was

constant for both solutions up to point A where a thin crust started forming on the surface. The crust was completed at B and assumed a hard consistency at C, at which point all drying practically stopped, in spite of the fact that the bulk moisture content was only about 50%.

c) Calculation of Drying Time

One of the most important steps in spray dryer design is the calculation of the time necessary to attain a desired value of the residual moisture content. If the spray consists of pure liquid droplets and if the size distribution at the nozzle is known and can be expressed in terms of a mathematical equation, then the approach of Probert (106) can be used to calculate the time required. In all industrial applications, however, the particles contain dissolved solids and furthermore the size distribution can not be readily expressed mathematically to any degree of accuracy.

Since the heat transfer coefficients are inversely proportional to the diameter and the surface area is proportional to the diameter squared, the rate of evaporation of a particle will be a direct function of the diameter. On the other hand, the amount of water that must be removed is proportional to the diameter cubed and the total drying time will therefore be proportional to the diameter squared. Consequently the small particles will be completely dry

much sooner, as can be seen from the experimental results of Run No. 20 shown in Figure 32, page 145. The droplets 14 microns and less in diameter were dry about 1.79 foot from the nozzle, while the large droplets decreased in size up to 11.19 feet from the nozzle.

Although no mean statistical diameter can be employed, the drying time can be calculated for each individual particle size. The differential amount of heat required for evaporation at the particle surface is given by the equation:

$$dQ = \lambda_w dm \dots\dots\dots(46)$$

and the rate of heat transfer at the droplets' surface can be expressed as:

$$dQ = hnr d^2(t - t_w) d\theta \dots\dots\dots(47)$$

The heat transfer coefficient given in equation (47) is the actual one, and in order to permit at high temperatures the use of the results obtained in the water tests, the corrected value must be used (equation 29A, page 38), giving, when equation (46) and (47) are combined together with equation (45)

$$dm = \left\{ 6hZ'(t - t_w) \right\} / \left\{ d\rho_s c \left[\lambda_w + C_{p_v}(t - t_w) \right] \right\} d\theta \dots\dots(48)$$

Since c and consequently ρ_s , d and t_w will be functions of dm ,

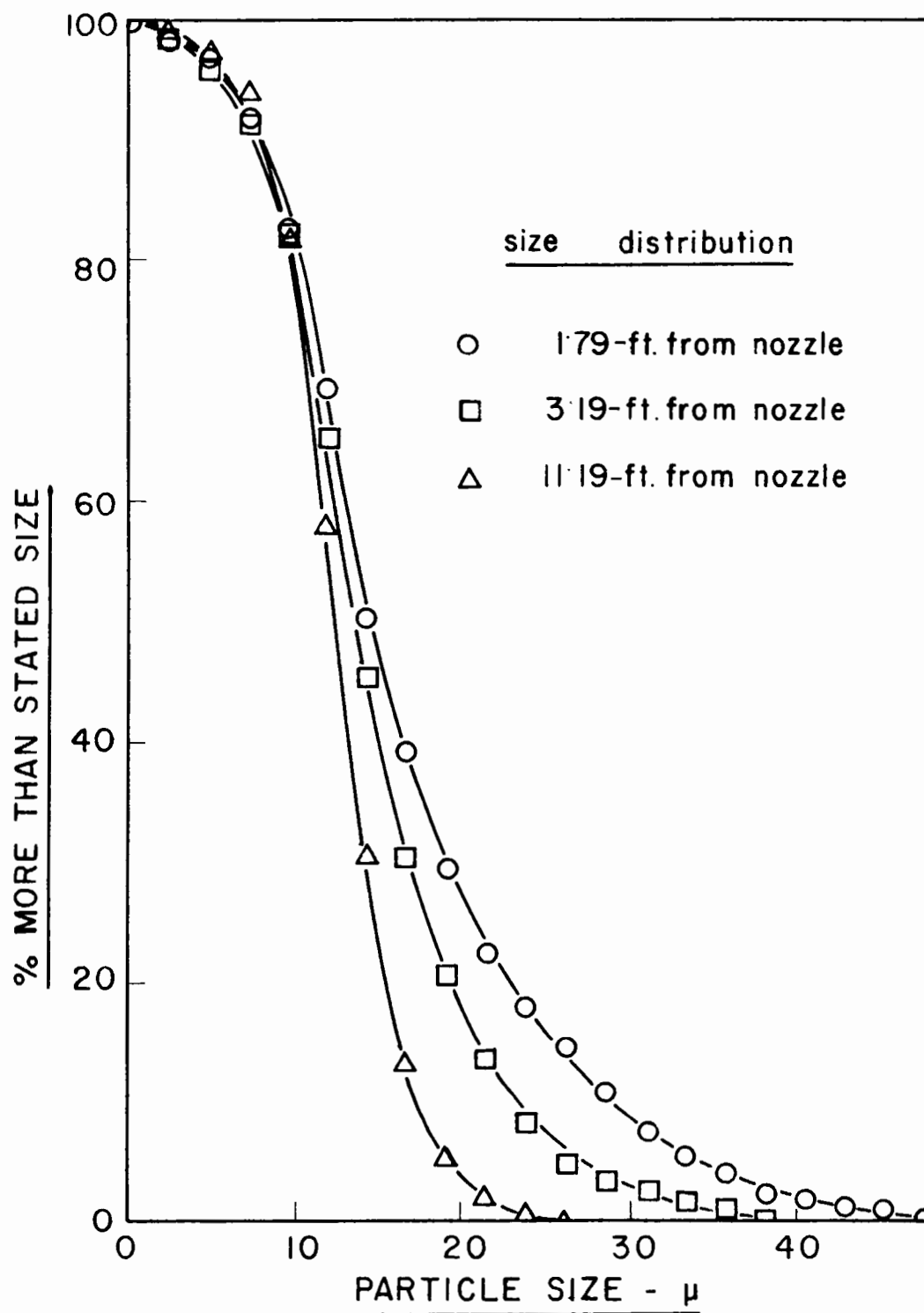


Fig. 32. Particle Size Distribution, Run No. 20

equation (48) can not be integrated directly. A stepwise calculation for the various group sizes is, however, possible, and was carried out to verify the experimental results of Runs No. 20, 22 and 23, the last of which was at a high temperature.

The particle spectrum was divided into six groups of drop sizes. The mass of bone dry Lignosol per hour contained in each group was calculated from the average diameter for that group and the experimental particle size distribution obtained on the dry product collected at the bottom of the chamber. Equation (48) was then used to calculate the change in concentration for each group in incremental intervals $\Delta\theta$, starting with the initial conditions in the atomized spray. More specifically, these calculations were based on the following procedure:

1. For each size group, the initial diameter of the droplet was back-calculated from equation (45) and its temperature determined from Figure 5, page 71, using the bulk concentration of the feed to determine the saturation vapour pressure.
2. The amount of water evaporated Δm in the time increment $\Delta\theta$ was calculated from equation (48), using the inlet conditions for all the values in the equation, and using Figure 19, page 114, to calculate the actual heat transfer coefficient.
3. The new conditions of air properties and particle properties following evaporation occurring during the incremental period $\Delta\theta$ were calculated from the change in concentration that was

obtained in step 2 during that time.

4. The calculations in step 2 were repeated, but this time using the prevailing conditions as obtained in step 3.
5. The values of Δm as calculated in steps 2 and 4 were averaged to give the proper change in concentration for each size group in the time interval $\Delta \theta$.
6. The stepwise calculations given in 1 to 5 were repeated for new time intervals $\Delta \theta$ until the average concentration of the spray was almost 100% solids.

The results of the stepwise calculations are shown in Tables XIX to XXI and the comparison between the calculated and the experimentally-determined moisture contents under the same conditions is shown in Figure 33, page 151. The very good agreement between all the data indicates the validity of the approach, and also serves to confirm the precision of the heat transfer coefficients shown in Figure 19, which were used in the calculations.

In Run No. 23 the dried product consisted of hollow particles, which expanded during the last stages of the drying process, (Figure 28). The particle size distribution could therefore not be determined experimentally from the dried product. Since the atomizing conditions in Run No. 23 were the same as in Run No. 20 and since the feed concentration was equal in both cases, the distribution obtained in the latter case was used in the calculation of the total drying time of

CALCULATED DRYING TIME FOR LIGNOSOL SOLUTIONS

(PARTICLE CONCENTRATION-%)

CONDITIONS AS IN RUN NO. 20

<u>diameter - μ</u>	<u>Z' - lb. dry Lignosol/hr.</u>
2.4	0.0002
7.2	0.0282
11.9	0.3458
16.7	0.4690
21.4	0.1530
26.2	0.0387

<u>θ</u> sec.	<u>DRY PARTICLE DIAMETER</u>						<u>$X_{ave.}$</u> <u>$\frac{lb.w.}{lb.Lig.}$</u>	<u>t</u> °F.
	2.4	7.2	11.9	16.7	21.4	26.2		
0	18.2	18.2	18.2	18.2	18.2	18.2	4.49	147.0
0.05	100	73.3	30.5	23.6	21.3	20.2	2.95	138.8
0.10	100	100	56.9	30.9	24.9	22.3	1.85	134.4
0.15	100	100	79.5	41.7	29.2	24.7	1.18	131.0
0.20	100	100	100	60.4	34.5	27.3	0.68	128.5
0.25	100	100	100	87.9	41.1	30.3	0.36	126.9
0.30	100	100	100	100	49.7	33.7	0.22	126.2
0.35	100	100	100	100	61.2	37.7	0.15	126.0
0.40	100	100	100	100	76.7	42.5	0.09	125.6
0.45	100	100	100	100	93.7	48.1	0.05	125.3
0.55	100	100	100	100	100	63.1	0.02	125.3

CALCULATED DRYING TIME FOR LIGNOSOL SOLUTIONS

(PARTICLE CONCENTRATION-%)

CONDITIONS AS IN RUN NO. 22

<u>diameter - μ</u>	<u>Z' - lb. dry Lignosol/hr.</u>					
2.4	0.0003					
7.2	0.0296					
11.9	0.3300					
16.7	0.3950					
21.2	0.2521					
23.8	0.0930					

<u>θ</u> sec.	<u>DRY PARTICLE DIAMETER</u>						<u>$X_{ave.}$</u> <u>lb.w.</u> lb.Lig.	<u>t</u> °F.
	2.4	7.2	11.9	16.7	21.2	23.8		
0	19.4	19.4	19.4	19.4	19.4	19.4	4.15	106.0
0.05	91.4	48.5	26.8	22.9	21.5	21.0	3.22	101.1
0.10	100	81.2	38.0	27.0	23.7	22.7	2.49	97.2
0.15	100	100	56.0	31.7	26.0	24.4	1.91	94.2
0.20	100	100	88.6	37.5	28.6	26.2	1.44	91.6
0.25	100	100	100	44.2	31.3	28.0	1.16	90.3
0.35	100	100	100	62.1	37.3	31.9	0.77	88.2
0.45	100	100	100	87.7	44.6	36.4	0.47	86.5
0.55	100	100	100	100	53.4	41.4	0.32	85.7
0.65	100	100	100	100	64.4	47.5	0.22	85.1
0.75	100	100	100	100	78.4	54.5	0.14	84.7
0.85	100	100	100	100	89.3	62.9	0.08	84.4
0.95	100	100	100	100	95.7	72.7	0.04	84.2
1.05	100	100	100	100	97.0	84.1	0.03	84.2

TABLE XXI
CALCULATED DRYING TIME FOR LIGNOSOL SOLUTIONS
(PARTICLE CONCENTRATION-%)

<u>CONDITIONS AS IN RUN NO. 23</u>								
	<u>diameter - μ</u>		<u>Z' - lb. dry Lignosol/hr.</u>					
	2.4		0.0002					
	7.2		0.0282					
	11.9		0.3458					
	16.7		0.4690					
	21.4		0.1530					
	26.2		0.0387					

<u>θ</u> sec.	<u>DRY PARTICLE DIAMETER</u>						<u>$X_{avg.}$</u> <u>lb.w.</u> <u>lb.Lig.</u>	<u>t</u> °F.
	2.4	7.2	11.9	16.7	21.4	26.2		
0	18.2	18.2	18.2	18.2	18.2	18.2	4.50	419
0.01	100	48.3	30.2	23.2	21.2	20.2	2.99	405
0.02	100	100	58.9	30.8	24.9	22.4	1.83	394
0.03	100	100	100	42.1	29.4	25.0	1.09	387
0.04	100	100	100	60.6	35.3	27.9	0.66	383
0.05	100	100	100	84.0	42.0	32.0	0.37	380
0.06	100	100	100	100	53.0	38.0	0.19	378

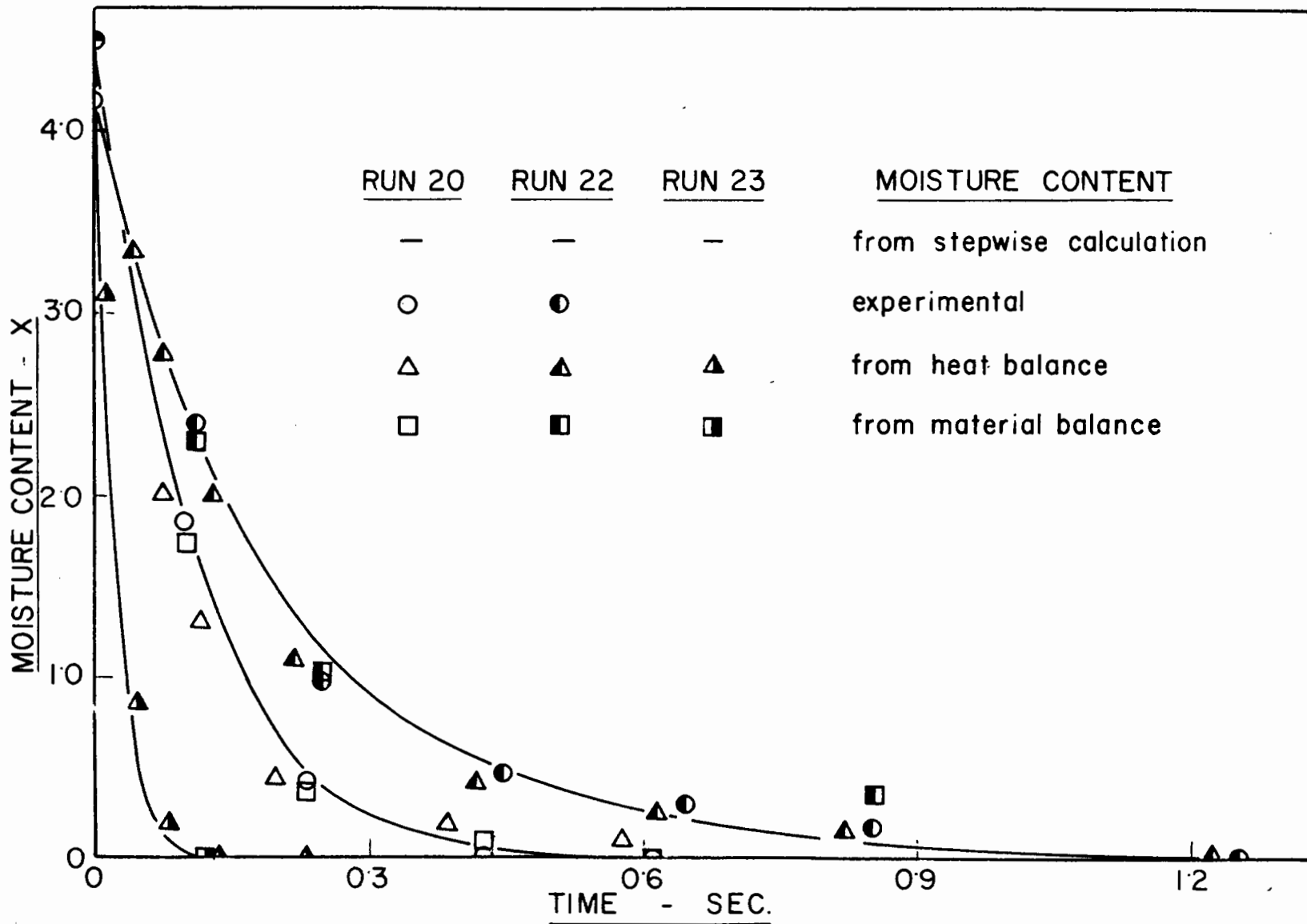


Fig. 33. Calculated and Experimental Rate of Drying of Lignosol Sprays

Run No. 23. Any correction for the sudden increase in the droplet diameter as they dried was negligible, because expansion occurred only near the end of the drying process; droplets were still liquid at an average concentration of at least 84%.

It may appear from the results, that in spite of the wide variation of the inlet air temperature, the capacity of the dryer remained unchanged. However, it should be pointed out that no effort was made to operate the unit at its full capacity; rather, the operating variables were maintained constant as far as possible, to facilitate analysis of the results.

NOMENCLATURE

a) Alphabetical Symbols

- A - heat or mass transfer area, ft.²;
- a - radius, ft.;
- c - solution concentration, lb.solids/lb.solution;
- C_{pa} - heat capacity of dry air, B.t.u./(lb.)(°F.);
- C_{pV} - heat capacity of water vapour, B.t.u./(lb.)(°F.);
- C_{pW} - heat capacity of liquid water, B.t.u./(lb.)(°F.);
- C_{pZ} - heat capacity of dry Lignosol, B.t.u./(lb.)(°F.);
- D_V - diffusivity of water vapour in air, ft.²/hr.;
- d - particle diameter, ft.;
- d_V - mean volume diameter, ft.;
- d_{vs} - mean Sauter diameter, ft.;
- g_c - conversion factor, lb.-mass/(lb.-force)(hr.²);
- h - heat transfer coefficient, B.t.u./(hr.)(ft.²)(°F.);
- H - air humidity, lb.water/lb.bone dry air;
- H₀ - inlet air humidity, lb.water/lb.bone dry air;
- H_w - saturation humidity at surface of particles, lb.water/lb.bone dry air;
- k - thermal conductivity of air, B.t.u./(hr.)(ft.)(°F.);
- kg - mass transfer coefficient, lb./(hr.)(ft.²)(Δp);
- k_{g'} - mass transfer coefficient, lb./(hr.)(ft.²)(ΔH);

- k_G - mass transfer coefficient, lb.-moles/(hr.)(ft.²)(Δp);
 L - rate of liquid spray, lb./hr.;
 L_f - feed rate, lb./hr.;
 M - molecular weight;
 M_m - average molecular weight of gases between the particle surface and the bulk air;
 m - diffusion or evaporation, lb.;
 m' - diffusion or evaporation, lb.-moles;
 n - rate of particles, no./hr.;
 p - vapour pressure in bulk air, p.s.f.a.;
 p_s - equilibrium vapour pressure at the particle surface, p.s.f.a.;
 p' - $(p_s - p)$, p.s.f.a.;
 P_f - $\pi - (p_s - p)/2$, p.s.f.a.;
 Q - amount of heat transfer, B.t.u.;
 q - air rate, c.f.m.;
 R_1 - radius of particle, ft.;
 R_2 - radius of outer limit of gas film surrounding the particle, ft.;
 s - humid heat of air, B.t.u./(lb. bone dry air)(°F.), also a shape factor;
 S - cross-sectional area of drying chamber, ft.²;
 S_w - surface area of particles, ft.²/lb.;
 T - absolute temperature, °R.;
 t - temperature of air, °F.;
 t_f - inlet temperature of feed, °F.;

- t_o - inlet temperature of air, °F.;
 t_w - temperature of particles, °F.;
 V - humid volume, c.f./lb.bone dry air;;
 v - air velocity, ft./sec.;
 v_T - terminal velocity of particles, ft./sec.;
 w - air rate, lb.dry air/hr.;
 X - moisture content, lb.water/lb.bone dry Lignosol;
 X_f - feed moisture content, lb.water/lb.bone dry Lignosol;
 x - distance from nozzle, ft.;
 Z - total rate of bone dry Lignosol per hour;
 Z' - rate of bone dry Lignosol per hour in each particle size group.

b) Greek Symbols

- β - $1/T$, °R.;
 θ - time, hours;
 λ - latent heat of evaporation, B.t.u./lb.;
 λ_w - latent heat of evaporation at the particle temperature, B.t.u./lb.;
 μ - symbol for micron; also viscosity, lb./(hr.)(ft.);
 π - atmospheric pressure; also mathematical symbol for 3.14159;
 ρ - density of air, c.f./lb.;
 ρ_v - density of vapour, c.f./lb.;
 ρ_s - density of particles, c.f./lb.;

- Σ - summation symbol;
 Φ - function.

c) Dimensionless Numbers

- Gr - Grashof Number, $(d^3 \rho^2 g_c / \mu^2)(\beta \Delta t)$;
Nu - Nusselt Number, hd/k ;
Nu' - Modified Nusselt Number, $k_G M_{in} dp_f / D_v \rho$;
Pr - Prandtl Number, $C_p \mu / k$;
Re - Reynolds Number, $d v \rho / \mu$;
Sc - Schmidt Number, $\mu / \rho D_v$.

CONCLUSIONS

As all rate processes, spray drying is governed by the concepts of driving force and resistance. More specifically, spray drying is a diffusional process, and as such the driving force is measured by a partial pressure or humidity difference, while the resistance can be recognized as that of an interphase film. The rate of evaporation and drying will therefore be equal to the ratio of these two factors, expressed in the proper units. Calculation of the resistance factor involves a knowledge of the area available for heat and mass transfer at the interface, since it is inversely proportional to the latter. Resistance may therefore be considered as the product of the reciprocal of the transfer area by the reciprocal of a transfer coefficient.

Because of the inherent difficulties in measuring the instantaneous values of the driving force and of the resistance, very few attempts have been made in the past to follow experimentally the continuous changes which these two factors undergo during the spray drying process. These difficulties in measurement were ascribed by other workers in the field chiefly to back-mixing and complexity of the air-flow pattern with resulting uncertainty in the estimation of the particle trajectory and residence time. It is believed that the use of a constant-diameter, concurrent chamber in this experimental study has largely eliminated most of these difficulties and has made it possible to obtain - for the first time - a complete step-by-step

picture of the spray drying process for a specific material. It is felt, moreover, that this picture was made quite accurate by the careful development of suitable techniques for the sampling and measurement of the various operating variables. The evidence for this particular aspect of the work has already been discussed at great length in the experimental section. It should be noted, however, that the determination of the air humidity by the specially-developed volumetric method was found to be particularly reliable, and that this method appears to have general applicability in any field in which simplicity of analysis combined with good accuracy are required, especially when only small samples are available.

From the experimental data which have been presented, several general conclusions of a fundamental nature can now be advanced which - it is hoped - might help to clarify certain aspects of spray drying.

Considering first the resistance concept, it has already been pointed out that it will be inversely proportional to the transfer area. Since for a given volume of liquid fed to the spray dryer, the latter will be inversely proportional to the droplet diameter, the profound influence which the degree of atomization exerts on the rate of evaporation and drying becomes at once obvious, quite apart from its effects on the physical properties of the dried product.

The other factor involved in the measurement of the resistance is the reciprocal of the heat and mass transfer coefficients. The published evidence, described in the historical section, clearly

indicates that for stationary drops, these coefficients will depend on the droplet diameter and on the relative velocity between the droplets and the air. This is best shown by the Marshall and Ranz expression (equation (23), page 29). However, application of this correlation to a cloud of freely-suspended, moving droplets certainly required experimental verification because of the uncertainties introduced by a number of possible secondary factors such as the doubtful value of the relative velocity, effect of the droplets on the air turbulence, proximity of the droplets, possible contributions from the droplet rotations, or from internal circulation in the droplets. It is believed that the present study has fully vindicated the views of most workers in the field to the effect that these secondary effects should be of negligible importance. The dependence of the heat transfer coefficients on the droplet diameter can be clearly seen from Figures 19 and 20 (Pages 114 and 115), and the experimental results indicate, furthermore, that the value of the Nusselt Number is equal to very nearly two, the exact experimental value being 2.07. This corresponds to the case of droplets evaporating in stagnant air and it is therefore apparent that the relative velocity is essentially equal to zero, or in other words, that the droplets follow the eddy diffusivity of the turbulent air stream. The theoretical analysis of Soo (135) and the results of Kesler (75) would confirm a behaviour of this nature. Since the scatter of the

experimental points is approximately the same as the difference between the average value (2.07) and two, it is difficult to ascribe a theoretical significance to the latter. The somewhat lower value of the modified Nusselt Number (1.89) can be attributed to uncertainties in the values of the diffusivity coefficients, as was done by other workers (107).

If the driving force concept is next considered, the major governing variable in this case is the inlet temperature of the drying air. It has already been pointed out that the surface temperature of pure liquid droplets evaporating in a gas will be the wet bulb temperature of the gas, and consequently the driving force for heat transfer will be the difference between the gas temperature and its wet bulb temperature, while for mass transfer it will be the difference between the saturation vapour pressure at the droplet surface and the vapour pressure of the diffusing component in the bulk gas stream. When a solution is being evaporated, however, the estimation of the driving force is complicated by the lowering of the vapour pressure and the uncertainty of the resulting droplet temperature. In the present study, it was assumed that the surface temperature of the droplets was governed by the saturated humidity corresponding to their bulk concentration, and not to a special condition at the drop surface. The excellent comparison between the calculated and experimental drying times appears to confirm this assumption. These views are in direct opposition to those of

Ranz and Marshall (107), who advanced that a saturated layer of solution would be very quickly formed at the droplet surface which would control the drying process from then on. Their evidence was based on the experimental observation of large, stationary drops fed from the center, and can hardly apply to small moving drops, of constantly shrinking diameter. Because of its considerable theoretical and practical significance, a great deal of attention was devoted to this particular point during the experimental work. Thus, it was repeatedly observed that - because of the extreme solubility of Lignosol in water - a crust did not form on the surface of the droplets until the very last stages of drying were reached. Undoubtedly, a true falling rate period became established at that point but its duration was too small to be detected. These observations contrast directly with the tray drying tests carried out with 1/8-in. layers of solution, where a crust formed at a bulk concentration of less than fifty per cent and effectively stopped any further evaporation. It must be realized, however, that the thickness of the crust thus obtained was larger than the whole diameter of the spray dried particles. This clearly indicates the impossibility of extrapolating results derived from conventional drying methods, or even from the drying of large drops, to the range of droplet size in-

volved in most spray drying operations.

On the practical side, crust formation has far-reaching effects on the physical nature of the spray dried products. At high air temperatures, the vapour pressure of the gases trapped inside the particles by the crust will result in expansion during the very last stages of drying such as was obtained in Run No. 23 at an inlet air temperature of 419°F. Whether the expanded particle will actually explode inside the drying chamber to give the typical fractured egg-shell structure so often reported in the literature remains to be established. It is more likely that the breaking of the hollow shells will occur during collection. At low temperatures, on the other hand, the internal vapour pressure will not be sufficiently large, and possible shrinking and surface checking of the particles will take place instead, with the result that they will remain solid. The physical properties of the product will be profoundly affected by this difference in behaviour, as shown by the work of Duffie and Marshall (30) and Knelman (78).

It is probable that some of the above comments will apply only within the range of variables investigated, and be specific to the material studied or to others similar to it. Several general conclusions can, however, be reached on the basis of the experimental results, and it would appear that the following steps should be

followed in spray dryer design:

1. The product specifications, including the moisture content, particle size and particle density, must first be established.
2. Pilot plant scale tests have to be carried out to determine the physical nature of the product and the temperature at which hollow particles - if any - are formed. The importance of the falling rate period with respect to the overall drying time must also be determined, and this can best be done in a concurrent dryer such as used in this study.
3. Some of the more important physical properties of the solution to be spray dried have to be known; these include the vapour pressure, density, specific heat and heat of solution.
4. From the specifications of the product particle size, a suitable type of atomizer can be selected; apart from the average particle size, the size distribution of the spray from the atomizer must also be given.
5. The minimum quantity of drying air required can be calculated from a material balance, bearing in mind that the outlet humidity cannot exceed the saturation humidity of the product, under the given conditions of air temperature.
6. The evaporation and drying time of the spray can then be calculated by the previously mentioned stepwise method; although the method is somewhat ponderous, it is necessary, since it is difficult

to express the physical properties mathematically to permit a direct integration. The overall time obtained will, of course, depend on the amount of excess air provided.

7. If a minimum moisture content in the product is desired, it will only be necessary to calculate the drying time of the largest droplets.

8. For a given inlet air temperature, the drying time will be a function of the ratio of the air rate and feed rate, since the excess air will determine the driving force throughout the chamber.

9. The size of the drying chamber required, that is its diameter and length, can then be determined from the necessary drying time and from the overall velocity of the particles, and hence of the air. Although this will be fairly simple for concurrent dryers and for dryers where complete mixing takes place, it will present certain difficulties in dryers for which the flow patterns have not been determined previously.

10. Since the residence time of the particles in the chamber must be at least equal to the drying time, an economic balance between the initial investment cost, which will depend on the size of the chamber, and the operating cost, which will depend on the quantity of hot air required, should determine the size of the installation.

11. Allowance must be made in the design for the relatively low amount of evaporation taking place in the nozzle zone when certain

types of atomizers are used.

Although the proposed design considerations are not completely general, they should greatly facilitate scale-up calculations, and the establishment of the heat transfer coefficients and droplet temperatures presented previously will undoubtedly contribute to a general spray drying theory. It is further hoped, that additional experimental studies of a similar type will in time establish a firm engineering basis for spray dryer design, and thus remove the empirical approach to commercial applications which is still largely used.

SUMMARY AND CONTRIBUTION TO KNOWLEDGE

Few unit operations in the field of chemical engineering have enjoyed a wider industrial expansion than spray drying during the past two decades. In spite of this, however, many aspects of the operation have remained unknown or uncertain, and design considerations are based mostly on empirical data and pilot plant tests.

A fundamental study was therefore carried out employing a vertical concurrent spray dryer, fourteen feet long and eight inches in diameter. Since the trajectory of the particles in the apparatus could be determined, it was possible to follow the progressive evaporation and drying of the atomized spray under known operating conditions. From the experimental results the following conclusions were reached:

1. Due to the fact that the velocity of the atomized spray emerging from a pneumatic atomizer is very high, the amount of evaporation taking place in the nozzle zone - approximately one foot long - is relatively small.
2. The evaporation of water droplets ranging in diameter from 11.5 to 38.5 microns, suspended in turbulent air streams of velocities from 3.9 to 14.8 feet per second, is essentially the same as the rate of evaporation of single droplets in stagnant air.
3. The eddy diffusivities of the droplets and of the air are almost equal, resulting in practically zero relative velocity.
4. The temperature of liquid droplets containing dissolved

solids corresponds to the wet-bulb temperature of the air, corrected for the reduced vapour pressure of the diffusing component at the surface of the droplets.

5. The reduction in vapour pressure will be a function of the average concentration of the droplet.

6. In the last stages of drying, a crust will form on the surface of the particles.

7. The formation of the crust will result in the establishment of a true falling rate period, with the accompanying difficulty of estimating the particle temperature and consequently the drying time.

8. At high air temperatures the vapour generated in the center of the particles will expand the crust, resulting in a hollow product.

9. At low air temperatures the vapour pressure will be insufficient and the product will be solid, although the surface of the particles will be checked.

10. In spray drying the crust will form at a much higher average concentration than in tray drying, due to the small dimensions of the particles involved.

11. The calculation of the drying time necessary up to the point of crust formation is possible by a stepwise method.

12. For many highly soluble materials, such as Lignosol, the duration of the falling rate period will be negligibly small.

13. If complete mixing takes place in the spray dryer, the drying time has to be estimated only for the largest drops, and the size of the drying chamber can be calculated from the necessary residence time.

14. If a concurrent spray dryer is employed, the temperature distribution in the chamber must be estimated from the drying time of various droplet size groups, and the length of the chamber can be calculated from the drying time of the largest droplets.

15. If only partial mixing takes place in the spray dryer, the trajectory of the air and of the particles must be determined before the size of the chamber can be estimated.

16. An accurate and simple method for the determination of humidities of small samples of air was developed.

BIBLIOGRAPHY

1. Abbott, N.J., Textile Research J., 24: No. 1, 59 (1954).
2. Adler, C.R., A.M. Mark, W.R. Marshall Jr., and R.J. Parent, Chem. Eng. Progr., 50: 14 (1954).
3. Adler, C.R., and W.R. Marshall Jr., Chem. Eng. Progr., 47: 515, 601 (1951).
4. Alden, E., "Design of Industrial Exhaust Systems", Ind. Press, New York (1940).
5. Alexander, L.G., and C.L. Coldren, Ind. Eng. Chem., 43: 1325 (1951).
6. Andrade, E.N. da C., Proc. Roy. Soc. (London), A134: 445 (1932).
7. Bergolits, M.K., Farmatsiya, 8: No. 3, 15 (1945).
8. Berte, G., Soap and Sanit. Chem., 23: No. 5, 38 (1947).
9. Biddle, S.B., Jr., and A. Klein, Am. Soc. Testing Materials, 36: P2, 310 (1936).
10. Blake, P.D., Chem. and Ind., 68: 138 (1949).
11. Bradley, R.S., M.G. Evans, and R.W. Whytlaw-Gray, Proc. Roy. Soc. (London), 186A: 368 (1946).
12. Briton, M.D., Ind. Eng. Chem., 47: 23 (1955).
13. Buckham, J.A., and R.W. Moulton, Chem. Eng. Progr., 51: 126 (1955).
14. Bullock, K., and J.W. Lightown, Quart. J. Pharm. Pharmacol., 16: 213 (1943).
15. Burkhart, W.H., and E.T. Marceau, U.S. 2152788 (1939).
16. Burton, W.G., J. Soc. Chem. Ind., 63: 213 (1944).
17. Calbeck, J.H., and H.R. Harner, Ind. Eng. Chem., 19: 58 (1927).
18. Calderbank, P.H., and I.J.O. Korchinski, Chem. Eng. Sci., 6: 65 (1956).
19. Carr, R.H., and G. Schild, Food Ind., 16: 809 (1944).
20. Carrier, W.H., and D.C. Lindsay, Mech. Eng., 47: 327 (1925).
21. Case, J.W., Instruments and Automation, 27: No. 7, 1076 (1954).

22. Castelman, R.A., Jr., J. Research Nat. Bur. Standards, 6, RP. 281, 369 (1931).
23. Chem. Processing, 17: No. 7, 100 (1954).
24. Coldren, C.L., and E.W. Comings, "Pneumatic Thermometer and Hygrometer", University of Illinois (1956).
25. Comings, E.W., and C.L. Coldren, Paper presented at the A.I.Ch.E. Meeting, Boston, Mass. (December, 1956).
26. Corbett, W.J., Food Ind., 20: 534 (1948).
27. Davies, C.N., Symp. on Part. Size Anal., Inst. Chem. Engrs. and Soc. Chem. Ind., p. 25 (February 4, 1947).
28. De Juhasz, K.J., O.F. Zahn, and P.H. Schweitzer, Penn. State Coll. Bull., No. 40, (1932).
29. Dorman, R.G., British J. App. Phys., 3: 189 (1952).
30. Duffie, J.A., and W.R. Marshall, Jr., Chem. Eng. Progr., 49: No. 8, 417 (1953).
31. Edeling, C., Beheifte, Angew. Chem., No. 57 (1949).
32. Electrical West., 95: No. 6, 89 (1945).
33. Fairs, G.L., Chem. and Ind., 62: 374 (1943).
34. Fogler, B.B., and R.V. Kleinschmidt, Ind. Eng. Chem., 30: 1372 (1938).
35. Fraser, R.P., and P. Eisenklam, Trans. Inst. Chem. Engrs. (London), 34: 294 (1956).
36. Frechette, J., and H.I. Sephton, Am. Cer. Soc. Bull., 28: 496 (1949).
37. Frevol, H.L., B.G. Edwards, A.L. Dunick, and M.M. Boggs, Ind. Eng. Chem., 38: 1079 (1946).
38. Friedman, S.J., F.A. Gluckert, and W.R. Marshall, Jr., Chem. Eng. Progr., 48: 181 (1952).
39. Froessling, N., Gerlands Beitr. Geophys., 52: 170 (1938).
40. Fuchs, N., Physik. Z. Sowjetunion, 6: 224 (1934).
41. Fuchs, N., and I. Petrjanoff, Nature, 139: 111 (1937).

42. Garner, H.F., Trans. Inst. Chem. Engrs. (London), 28: 88 (1950).
43. Geist, J.M., J.L. York, and G.G. Brown, Ind. Eng. Chem., 43: 1371 (1951).
44. Glasston, S., "Textbook of Physical Chemistry", 2. ed., p.632 D. van Nostrand, New York, (1946).
- 44A. Godsave, G.A.E., Collected Papers of the 4th Int. Symp. on Combustion, Cambridge, Mass. (September, 1952).
45. Golitzine, N., National Aeronautical Est., Can., Note 6, ME- 177 (1951).
46. Gooden, E.L., and C.L. Smith, Ind. Eng. Chem. (Anal. Ed.), 12: 479 (1940).
47. Guyton, A.C., J. Ind. Hug. Toxicol., 28: 133 (1946).
48. Greene, J.W., R.M. Conrad, A.L. Olsen, and C.E. Wagoner, Paper presented at the A.I.Ch.E. Meeting, Detroit, Michigan (November 12, 1947).
49. Gwyn, J.E., J.C. Garver, and W.R. Marshall, Jr., Paper presented at the A.I.Ch.E. Meeting, Boston, Mass. (December, 1956).
50. Hagerty, W.W., and J.F. Shea, Paper No. 55- AFM- 21, A.S.M.E. (1954).
51. Hamilton, W.F., Ind. Eng. Chem. (Anal. Ed.) 2: 234 (1930).
52. Hanson, A.R., "Ohio State University Studies in Engineering", XXI: No. 3, 415 (1952).
53. Harkins, W.D., and F.E. Brown, Am. Chem. Soc. J., 41: 499 (1919).
54. Hawksley, P.G.W., Nature, 170: 984 (1952).
55. Heidbrink, W., Fats and Soaps, 53: 291 (1951).
56. Herring, W.M., Jr., and W.R. Marshall, Jr., Am. Inst. Chem. Engrs. J., 1: 200 (1955).
57. Heyword, H., Symp. on Part. Size Anal., Inst. Chem. Engrs. and Soc. Chem. Ind., p. 14 (February 4, 1947).
58. Hillier, J., U.S. 2491441 (1950).
59. Hinze, J.O., and H. Milborn, J. Appl. Mechanics, 17: 145 (1950).
60. Houghton, H.G., Physics, 2: 467 (1932).
61. Ibid. 4: 419 (1933).

62. Houghton, H.G., and W.H. Radford, Papers Phys. Oceanog. Meteorol., Mass. Inst. Tech. and Woods Hole Oceanog. Inst., 6: No. 3, 4 (1938).
63. Hu, S., and R.C. Kintner, Am. Inst. Chem. Engrs. J., 1: 42 (1955).
64. Hughes, R.R., and E.R. Gilliland, Chem. Eng. Progr., 48: 497 (1952).
65. Ingebo, R.D., Natl. Advisory Comm. Aeronaut., Tech. Mem. 2368 (1951).
66. Ibid., 3265 (1954).
67. International Critical Tables, V: 62 (1929).
68. Isenberg, P.H., Ind. Eng. Chem., 46: No. 11, 105A (1954).
69. Johnson, J.C., J. App. Phys., 21: 22 (1950).
70. Johnstone, H.F., and D.K. Eads, Ind. Eng. Chem., 42: 2293 (1950).
71. Johnstone, H.F., and R.V. Kleinschmidt, Trans. Am. Inst. Chem. Engrs., 34: 181 (1938).
72. Johnstone, H.F., R.L. Pigford, and J.H. Chapin, Trans. Am. Inst. Chem. Engrs., 37: 95 (1941).
73. Johnstone, H.F., and G.C. Williams, Ind. Eng. Chem., 31: 993 (1939).
74. Kersten, H., Science, 121: 98 (1954).
75. Kesler, G.H., D.Sc. Thesis, Mass. Inst. Technol., (1952).
76. Kestner Evaporator and Eng. Co. (London), Food, 5: 425 (1936).
77. Knapp, T., Ind. Eng. Chem. (Anal. Ed.), 6: 66 (1934).
78. Knelman, F.H., M. Eng. Thesis, McGill University, Montreal (1950).
79. Kyte, J.R., A.J. Madden, and E.L. Piret, Chem. Eng. Progr., 49: 653 (1953).
80. Lane, W.R., Ind. Eng. Chem., 43: No. 6, 1312 (1951).
81. Langmuir, I., Phys. Rev., 12: No. 2, 368 (1918).
82. Langstroth, G.O., G.H.H. Diehl, and E.J. Winhold, Can. J. Res., 28A: 580 (1950).
83. Leman, J.I.G., Swed., 149, 638 (1955).

84. Lewis, H.C., D.G. Edwards, H.J. Goglia, R.I. Rice, and W.L. Smith, *Ind. Eng. Chem.*, 4D: 67 (1948).
85. Lignosol Chemicals, Ltd., Private Communication, (June, 1955).
86. Liu, Vi-Cheng, Dept. of U.S. Air Force, Project 2160 (1955).
87. Longwell, J.P., D.Sc. Thesis, Mass. Inst. Technol., (1943).
88. Longwell, J.P., and M.A. Weiss, *Ind. Eng. Chem.*, 45: 667 (1953).
89. Luchak, G., and G.O. Langstroth, *Can. J. Res.*, 28A: 574 (1950).
90. Manning, W.P., Private Communication, (July, 1956).
91. Marshall, W.R., Jr., "Atomization and Spray Drying", *Chem. Eng. Progr.*, Monograph Series, 50: No. 2, (1954).
- 91A. Marshall, W.R., Jr., *Chem. Can.*, 7: 37 (1955).
92. Marshall, W.R., Jr., *Trans. Am. Soc. Mech. Engrs.*, 77: 1377 (1955).
93. Marshall, W.R., Jr., and E. Seltzer, *Chem. Eng. Progr.*, 46: 501, 575 (1950).
94. Mathieu, M.E., *Theorie de la Capillarite*, p. 134, Gauthier-Villars, Imprimeur Libraire, Paris, (1883).
95. Maxwell, J.C., "Diffusion", *Sci. Papers*, 2: Cambridge University Press, (1890).
96. May, K.R., *J. App. Phys.*, 20: 932 (1949).
97. Morse, H.W., *Proc. Am. Acad. Arts and Sci.*, 45: 363 (1910).
98. Nukiyama, S., and Y. Tanasawa, *Trans. Soc. Mech. Engrs. (Japan)*, 4: No. 14, 5-13 (1938). 4: No. 15, 5-24 (1938). 5: No. 18, 5-14 (1939). 5: No. 18, 5-15 (1939). 6: No. 22, 5-7 (1940). 6: No. 23, 5-18 (1940).
99. Oktay, C.M., Ph.D. Thesis, University of Florida, (1955).
100. Oyama, Y., M. Egutti, and K. Endon, *Chem. Eng. (Japan)*, 17: 296 (1953).
101. Perruchie, L., *Nature* 159: 184 (1947).
102. Perry, J.H., "Chemical Engineers' Handbook", 3 ed., p. 846, McGraw-Hill, New York, (1950).
103. *Ibid.*, p.1022.

104. Pigford, R.L., and C. Pyle, *Ind. Eng. Chem.*, 43: 1649 (1951).
105. Pinder, K.L., M. Eng. Thesis, McGill University, Montreal (1952).
106. Probert, R.P., *Phil. Mag.*, 37: 94 (1946).
- 106A. Ranz, W.E., *Trans. Am. Soc. Mech. Eng.*, 78: 909 (1956).
107. Ranz, W.E., and W.R. Marshall, Jr., *Chem. Eng. Progr.*, 48: 141, 173 (1952).
108. Ranz, W.E., and J.B. Wong, *Ind. Eng. Chem.*, 44: 1371 (1952).
109. Rasbash, D.J., *J. Sci. Instrum.*, 30: 189 (1953).
110. Rayleigh, Lord, *Proc. London Math. Soc.*, 10 (1878).
111. Reavell, J.A., *Chem. and Ind.*, 46: 925 (1927).
112. *Ibid.*, 56: 618 (1937).
113. Reavell, J.A., *Soap Perfumery Cosmetics*, 17: 816 (1944).
114. Reavell, J.A., *Trans. Inst. Chem. Engrs. (London)*, 6: 115 (1928).
115. Richardson, E.G., *App. Sci. Res.*, A4: 374 (1954).
116. Richardson, E.G., "Dynamics of Real Fluids", p. 102, Edward Arnold and Co., London, (1950).
117. Richardson, E.G., *Proc. Phys. Soc. (London)*, 55: 48 (1943).
118. Ripka, L.V., *Chem.-Ing.-Tech.*, 26: 440 (1954).
119. Rizika, J.W., Paper No. 55-A-154, A.S.M.E. (1954).
120. Roberts, F., and Y.Z. Young, *Proc. Inst. Elec. Engrs. (London)*, 99: pt. III. A, No. 20, 747 (1952).
121. Rupe, J.H., "Third Symposium on Combustion Flame and Explosion Phenomena", The Williams and Wilkins Co., Baltimore, (1949).
122. Santer, J., *Forsch. Gebiete Ingenieurw.*, No. 297 (1926).
123. Schmidt, J.M., *Jet Prop. Lab., Cal. Inst. Tech., Prog. Rep. No. 3-18* (1948).
124. Schweitzer, P.H., *J. App. Phys.*, 8: 513 (1937).
125. Scott, A.W., *Hanna Dairy Res. Inst. (G.B.)*, Publication, (1932).
126. Scott, G. and Son, Ltd., *Food*, 16: 342 (1947).

127. Shereshefsky, J.L., and S. Steckler, *J. Chem. Phys.*, 41: 108 (1936).
128. Sherwood, T.K., and G.C. Williams, *Natl. Defence Res. Comm. Prog. Rep.*, P.B. 6538 (1941).
129. Sherwood, T.K., and B.B. Woertz, *Ind. Eng. Chem.*, 31: 1034 (1939).
130. Sjenitzen, F., *Chem. Eng. Sci.*, 1: 101 (1952).
131. Skimmer, P.G. and S. Boas-Traube, *Symp. on Part. Size Anal., Inst. Chem. Engrs. and Soc. Chem. Ind.*, p. 57 (February 4, 1947).
- 131A. Sleicker, C.A., Jr., and S.W. Churchill, *Ind. Eng. Chem.*, 48: 1819 (1956).
132. Slipecevich, C.M., J.A. Consiglio, and F. Kurata, *Ind. Eng. Chem.*, 42: 2353 (1950).
133. Smith, D.A., *Chem. Eng. Progr.*, 45: 703 (1950).
134. Smith, M.W., *Chem. Age (London)*, 64: 443 (1951).
135. Soo, S.L., *Chem. Eng. Sci.*, 5: 57 (1956).
136. Spencer-Gregory, H., and E. Rouke, *Instrument Practice*, 7: No. 5, 335 (1953).
137. Stamford Research Institute, *News Bull.*, 5: No. 5, 4 (1953).
138. Stewart, E.D., *Chem. and Met. Eng.*, 35: 470 (1928).
139. Stockmann, G.J., *Oils and Oilseeds J. (India)*, 7: No. 12, 8 (1955).
140. Stoker, R.L., *J. App. Phys.*, 17: 243 (1946).
141. Straus, R., *Ph.D. Thesis, University of London* (1949).
142. Tang, Y.S., *Ph.D. Thesis, University of Florida* (1952).
143. Tate, R.W., and W.R. Marshall, Jr., *Chem. Eng. Progr.*, 49: 169, 226 (1953).
144. Taylor, E.H., and D.B. Harmon, Jr., *Ind. Eng. Chem.*, 46: 1455 (1954).
145. Taylor, T.H.M., *Chem. Eng. Progr.*, 43: 153 (1947).
146. Tolman, R.C., R.H. Gerke, A.P. Brooks, A.G. Herman, R.S. Mulliken, and H. Dew-Smyth, *J. Am. Chem. Soc.*, 41: 575 (1919).
147. Tonn, H., *Chem. Eng. Progr.*, 49: 388 (1953).

148. Turner, G.M., and R.W. Moulton, Chem. Eng. Progr., 49: 185 (1953).
149. Walton, W.H., Nature, 169: 518 (1952).
150. Walton, W.H., and W.C. Prewett, Proc. Phys. Soc. (London), 62B:
341 (1949).
151. Webb, P., and M.K. Neugebauer, Rev. Sci. Instr., 25: 1212 (1954).
152. White, W.C., Elec. Eng., 73: 1084 (1954).
153. York, J.L., and H.E. Stubbs, Trans. Am. Soc. Mech. Engrs., 74:
1157 (1952).
154. Yorston, F.H., Private Communication, (October, 1954).